

AD A138080

1

DISCRETE ELEMENTS METHOD
OF
NEUTRAL PARTICLE TRANSPORT

DISSERTATION

AFIT/DS/PH/83-5

Kirk A. Mathews
LCDR USN

Approved for public release; distribution unlimited

DTIC
ELECTE
S FEB 22 1984

D

84 02 21 18Z

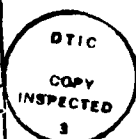
DTIC FILE COPY

THE DISCRETE ELEMENTS METHOD
OF
NEUTRAL PARTICLE TRANSPORT

DISSERTATION

Presented to the Faculty of the School of Engineering
of the Air Force Institute of Technology
Air University
in Partial Fulfillment of the
Requirements for the Degree of
Doctor of Philosophy

Accession For	
NTIS GRA&I	<input checked="checked" type="checkbox"/>
DTIC TAB	<input type="checkbox"/>
Unannounced	<input type="checkbox"/>
Justification	
By	
Distribution/	
Availability Codes	
Dist	Avail and/or Special
RI	



by

Kirk A. Mathews, B.S., M.S.

LCDR

USN

DS/PH/83-5

DISCRETE ELEMENTS METHOD
OF
NEUTRAL PARTICLE TRANSPORT

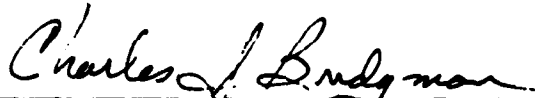
by

Kirk A. Mathews

LCDR

USN


Approved:




Charles J. Bridgman, Chairman



Edward W. Larsen



David A. Lee

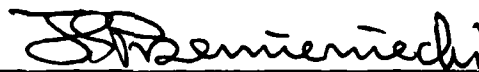


Donn G. Shankland



John Jones, Jr.

Accepted:



Janusz S. Przemieniecki
Dean, School of Engineering

Acknowledgments

I would like to thank all those whose assistance has made it possible for me to complete this project in the (limited) time available. The members of my doctoral committee are certainly among this group. They are Charles J. Bridgman (Chairman), Edward W. Larsen, David A. Lee, Donn G. Shankland, and John Jones, Jr. (Dean's Representative). I also owe Professor Bridgman particular thanks as my advisor at AFIT.

I would like to thank Dr. Larsen (of the Los Alamos National Laboratory) for serving on my committee by long-distance, and for running sample problems in S_N which were used to validate my computer programs, and for providing conventional S_N results for the vacuum duct problem. His readiness to discuss the project whenever I telephoned has been greatly appreciated.

Other members of the laboratory who helped include William T. Urban, who provided the Monte Carlo benchmark solution to the duct problem; Ray E. Alcouffe, who provided me with a copy of his reference library on quadrature sets; and Kaye D. Lathrop, who stressed the importance of a sound theoretical basis for numerical methods.

Lastly, I would like to thank Captain Paul L. Callahan, USN, whose assistance (as Commanding Officer of USS Birmingham, SSN 695) obtained me a billet at the Air Force Institute of Technology.

Table of Contents

	<u>Page</u>
Acknowledgments.....	iii
List of Figures.....	vii
List of Tables.....	vii
Abstract.....	viii
I. Introduction.....	I-1
A. Background.....	I-1
B. Statement of the Problem.....	I-4
C. Scope.....	I-5
D. General Approach and Sequence of Presentation.....	I-6
II. Derivation of the Discrete Elements Transport Method.....	II-1
A. Angular Coordinates and Elements of Angle.....	II-1
B. Discretization of the (Angular) Flux.....	II-3
C. Discretization of the Transport Equation.....	II-4
D. The Flux-Weighted Mean Angle.....	II-6
E. Approximating the Flux-Weighted Streaming Directions.....	II-7
F. The Discrete Elements Method Algorithm.....	II-9
G. Summary.....	II-11
III. Angular Quadrature in the S_N and L_N Methods.....	III-1
A. Global Basis Functions and Gaussian Quadrature.....	III-1
B. Local Basis Functions and Composite Quadrature.....	III-2
C. Behavior of the Directional Flux in Heterogeneous Problems.....	III-2
D. Totally Symmetric Quadrature Sets (S_N) and Related Types.....	III-3
E. Product Quadrature Sets.....	III-4
1. Single Range Quadrature.....	III-5
2. Multiple Range (S_{KG}, L_Q) Quadrature.....	III-5
3. Rotationally Symmetric Azimuthal (S_{KG}, L_R) Quadrature.....	III-6
F. Discrete Elements Composite Quadratures.....	III-7
1. One-dimensional Equal Weight (L_N) Quadrature.....	III-7
2. One-dimensional Gaussian Weight (L_{NGW}) Quadrature.....	III-8
3. Equal Weight Composite Product ($L_{K,L}$) Quadrature.....	III-8
G. Hybrid Gauss-Christoffel/Composite (L_{KG}, L) Quadrature.....	III-9
H. Diffusion Limit Considerations.....	III-9
I. Summary.....	III-13
IV. Quadrature Rules for Discrete Element Flux Modelling.....	IV-1
A. Simpson's Rule.....	IV-1
B. Three-Point Gauss-Legendre Rule.....	IV-2
C. Newton-Cotes Closed (Five-Point) Rule.....	IV-4
D. Summary.....	IV-6

V. Spatial Quadrature Methods.....	V-1
A. One-Dimensional (Slab) Spatial Quadrature.....	V-1
1. Coordinates and Symbols.....	V-1
2. Balance Equation.....	V-2
3. Conservation Considerations.....	V-3
4. Step Method.....	V-4
5. Diamond Difference.....	V-5
6. Negative Flux Fixup for the Diamond Difference Method....	V-6
7. Considerations Regarding the Use of Fixups.....	V-7
8. Step Characteristic Method.....	V-8
9. Linear Characteristic Method.....	V-9
B. Two-Dimensional (xy) Spatial Quadrature.....	V-10
1. Coordinates and Symbols.....	V-10
2. Balance Equation.....	V-11
3. Step Method.....	V-11
4. Diamond Difference.....	V-12
5. Negative Flux Fixup for the Diamond Difference Method...	V-13
6. Step Characteristic.....	V-15
C. Summary.....	V-18
VI. Interaction of Angular and Spatial Quadrature:	
Ray Effects and Quasi-Ray Effects..	VI-1
A. The Square-in-a-Square Problem: Without Scatter.....	VI-1
B. Angular Truncation Error and Ray Effect.....	VI-3
C. Quasi-Ray Effect and Spatial Truncation Error.....	VI-5
D. Combined Angular and Spatial Truncation Errors.....	VI-8
E. Summary.....	VI-10
VII. Versions of the Discrete Elements Method.....	VII-1
A. Specification of a Discrete Elements Numerical Scheme.....	VII-1
B. Coupling of Auxiliary and Main Fluxes.....	VII-2
C. Optimization.....	VII-3
VIII. Computer Implementation.....	VIII-1
A. Problem and Quadrature Dimensions.....	VIII-1
B. Discrete Ordinates Memory Requirements.....	VIII-1
C. Discrete Elements Memory Requirements.....	VIII-2
D. Example Comparison of Storage Requirements.....	VIII-5
E. Execution Times for S_N Spatial Quadratures.....	VIII-5
F. Execution Times for L_N Streaming Direction Averaging.....	VIII-7
G. Example Execution Cost Comparison.....	VIII-8
H. Computer Programs for Testing the Discrete Elements.....	VIII-8
I. Conclusions.....	VIII-9
IX. Test Cases in One-Dimensional Geometry and Results.....	IX-1
A. Scatter-Free Shield Penetration.....	IX-1
1. Step vs. SC for Auxiliary Fluxes.....	IX-3
2. Simpson's Rule vs. Gauss-Legendre (3-point) Quadrature..	IX-3
3. Equal Weight vs. Gaussian Weight Discrete Elements.....	IX-3
4. Discrete Elements vs. Discrete Ordinates.....	IX-3

B. Two-Region Problem.....	IX-4
1. Error "Norms".....	IX-5
2. Step/LC vs. Step/DDF.....	IX-6
3. Equal Weight vs. Gaussian Weight Elements.....	IX-7
4. LC/LC vs. Step/LC.....	IX-8
5. G3 vs. SR Element Quadrature.....	IX-9
6. Discrete Elements vs. Discrete Ordinates.....	IX-9
C. Conclusions.....	IX-10
X. Test Cases in Two-Dimensional Geometry and Results.....	X-1
A. Ray Effect Problem and Comparison of Results.....	X-1
1. Conventional Discrete Ordinates.....	X-1
2. Rotationally Symmetric Discrete Ordinates.....	X-2
3. "Consistent" Discrete Ordinates.....	X-2
4. Spherical-Harmonics-Like Discrete Ordinates.....	X-2
5. Compatible Product Quadrature Discrete Ordinates.....	X-3
6. Discrete Elements.....	X-3
B. Vacuum Duct Problem: Qualitative Comparison of Results.....	X-8
1. The Test Problem.....	X-8
2. Monte Carlo Benchmark Solution.....	X-9
3. Conventional Discrete Ordinates.....	X-9
4. Product Quadrature Discrete Ordinates.....	X-13
5. Discrete Elements.....	X-13
C. Vacuum Duct Problem: Quantitative Comparison of Results....	X-16
1. Convergence of Conventional S_N	X-16
2. Convergence in Polar Quadrature.....	X-18
3. Convergence in Azimuthal Quadrature.....	X-18
4. Convergence of Spatial Quadrature.....	X-19
5. Confidence of Results.....	X-20
D. Interaction of Spatial and Angular Quadrature.....	X-21
1. Leakage Through the Shield.....	X-21
2. Leakage Through the Duct.....	X-22
E. Conclusions.....	X-25
XI. Conclusions and Recommendations.....	XI-1
A. Conclusions.....	XI-1
1. Sound Theoretical Basis.....	XI-1
2. Practical for Computer Implementation.....	XI-1
3. Amelioration of Ray Effects.....	XI-1
4. Accuracy	XI-2
5. Cost Effectiveness.....	XI-2
6. Element Quadrature Rules.....	XI-2
7. Angular Quadrature for XY-Geometry.....	XI-2
8. Spatial Quadrature.....	XI-2
B. Recommended General Purpose Discrete Elements Schemes.....	XI-3
C. Recommended Topics for Further Research.....	XI-4
1. Evaluation with Higher Order Spatial Quadratures.....	XI-4
2. Extension to Curvilinear Coordinates.....	XI-4
3. Extension to Anisotropic Scatter.....	XI-4
4. Higher Order Space-Angle Coupling.....	XI-5
Bibliography.....	BIB-1
Vita.....	Vita-1

List of Figures

	<u>Page</u>
II-1: Discrete Element Auxiliary Directions for Simpson's Rule.....	II-8
III-1: Example Problem: Homogeneous Reactor with Control Rod.....	III-3
V-1: Step Characteristic Unit Cell.....	V-15
VI-1: Square-in-a-Square, Non-scattering Absorber Problem.....	VI-2
VI-2: Discrete Ordinates Solution with Analytic Spatial Quadrature.....	VI-4
VI-3: Quasi-Ray Effect in Step Characteristic Method.....	VI-6
VI-4: Discrete Angular and Spatial Quadrature Results.....	VI-9
VIII-1: Quadrature Set for $SR-L_{2G,3}$	VIII-3
VIII-2: Quadrature Set for $SR-L_{2,3}$	VIII-4
X-1: Ray Effects: Conventional S_N [Ref.8:257].....	X-4
X-2: Ray Effects: Rotationally Symmetric S_N [Ref.8:258].....	X-5
X-3: Ray Effects: "Consistent" Discrete Ordinates [Ref.8:259].....	X-5
X-4: Ray Effects: Spherical-Harmonics-Like S_N [Ref.8:263].....	X-6
X-5: Ray Effects: Gauss-Christoffel/Quadruple-Range S_N [Ref.2:313].....	X-6
X-6: Ray Effects: Discrete Elements $G3-L_{2G,3}^{SC/DDF}$	X-7
X-7: Ray Effects: Discrete Elements $G3-L_{2G,3}^{SC/SC}$	X-7
X-8: Vacuum Duct Problem Parameters.....	X-8
X-9: Vacuum Duct: Conventional S_N^{DDF}	X-10
X-10: Vacuum Duct: Conventional S_N^{SC}	X-11
X-11: Vacuum Duct: Conventional S_N^{LC}	X-12
X-12: Vacuum Duct: Product Quadrature Discrete Ordinates $S_{2G,3R}^{SC}$	X-14
X-13: Vacuum Duct: Discrete Elements $G3-L_{2G,3}^{SC/SC}$	X-15
X-14: SC and LC Shield Penetration Errors.....	X-22
X-15: Paths Through the Vacuum Duct.....	X-23

List of Tables

IV-1: Flux-Weighted Mean Angle Formulas.....	IV-5
VIII-1: Example Case Memory Requirements.....	VIII-5
VIII-2: Cray-1 Floating Point Execution Times.....	VIII-6
VIII-3: Discrete Ordinates Spatial Quadrature Subroutine Costs.....	VIII-6
VIII-4: Execution Times for L_N Streaming Direction Averaging.....	VIII-7
IX-1: Error Ratio of Shield Penetration Current.....	IX-2
IX-2: Parameters for Two Region Test Problem.....	IX-4
IX-3: Error Ratio of Scalar Flux Integrated over Source Region.....	IX-5
IX-4: Error Ratio of Scalar Flux Integrated over Shield Region.....	IX-6
IX-5: Average Error Ratio of Scalar Flux in the Source Region.....	IX-7
IX-6: Average Error Ratio of Scalar Flux in the Shield Region.....	IX-8
X-1: Vacuum Duct: Error Norms for L_N and S_N Results.....	X-17

Abstract

A new "discrete elements" (L_N) transport method is derived and compared to the discrete ordinates S_N method, theoretically and by numerical experimentation. The discrete elements method is more accurate than discrete ordinates and strongly ameliorates ray effects for the practical problems studied. The discrete elements method is shown to be more cost effective, in terms of execution time with comparable storage to attain the same accuracy, for a one-dimensional test case using linear characteristic spatial quadrature. In a two-dimensional test case, a vacuum duct in a shield, L_N is more consistently convergent toward a Monte Carlo benchmark solution than S_N , using step characteristic spatial quadrature. An analysis of the interaction of angular and spatial quadrature in xy-geometry indicates the desirability of using linear characteristic spatial quadrature with the L_N method.

The discrete elements method is based on discretizing the Boltzmann equation over a set of elements of angle. The zeroth and first angular moments of the directional flux, over each element, are estimated by numerical quadrature and yield a flux-weighted average streaming direction for the element. (Data for this estimation are fluxes in fixed directions calculated as in S_N .) The spatial quadrature then propagates the element flux in this "steered" direction. Since the quadrature directions are not fixed, but are coupled to the fluxes, the method strongly ameliorates ray effect. This is verified using the square-in-a-square test case originated by Lathrop. A variety of spatial, angular, and element quadrature schemes are evaluated for both L_N and S_N . The best discrete elements method uses a hybrid of Gauss-Christoffel polar and composite 3-point Gauss-Legendre azimuthal quadrature.

I. Introduction

The research reported here has developed a new numerical method for solution of the Boltzmann neutral particle transport equation, the method of discrete elements (L_N), and tested its performance on problems in one- and two-dimensional Cartesian coordinates. These problems have been selected as a proof of concept.

A. Background

The Boltzmann equation, in the form of equation (I-1), is a balance equation for the flux of neutral particles at any point in seven-dimensional phase space. This flux, ψ , is a function of particle position (x, y, z), direction of particle motion (θ, ϕ), particle speed (v) or energy (E), and time (t). For the monoenergetic, steady state, one- and two-dimensional problems considered in this research, the time and energy dependences are suppressed, as are one (z) or two (y, z) of the spatial dependences.

$$\hat{\Omega} \cdot \nabla \psi + \sigma_t \psi = c \sigma_s \phi + S \quad (I-1)$$

where

σ_t is the total cross-section for interaction (absorption or scatter)

σ_s is the scattering cross-section

$$c = \sigma_s / \sigma_t$$

$\hat{\Omega}$ is the direction of motion unit vector, (θ, ϕ) in spherical coordinates, and

ϕ is the scalar flux, and is related to the (directionally dependent) flux, ψ , by

$$\phi(x, y, z) = \int_{4\pi} \psi(x, y, z, \hat{\Omega}) d\hat{\Omega} \quad (I-2)$$

Equation (I-1) represents the balance between loss rate (left side) and gain rate (right side) which exists at each point of phase space under steady state conditions. The first term on the left is the loss rate of particles due to divergence, or spreading of the flux. The second term is the loss rate due to interactions of the particles with the medium, either absorption, which destroys the particle, or scatter, which changes its direction of motion (and, more generally, energy, although that dependence is suppressed here), removing the particle from its original element of phase space. The first term on the right is the gain rate due to particles which are present at the given space location, but traveling in other directions, and which scatter, changing to the given direction of motion. The final term is the gain rate due to creation of new particles by any source mechanism, for example, radioactive decay.

Actually, the (phase space) flux, ψ , is usually of interest only in so far as it is needed to obtain its zeroth angular moment, the scalar flux, ϕ , or its first angular moment, the (vector) current, \underline{J} . The

scalar flux is of physical interest because it determines rates of reactions, such as fission or neutron activation. The current is of physical interest in determining the leakage rates of particles from one region to another, through boundary surfaces.

Equation (I-1) is an integro-differential equation, solution of which is particularly difficult. It is solved (except for very simple cases) by numerical means, such as the method of discrete ordinates, rather than analytically.

Since its development in the 1960's, the discrete ordinates S_N method of numerical neutral particle transport has been a mainstay of nuclear design. Its simple, iterative computational structure supports computer solution of problems with large spatial grids and multiple energy groups without prohibitive storage requirements. This is accomplished by treating the spatial and angular integrations, or quadratures, independently. Finite element methods which couple the spatial and angular representations of the flux have the potential for accurate solutions with coarse meshes, but are complicated and very costly in storage.

Discrete ordinates methods have serious drawbacks, however. The use of discretized angular and spatial representations inevitably entails truncation errors. These often take the form of random errors which limit the accuracy of the method, but when the truncation errors appear systematically, they can cause results which are qualitatively incorrect. Such systematic errors have been known as ray effects, since the discrete ordinates method represents particle motion only in fixed directions, or "rays". Another limitation of discrete ordinates is that it provides poor accuracy for some types of problems which are important

in nuclear design. Streaming ducts in shields cause such difficulties because the discrete ordinates angular representation is not well adapted to a distribution of flux which is strongly peaked along the axis of the duct. If the duct is not aligned along one of the quadrature set directions, the discrete ordinates calculation may be very insensitive to the presence of the duct. Monte Carlo methods can be used in such cases, but are computationally costly. The performance of the S_N method is sensitive to the choice of the angular quadrature direction set, in a problem-dependent way. One of the limitations of the method is that when different quadrature sets give widely varying results, it is difficult to have much confidence in any of them.

The discretized spatial representation can also lead to systematic errors which result in qualitatively incorrect solutions, here called "quasi-ray effect". Recent progress has been made in developing higher order spatial quadrature schemes which reduce these truncation errors.

Various schemes have been proposed for improving the performance of discrete ordinates calculations. Some of these are reviewed in the body of this report.

B. Statement of the Problem

The objective of this research is to derive the discrete elements equations, and to develop, implement, and evaluate the performance of the discrete elements method. The method should use an improved angular representation which couples angular and spatial quadrature in order to reduce truncation errors and ray effects, while retaining the computational simplicity of the S_N method.

C. Scope

The scope of the research includes development and demonstration of the discrete elements method and analysis of its computational costs in terms of computer storage and execution time. Its performance is compared to discrete ordinates calculations with various quadrature sets. The method is tested with various angular and spatial quadratures and the optimum scheme identified. Two 1-dimensional and two 2-dimensional test problems are used. These test problems incorporate the following assumptions:

- Geometries: 1-D and 2-D Cartesian
- Sources:
 - Uniformly distributed (by region)
 - Isotropic
- Media:
 - Uniform by region
 - Isotropic
 - Non-Multiplying
- Scatter: Isotropic (in Lab Frame)
- Energy Dependence: Monoenergetic (i.e. One Group)
- Time Dependence: Steady State

Since the discrete element method retains much of the computational structure of discrete ordinates methods, the extension to multiple energy groups, anisotropic scatter, and time dependent problems is immediate and so need not be explicitly demonstrated here.

D. General Approach and Sequence of Presentation

The discrete elements equations are derived, in chapter II, by discretizing the integro-differential form of the Boltzmann transport equation over elements of solid angle. The computer algorithm for the method is then developed as an extension of the discrete ordinates algorithm. Angular quadrature sets for S_N methods are reviewed in chapter III, and corresponding quadrature grids for L_N are proposed. Three quadrature rules are considered in chapter IV. These are used within each element of angle for coupling the angular and spatial quadratures. Potential advantages and disadvantages of the three methods are evaluated. Chapter V reviews the spatial quadrature schemes that are to be used in the testing in later chapters. The review is conducted in detail in order to support the later analysis of the performance of the discrete elements method using these schemes. Smoothness, pointwise accuracy, global accuracy, and tendencies toward systematic error are considered. Having established the angular and spatial quadratures available, the interaction of the two forms of quadrature is investigated in chapter VI. Formal definitions are given for ray effect and quasi-ray effect, and examples of each are given. In evaluating the performance of the L_N method, it is important to be able to distinguish between faults of the angular representation and quadrature and faults of the spatial discretization and quadrature.

Since there are many possible combinations of quadrature schemes to be employed as a discrete elements method, chapter VII defines a notational system for identifying the different schemes, and discusses the possibilities for optimization of the method. Chapter VIII then analyses the computational costs of implementing these various schemes.

The discrete elements method was programmed and tested in both one- and two-dimensional Cartesian geometry. Chapter IX presents an analysis of the results for the one-dimensional problems: a pure absorber (no scatter, no source) with an isotropic flux incident on one side; and a highly scattering source region with a low scatter shield and vacuum outer boundary. Chapter X treats two 2-dimensional problems: a square source in a larger square absorber; and a shielded source with a vacuum duct in the shield. Both chapters present the results of calculations with various L_N schemes, as well as with competing S_N schemes, and, in most cases, analytic or Monte Carlo benchmark solutions. The methods are analyzed for accuracy, convergence, and cost-effectiveness. Causes of the observed errors are also considered. Chapter XI summarizes the conclusions drawn in the previous chapters and presents recommendations for use of the discrete element method and for future research.

II. Derivation of the Discrete Elements Transport Method

This chapter presents the derivation of a new method of discretizing and solving the integro-differential form of the Boltzmann neutral particle transport equation. The method has some features in common with the discrete ordinates S_N method, but differs from it in two major ways. First, the Boltzmann equation is discretized over a collection of elements of solid angle, rather than into a point-set of fixed directions as in S_N . Second, the method of approximating and solving the discrete element equations explicitly couples the angular dependence of the directional flux into the spatial quadrature scheme, so that the directions of streaming are interpolated to better represent the motion of the particles in each angular element. A motivation for this scheme is the anticipation that the steered streaming of the discrete elements method should ameliorate the ray effects seen in the discrete ordinates method as a result of its fixed streaming directions.

A. Angular Coordinates and Elements of Angle

Three related angular coordinate systems are used here. These are:

1 - polar coordinates (θ, ϕ) where θ is the polar angle, measured from the z-axis, and ϕ is the azimuthal angle, measured from the x-axis toward the y-axis.

2 - polar cosine / azimuthal angle coordinates (τ, ϕ) where $\tau = \cos(\theta)$ and ϕ is the azimuthal angle, as above.

3 - direction cosine coordinates (μ, η) where μ is the x-direction cosine and η is the y-direction cosine.

These coordinates are related by

$$\tau = \cos (\theta) \quad (II-1)$$

$$\mu = \sin (\theta) \cos (\phi) = \sqrt{1 - \tau^2} \cos (\phi) \quad (II-2)$$

$$\eta = \sin (\theta) \sin (\phi) = \sqrt{1 - \tau^2} \sin (\phi) \quad (II-3)$$

The transport equation will be discretized into a system of equations, each describing the flux over an element of angle. These elements of solid angle are like wedges or cones which together form the unit sphere of solid angle. The angular mesh used here is similar to a product quadrature set, and is formed by dividing the polar and azimuthal coordinates, independently, into segments. This is perhaps most easily visualized as a partitioning of the surface of a globe along lines of latitude and of longitude. This partition maps as a rectangular mesh on the (τ, ϕ) plane, where the weight of an element is proportional to its area. The element weight can also be expressed as the product of the τ -weight and the ϕ -weight:

$$W_{k,l} = \int_{D_m} \sin (\theta) d\theta d\phi / 2\pi = \Delta\tau_k \Delta\phi_l / 2\pi \quad (II-4)$$

where D_m is the domain of angle of the m 'th discrete element and where the normalization factor is 2π rather than 4π , since only the upper hemisphere of directions need be considered (due to the z -symmetry of xy -geometry). Except where explicitly needed, the indices, k and l , will be expressed as a single index, m , ranging from 1 to M .

B. Discretization of the (Angular) Flux

In order to discretize the the transport equation, it is useful to first treat the flux, $\psi(x,y,\tau,\phi)$. The flux may be considered as a union of M functions, $\psi_m(\tau,\phi)$, each over a domain restricted to a single angular mesh cell, D_m , of area W_m . One reason for doing this is that these functions could be approximated by a truncated power series expansion. This representation of the flux as a piecewise polynomial is similar to a finite elements method approach. Differences are (1) finite elements typically uses basis elements which overlap in support and (2) finite elements typically uses differentiability constraints, resulting in coupling among the discretized equations, and thus requiring the assembly of global matrices and solution of linear algebra problems. The discrete elements method, however, uses basis elements that are discrete in domain (non-overlapping) and does not require differentiability, or even continuity, at the boundaries between elements, thus avoiding the complications and computational difficulties of finite elements.

Each flux, ψ_m , can be characterized by its angular moments. The zeroth and first moments are central to the discrete element method. Notation for these flux moments is defined as follows:

$$F_m = (1/W_m) \int_{D_m} \psi(\tau,\phi) d\hat{\Omega} \quad (\text{II-5})$$

$$J_m = (1/W_m) \int_{D_m} \hat{\Omega} \psi(\tau,\phi) d\hat{\Omega} \quad (\text{II-6})$$

where the directional unit vector, $\hat{\Omega}$, is defined as

$$\hat{\Omega} = \mu \hat{i} + \eta \hat{j} + \tau \hat{k} \quad (\text{II-7})$$

F_m may be physically interpreted as the average flux of particles traveling in directions which fall within the m 'th element of solid angle. Similarly, the vector quantity, $\hat{\Omega}\phi(\hat{\Omega})$, is a (directionally dependent) current. It bears the same relationship to the (scalar) current vector, \underline{J} , of diffusion theory as does the (directional) flux of transport theory to the (scalar) flux of diffusion theory. Thus, \underline{J}_m is the average current vector for the m 'th element of solid angle.

C. Discretization of the Transport Equation

The transport equation is usually written in the form

$$\hat{\Omega} \cdot \nabla \psi + \sigma \psi = c \sigma \phi + S \quad (\text{II-8})$$

where $c = \sigma_s / \sigma_t$ and ϕ is the scalar flux. Since the current is physically meaningful, as discussed in the previous section, the first step in the discretization is to bring the unit direction vector back inside the divergence operator:

$$\nabla \cdot (\hat{\Omega} \psi) + \sigma \psi = c \sigma \phi + S \quad (\text{II-9})$$

In order to discretize this transport equation, it is averaged over each element of solid angle. More precisely, the zeroth angular moment of the equation is taken, over the domain D_m , and normalized by the weight, W_m :

$$\frac{1}{W_m} \int_{D_m} \nabla \cdot (\hat{\Omega} \psi) d\hat{\Omega} + \frac{1}{W_m} \int_{D_m} \sigma \psi d\hat{\Omega} = c \tau \phi + S \quad (\text{II-10})$$

Since the spatial divergence and angular moment operators apply to independent variables, the divergence operator may be taken outside the integral. Recalling the definitions of F_m and \underline{J}_m , the result is

$$\nabla \cdot \underline{J}_m + \sigma F_m = c \sigma \phi + S \quad (\text{II-11})$$

Two simplified forms of this equation are convenient. In a vacuum, it reduces to

$$\nabla \cdot \underline{J}_m = S \quad (\text{II-12})$$

and otherwise, since the cross-section is non-zero, it may be written

$$\frac{1}{\sigma} \nabla \cdot \underline{J}_m + F_m = Q \quad (\text{II-13})$$

where Q is the effective source term, with dimensions of flux, defined as

$$Q = c \phi + \frac{S}{\sigma} \quad (\text{II-14})$$

The scalar flux is eliminated from this system of equations by expressing it in terms of the F_m :

$$\phi = \int_{4\pi} \psi \, d\hat{\Omega} = \sum_m W_m F_m \quad (\text{II-15})$$

Thus

$$Q = \frac{S}{\sigma} + c \sum_m W_m F_m \quad (\text{II-16})$$

Equations (II-16) and (II-13), or (II-12) in vacuum, are the discrete elements equations. These equations are exact, which is to say that no approximations have been made yet. If they were solved analytically, the exact scalar flux and current would be obtained, although the directional flux, ψ , would not be fully specified. Approximations to the second or higher angular flux moments could be devised, but the first moment is determined exactly by

$$\underline{J} = \sum_m w_m \underline{J}_m \quad (\text{II-17})$$

Although equation (II-16) assumes isotropic scatter, equation (II-17) could be used to include linearly anisotropic scatter in a straightforward manner. For simplicity in implementing and evaluating the discrete elements method, isotropic scatter is assumed.

D. The Flux-Weighted Mean Angle

The discrete elements equations appear very much like the discrete ordinates equations. In fact, if an assumption were made that the discrete fluxes and currents were related by $\underline{J}_m = \hat{\Omega}_m F_m$ where the direction (or "ordinate"), $\hat{\Omega}_m$, is a fixed direction established by the choice of angular quadrature set, then the discrete elements equations would reduce to the discrete ordinates equations. Without this assumption, the relationship of \underline{J}_m and F_m defines the element mean streaming direction to be

$$\hat{\Omega}_m = \underline{J}_m / F_m \quad (\text{II-18})$$

Substituting equations (II-5) and (II-6), and canceling the weights, w_m ,

$$\hat{\Omega}_m = \frac{\int_{D_m} \hat{\Omega}(\hat{\Omega}) d\hat{\Omega}}{\int_{D_m} \psi(\hat{\Omega}) d\hat{\Omega}} \quad (\text{II-19})$$

The components of $\hat{\Omega}_m$ are designated by θ_m , ϕ_m , μ_m , η_m , and τ_m . Equation (II-19) shows $\hat{\Omega}_m$ to be the element flux-weighted mean angle. If these angles were somehow known, then the well-developed techniques for solving the discrete ordinates equations could be used to solve the discrete elements equations. Numerical methods of approximating the $\hat{\Omega}_m$ are considered next.

E. Approximating the Flux-Weighted Streaming Directions

The flux-weighted mean angles, $\hat{\Omega}_m$, are approximated by using numerical quadrature rules to approximate the integrals in equation (II-19). Separation of variables in (τ, ϕ) coordinates is assumed within each discrete element, and the integrals in the two coordinates are done independently. Thus, for each element, there is a flux-weighted mean τ_m , and a flux-weighted mean ϕ_m :

$$\tau_m = \frac{\int_{D_m} \tau \psi(\tau) d\tau}{\int_{D_m} \psi(\tau) d\tau} \quad (\text{II-20})$$

$$\phi_m = \frac{\int_{D_m} \phi \psi(\phi) d\phi}{\int_{D_m} \psi(\phi) d\phi} \quad (\text{II-21})$$

These one-dimensional integrals are then approximated by a quadrature rule, e.g. Simpson's rule. The application of Simpson's rule requires knowledge of the flux in three fixed directions distributed in azimuth and three fixed directions distributed polarly, within each element. Figure II-1 shows these fixed "auxiliary" directions, labelled as north, south, east, west, and center. This nomenclature is chosen to be analogous to the sides of a rectangle of latitude and longitude on the surface of a globe, eastward being increasing ϕ , and northward being increasing τ .

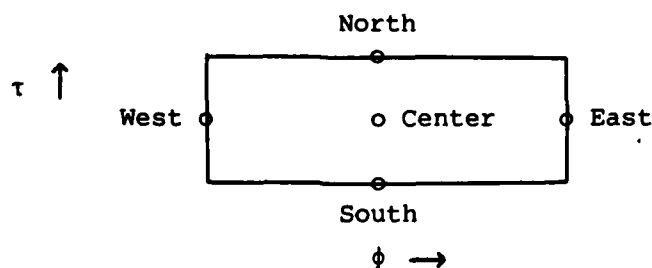


Fig. II-1: Discrete Element Auxiliary Directions for Simpson's Rule

These directions are fixed by the choice of the discrete element angular mesh and the choice of Simpson's rule. The flux in these fixed directions therefore obeys the discrete ordinates transport equations and may be calculated using conventional S_N spatial quadrature. The source term for these auxiliary calculations is the same Q as is used in the discrete elements equations. The algorithm for this method is considered in the next section.

First, an alternative view of this approximation scheme is considered. If the flux is expanded in a Taylor's series (in angle) about the element center, (τ_0, ϕ_0) , it is expressed as a series in powers of $(\tau - \tau_0)$ and $(\phi - \phi_0)$. Retaining terms through quadratic, including the

bilinear term, and performing the integrations in equation (II-19) analytically, it may be shown that the bilinear term vanishes from both integrals. (Thus, the assumption of separability is actually required only if terms higher than quadratic are retained.) The use of Simpson's rule is equivalent to finding a quadratic flux which equals the calculated fluxes at the five auxiliary directions and exactly evaluating the flux-weighted mean streaming direction for that flux.

F. The Discrete Elements Method Algorithm

The discrete elements algorithm is based as closely as possible upon that used in discrete ordinates. The essential feature of S_N is the separation of the angular and spatial quadratures in an iterative scheme. The source term, Q , is assumed known (from the previous iteration, or by a guess), and the spatial quadrature is performed as a walk through a mesh of space cells, using the fixed directions of the angular quadrature set. As the directional fluxes are found, they are folded into a new scalar flux at each point, thus performing the angular quadrature to get an improved scalar flux. After the spatial walk is completed, the source term, Q , is updated in preparation for the next iteration. This scheme minimizes storage requirements so that real engineering problems can be fit into the computer. The discrete elements algorithm retains this structure, with its computational advantages, but adds the steps necessary to approximate the (no longer fixed) streaming directions and use them in the spatial quadrature of the element fluxes, F_m . Once the streaming direction is found, the spatial quadrature of F_m uses the same methods as in S_N .

The discrete elements iterative scheme is:

1. Perform space quadrature in fixed directions to get auxiliary directional fluxes.
2. Perform angular quadrature within each element of angle to obtain the steered $\hat{\Omega}_m$
3. Perform space quadrature in the (adjusted) directions to get discrete element ("main") directional fluxes.
4. Accumulate the (weighted) main fluxes to get the scalar flux at each space cell.
5. Update the source term, Q , and return for next iteration, if the results are not yet converged.

The actual algorithm combines steps 1 through 4 in order to minimize storage requirements, as follows:

Repeat

For each angular element

For each space cell

1. Step the associated auxiliary fluxes across the cell
2. Find the mean direction for the main flux
3. Step the main flux across the cell
4. Accumulate the contribution to the scalar flux in the "new-flux" array

Next space cell

Next angular element

For each space cell

1. Test for convergence
2. Update the "old" scalar fluxes to the "new"
3. Re-evaluate the source, Q , for the cell

Next space cell

Until convergence criteria are met.

G. Summary

The discrete elements equations and algorithm have been developed in this chapter. The method is similar to a finite elements method in that the flux is represented by piecewise polynomial functions. The advantages of finite elements may be expected, specifically, better performance for problems with strong local sources and absorbers, since the resulting ill-behaved flux functions are better approximated by the piecewise basis. Unlike the finite elements method, however, the elements are discrete and are solved by an iterative spatial and angular mesh walk rather than simultaneously with matrix algebra. In this respect, the method retains the practicality of the discrete ordinates method. Unlike S_N , however, the spatial and angular quadratures are explicitly coupled through the flux-weighted mean streaming angles. In effect, this coupling steers the streaming in the average directions of particle flow and should strongly ameliorate the ray effects caused by using fixed streaming directions in S_N .

Before the L_N method can be implemented and evaluated by comparison with S_N , the details of the angular and spatial quadrature methods must be filled in. Chapter III covers angular quadrature: choice of streaming directions and weights in S_N , and choice of angular mesh in L_N . Chapter IV covers the angular quadrature used within each element to evaluate the mean streaming direction. Chapter V presents the spatial quadrature methods used to step the fluxes across each spatial grid cell. Chapter VI considers the interaction of the spatial and angular discretized quadratures and the inherent deficiencies of discretization, such as ray effect.

III. Angular Quadrature in the S_N and L_N Methods

In the discrete ordinates method, a quadrature set is a set of directions, $\hat{\Omega}_m$, and weights, w_m , used to approximate angular integration by the following quadrature rule:

$$\int_{D_m} f(\hat{\Omega}) d\hat{\Omega} \approx \sum_m w_m f(\hat{\Omega}_m) \quad (\text{III-1})$$

where $f(\hat{\Omega})$ is any function, for example, ψ . If equation (III-1) is exact for $f(\hat{\Omega}) = \mu^n$, then the quadrature set is said to match the n 'th angular moment (with respect to the x -axis, in this case). This chapter reviews some of the quadrature sets proposed or in use for S_N , and defines quadrature sets for use in one- and two-dimensional (slab and xy) geometry with the L_N method.

A. Global Basis Functions and Gaussian Quadrature

S_N conventionally uses quadrature sets which match as many angular moments of the integrand as possible. (Various symmetry constraints are usually imposed, as well.) If the integrand is well-behaved, in that it has high orders of differentiability, then it can be expanded in a power series in the direction cosines. The quadrature set then integrates, exactly (or nearly exactly), as many of the terms as possible. Gaussian quadrature is an example in one dimension. This works well if the flux is well represented by a truncated power series in the direction cosines. An alternative approach is discussed next.

B. Local Basis Functions and Composite Quadrature

L_N models the flux with piecewise low order polynomials in one or two angular coordinates, τ and/or ψ . These are integrated by low-order methods such as Simpson's rule. The summation of the integrals over the pieces constitutes a composite quadrature. If the integrand of a composite integration is actually well-behaved, the composite integration works well, although a Gaussian would be more cost effective. But, if the integrand is ill-behaved (in that its low-order derivatives are small but its high-order derivatives are large or unbounded), the composite rule improves in accuracy as more subintervals are used, while Gaussian quadrature may become less accurate as more points are used.

C. Behavior of the Directional Flux in Heterogeneous Problems

A difficulty encountered in transport problems is that the flux, as a function of angle, can be rapidly varying (nearly discontinuous), and that the discontinuities can exist at angles that are not necessarily parallel to material interfaces. As an example, consider the flat control rod in an otherwise homogeneous reactor shown in figure III-1. Suppose that for some energy group, the neutron mean free path is large compared to the width of the control rod, but that the rod is strongly absorbing. Then the flux at point "A" is fairly uniform, except in those directions for which particles would have to have penetrated the rod. In these directions, the flux is depressed. The flux is rapidly varying with azimuthal angle for the direction coming from the edge of the control rod. Because of this type of ill behavior, composite angular quadrature may outperform global quadrature in those kinds of problems

where transport methods are most needed. Some global quadrature sets are more successful in handling this difficulty than others. Some of these quadrature sets will be covered next.

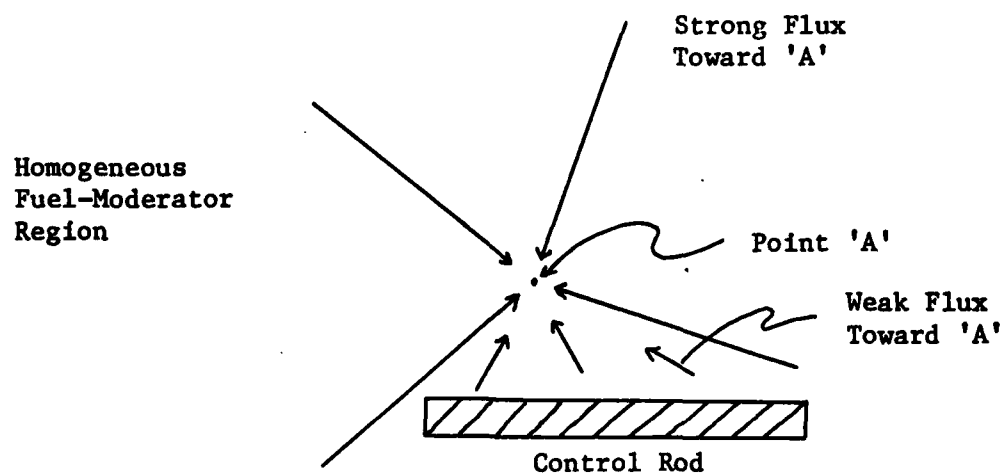


Fig. III-1: Example Problem: Homogeneous Reactor with Control Rod

D. Totally Symmetric Quadrature Sets (S_N) and Related Types

Lathrop and Carlson developed a family of quadrature sets which meet various symmetry constraints and use the remaining degrees of freedom to match angular moments. [Ref. 9 is perhaps the most useful of many available references on the subject.] The most popular of these is the totally symmetric quadrature sets. These are the sets implied if the term " S_N " is used without qualification as to quadrature set. They provide symmetry under interchange of any pair of axes, under 90-degree rotation about any of the three (x, y, and z) axes, and under reflection through any cardinal (xy, yz, zx) plane. These constraints ensure that the results computed for a problem will not depend on the choice of assignment of axis labels, clearly a physically desirable property.

However, these symmetries are of more importance in three dimensional transport than in the two dimensional cases of concern here. The interchangeability of the x and z axes, for example, is a waste of degrees of freedom that could better have been used matching moments, for example. Lathrop [Ref. 8] has shown that the totally symmetric quadratures are very prone to ray effect, and has proposed a rotationally symmetric quadrature which reduces ray effect. This set is discussed below, along with other product quadratures.

E. Product Quadrature Sets

Product quadrature sets are formed as the product of independent quadrature sets in τ and ϕ , such that $\hat{\Omega}_{k,l} = (\tau_k, \phi_l)$ with weight $W_{k,l} = W_{\tau k} W_{\phi l}$ and with k ranging from 1 to K and l from 1 to L.* Product quadratures of this type are particularly appropriate for use in two dimensional (xy) geometry, since they relax the x,z and y,z interchange symmetries, but (usually) retain the x,y interchange symmetry, as discussed above. The example in figure III-1 showed that the flux can be ill-behaved in azimuth. However, variations in polar angle (for any fixed azimuthal direction) result only in smooth variations in flux due to the z-symmetry of these problems. In a sense then, the polar quadrature is an easier problem than the azimuthal quadrature. Product quadrature sets allow the apportionment of more computational effort to the latter and less to the former. Some specific product quadratures are described below.

* The set is usually only specified for the principal octant, where all three direction cosines are positive. The other octants are defined by reflections of the principle octant. Since only the $\tau > 0$ hemisphere is used in xy-geometry, the total number of directions in the product quadrature set is 4KL.

1. Single Range Quadrature

Single range quadrature assumes continuity and differentiability of the flux throughout the (τ, ϕ) plane and implicitly represents the flux as a single polynomial in τ , $\sin(\phi)$, and $\cos(\phi)$ over the entire domain. Lathrop and Carlson developed product quadrature sets using Gauss-Legendre quadrature for τ in the range $(-1,1)$ and Gauss-Chebyshev quadrature in azimuth [Ref. 9]. They reported improved calculation of critical radii in cylindrical coordinates, compared to conventional S_N . However, this scheme is closely related to a P_N type flux representation, and shares its inability to exactly represent vacuum boundary conditions. Yvonne's method, DP_N , uses a double range Gaussian quadrature (in one dimensional problems) to correct this deficiency. In two dimensional discrete ordinates, the analogue to this approach is the use of multiple range quadrature sets.

2. Multiple Range ($S_{KG,LQ}$) Quadrature

Recently, Abu-Shumays has developed a Gauss-Christoffel quadrature in $\sin(\theta)$ over the range $(0,1)$ {i.e. θ in $(0, \pi/2)$ } [Ref. 2]. This is a double-range polar quadrature which takes advantage of the xy-plane mirror symmetry of the problems considered here. He also developed three forms of quadruple-range azimuthal quadrature, one of which retains xy-interchange symmetry. This azimuthal quadrature is defined for ψ in the range $(0, \pi/2)$ and extended to the other quadrants by reflection through the xz- and/or yz-plane. It can exactly represent vacuum and material interface boundaries oriented parallel to these planes. The combined Gauss-Christoffel polar / symmetric quadruple-range azimuthal quadrature has demonstrated excellent performance in reducing ray effect.

Based on Abu-Shumays findings, discrete ordinates results obtained with the combined Gauss-Christoffel / symmetric quadruple-range quadrature are here assumed to be the best of the available Gaussian-type S_N results and are used for comparison with the L_N results. The notation used to designate this quadrature is $S_{KG,LQ}$ indicating K latitude lines with Gauss-Christoffel spacing and weights, each with L azimuthal points per quadrant with quadruple-range spacing and weights.

3. Rotationally Symmetric Azimuthal ($S_{KG,LR}$) Quadrature

Lathrop [Ref. 8] suggested the possibility of using product quadrature with equally weighted directions equally spaced in azimuth. Such a quadrature set is invariant under rotations about the z-axis by angles which are multiples of the azimuthal spacing. For any choice of L, this provides the maximum rotational symmetry. This quadrature reduced ray effect compared to conventional sets. Not only does it better model the rotational symmetry of the integro-differential transport equation, as Lathrop observed, but it also has the advantages of a local basis representation for ill-behaved fluxes. This latter point is a consequence of the fact that the rotational quadrature set is equivalent to a composite quadrature using the midpoint rule. S_N with rotational quadrature is thus a degenerate case of the discrete elements method where the element angular quadrature is performed by the midpoint rule. The notation used to designate discrete ordinates with this quadrature is $S_{KG,LR}$, indicating K latitude lines with Gauss-Christoffel spacing and weights, each with L azimuthal points per quadrant, equally spaced and weighted.

Lathrop abandoned the rotational quadrature sets with the observations that they reduce but do not eliminate ray effect and that they require more directions for the same number of latitudes than the standard sets: "256 vs 144 for $N = 16$ " [Ref. 8:258]. This implicit assumption of the need for a square mesh is not really necessary, however. It may be that only a few latitudes, with Gauss-Christoffel quadrature, will provide accurate polar quadrature, allowing the use of a relatively fine azimuthal mesh. From the data presented in reference 8, it appears that an $S_{2G,8R}$ solution (16 directions/octant) has less ray effect than an S_{16} solution (36 directions/octant) at 44% of the cost. An $S_{3G,8R}$ would improve the accuracy of polar quadrature, with similar ray effect and still have only 67% of the cost. For this reason, S_N results using the combined Gauss-Christoffel / rotationally symmetric quadrature are used for comparison with L_N results obtained with the analogous quadrature.

F. Discrete Elements Composite Quadratures

The discrete elements method uses composite quadratures in which the choice of a quadrature set entails the specification of the arrangement and weights of the elements, subject to the constraint that the set of elements tile the (τ, ϕ) plane. Both one-dimensional (slab) and two dimensional (xy) test cases are used in evaluations of the discrete elements method. The quadrature sets used are described below.

1. One-dimensional Equal Weight (L_N) Quadrature

In one space dimension (slab geometry), the angular coordinates are oriented so that the problem is symmetric in azimuth. Therefore, only polar quadrature need be considered. The simplest scheme

is to divide the range of $\tau(-1,+1)$ into N equal intervals, as is usually done in composite numerical integration. The error bound for the quadrature over each element is proportional to the width of the interval (i.e. the element weight) raised to a power determined by the element quadrature rule. For example, with Simpson's rule the error is proportional to W^5 . Hence, using equal weights tends to minimize the sum of the errors over the set of elements. Another advantage is discussed in reference to diffusion limit considerations, below.

2. One-dimensional Gaussian Weight (L_{NGW}) Quadrature

A feature of the Gauss-Legendre quadrature for one-dimensional S_N is that it biases the placement of directions towards the poles, i.e., forward and backward through the problem, and puts reduced emphasis upon the equatorial (sideways) directions. A composite quadrature set which uses elements unequal in size, such that the element weights are those of the Gauss-Legendre ordinates, would retain this feature. It may be conjectured that good resolution in the polar fluxes is more important than for the equatorial fluxes, so that a "Gauss-like" composite quadrature might prove more effective than an equal weight composite quadrature. Gaussian weight composite quadrature is used to test this conjecture.

3. Equal Weight Composite Product ($L_{K,L}$) Quadrature

For two-dimensional (xy) problems, the discrete elements method, as derived in section III-C, uses composite product quadrature. Although any collection of rectangular elements which tiles the (τ,ϕ) coordinate plane could be employed, a division into discrete elements of equal area is most natural. The advantages of this quadrature are that uniform weights minimize the sum of the error terms and that the set

most nearly meets the diffusion limit criteria, as explained below. This quadrature set also retains the advantage of rotational symmetry in modeling the rotational symmetry of the Boltzmann transport equation and could be used for three-dimensional problems.

G. Hybrid Gauss-Christoffel/Composite ($L_{KG,L}$) Quadrature

In two-dimensional problems, as observed above, the flux is well-behaved with respect to τ , but may be ill-behaved with respect to ϕ . Consequently, a hybrid quadrature scheme is proposed. This scheme uses Gauss-Christoffel quadrature in the polar variation and equal weight discrete elements for the azimuthal quadrature. The fixed latitudes of the polar quadrature take advantage of the well-behaved character of the flux to provide the accuracy of a high order global quadrature, while the equal weight composite quadrature accommodates the potential ill-behavior of the flux. This method provides the advantage of coupled angular and spatial quadrature to steer the flux, but only in azimuth. However, steering in azimuth should suffice to reduce ray effect. Since fewer auxiliary fluxes are required, none being needed for polar steering, the method would be more cost effective than the $L_{K,L}$ quadrature, if it were at least as accurate.

H. Diffusion Limit Considerations

Although numerical transport methods are needed for accurate flux determinations where diffusion theory does not apply, it is desirable that the numerical method produce the same result as diffusion theory for problems where diffusion theory is valid. A numerical method which does this is said to satisfy the diffusion limit.

A discrete ordinates quadrature set which meets the criteria enumerated below will satisfy the diffusion limit. This can be shown by assuming that the flux is of the form $\psi(\hat{\Omega}) = \phi + \hat{\Omega} \cdot \underline{J}$. Then, in the limit of small \underline{J} , discrete quadrature with a quadrature set meeting these constraints can be used in place of analytic quadrature in the derivation of Fick's law or of the diffusion equation. The criteria are:

$$\sum_m w_m = 1 \quad (\text{III-2})$$

$$\sum_m \mu_m w_m = 0 \quad (\text{III-3})$$

$$\sum_m \eta_m w_m = 0 \quad (\text{III-4})$$

$$\sum_m \mu_m \eta_m w_m = 0 \quad (\text{III-5})$$

$$\sum_m \mu_m^2 w_m = 1/3 \quad (\text{III-6})$$

$$\sum_m \eta_m^2 w_m = 1/3 \quad (\text{III-7})$$

The physics behind these constraints is of interest. Equation (III-2) assures conservation in that the calculation of ϕ (hence of Q) will not lose or invent particles. Equations (III-3) and (III-4) serve the same purpose with respect to current. If the directional flux is isotropic, for example, they ensure that the current components, J_x and J_y , respectively, are properly computed as zero. Equation (III-5) causes cross product terms to vanish from the diffusion equation; the last two constraints produce the factor of 1/3 in the diffusion coefficient.

In the limit of isotropic flux, the flux-weighted element streaming directions go to the element center directions and the discrete elements

method becomes equivalent to a discrete ordinates method with those directions and weights as its quadrature set. The $L_{KG,L}$ becomes, in this degenerate case, $S_{KG,LR}$, for example. It is desirable for the discrete element quadrature sets to meet the diffusion limit.

All the (xy-geometry) quadrature sets described in this chapter, and used in this report, are constructed by specifying the set on the primary octant and filling in the other octants by reflection. Therefore, they have mirror symmetry through the yz-plane, which ensures equation (III-4) is satisfied, and through the xz-plane, for equation (III-3). Either of these two symmetries, alone, is sufficient to satisfy the cross-product constraint, equation (III-5). The conservation constraint is met by proper normalization of the weights. All of the sets used here are symmetric about $\phi = \pi/4$ and so are invariant under interchange of the x and y axes. Thus, if either of equations (III-6) and (III-7) are met, then so is the other. The standard S_N quadrature sets, and the $S_{KG,LQ}$ sets (for $K>1$) satisfy enough moment conditions to ensure satisfying equations (III-6) and (III-7). These quadratures satisfy the diffusion limit exactly.

An advantage of the Gauss-Christoffel polar quadrature (upon which Abu-Shumays did not remark, in Ref. 2) is that it satisfies the diffusion limit exactly, for $K>1$, when used with any azimuthal quadrature with the symmetries described in the previous paragraph. This is because, in equation (III-6), $\mu_m^2 = \cos^2(\phi) \sin^2(\theta)$ and the symmetry about $\pi/4$ allows the quadrature points to be arranged in pairs with complementary azimuths. Then the identity $\sin^2(\phi) + \cos^2(\phi) = 1$ causes the choices of azimuths and weights to drop out of equation (III-6). As a result, the Gauss-Christoffel polar / rotationally symmetric

azimuthal quadrature, $S_{KG,LR}$ and the corresponding discrete elements quadrature, $L_{KG,L}$ both satisfy the diffusion limit exactly.

The $L_{K,L}$ quadrature (considered as a fixed quadrature set) does not meet the diffusion limit exactly. For the reasons given in the last paragraph, the summation in equation (III-6) is independent of the azimuthal points and depends only on the choice of K . It reduces to

$$(1/K) \sum_k \sin^2(\theta_k) = (1/K) \sum_k (1-\tau_k^2) \quad (\text{III-8})$$

where

$$\tau_k = (2k-1) / (2K) \quad (\text{III-9})$$

which can be solved to obtain

$$\sum_m \mu_m^2 w_m = \frac{1}{3} [1 + 1/(8K^2)] \quad (\text{III-10})$$

In practice, equation (III-6) need not be met exactly, but the method will perform poorly under some circumstances if the summation differs from $1/3$ significantly. In this case, the method converges rapidly to $1/3$; for K as small as 2, the error is only about 3%, even if the quadrature set is used with discrete ordinates. The composite quadrature of the discrete elements method further reduces this error. Consequently, for practical purposes, the diffusion limit is met. Similar arguments can be made for the one-dimensional quadrature, L_N , for which the summation is given by $\frac{1}{3} (1 - 1/N^2)$. Also, it can be shown that these equal weight schemes are closest to meeting the diffusion limit, in that, if the weight of one element is increased and that of another correspondingly decreased, the approximation to $1/3$ is less accurate.

I. Summary

For xy-geometry, there are two natural choices of quadrature for the discrete elements method. With steering of the streaming angles in both polar and azimuthal coordinates, the equal weight product quadrature, $L_{K,L}$ is used. With steering only in azimuth, the hybrid Gauss-Christoffel polar / equal weight (rotationally symmetric) azimuthal product quadrature, $L_{KG,L}$ is used.

The performance of discrete ordinates is strongly dependent upon the choice of quadrature set, and the optimum choice is problem dependent. A meaningful performance comparison between discrete elements and discrete ordinates requires comparison with several discrete elements quadratures:

1 - Conventional (Totally Symmetric) S_N

This is often a sub-optimal performer, but the production codes in current use are designed around this quadrature set, so that it is used by default. Product quadratures are awkward to use and inefficiently implemented. DOT-4.3 is an example [Ref. 12]. In a practical sense, S_N is the standard of performance.

2 - Gauss-Christoffel / Rotationally Symmetric $S_{KG,LR}$

This quadrature underlies the hybrid $L_{KG,L}$ scheme. Comparison of these two will determine, if the discrete elements method works well, whether it works because of its underlying quadrature set or because of its composite quadrature within each element.

3 - Equal Weight / Rotationally Symmetric $S_{KE,LR}$

This quadrature underlies the $L_{K,L}$ scheme and comparison would have the same benefits as in the previous paragraph. However, $S_{KE,LR}$ is never as accurate as $S_{KG,LR}$ while showing essentially the same

ray effects. These two S_N methods have equal computational cost. Therefore, comparison of $L_{K,L}$ with $S_{KG,LR}$ is reported here.

4 - Gauss-Christoffel / Quadruple Range $S_{KG,LQ}$

This is a special quadrature set, ideally adapted to the test problems used here. Comparison with this quadrature is a demanding test of the discrete elements method. It should be noted, however, that such ideal discrete ordinates quadratures are not available for many practical problems. For example, the presence of diagonally oriented absorbers, material interfaces, or vacuum ducts would invalidate the assumptions of the quadruple-range azimuthal quadrature but would not be expected to degrade the performance of discrete elements.

All the quadrature schemes considered here meet, or very nearly meet, the diffusion limit constraints, equations (III-2) through (III-7).

IV. Quadrature Rules for Discrete Element Flux Modelling

The previous chapter noted that there are many possible choices of quadrature sets for discrete ordinates. The corresponding freedom in the discrete elements method is in the choice of quadrature rule within each element. This quadrature rule determines several characteristics of the flux model: whether it is piecewise continuous or discontinuous, the order of polynomial used as the basis function within each element, and the possible range of variation of the flux-weighted streaming direction. Three quadrature rules were tested: Simpson's rule, three-point Gauss-Legendre rule, and the Newton-Cotes (five-point) rule. This chapter reviews the rules and their Taylor series error bounds and considers their relative advantages and disadvantages. Table IV-1 provides the formulas for flux-weighted mean angle, optimized for minimum computational operations. The parameter "s" in these formulas represents τ or ϕ . The mean azimuth formulas are for use with $L_{K,L}$ and $L_{KG,L}$. Corresponding mean τ formulas are used with $L_{K,L}$ and L_N .

A. Simpson's Rule

Simpson's (three-point) rule is the lowest-order scheme considered. A convenient form for use here is

$$\int_{a-h}^{a+h} f(x) dx = h [f(a-h) + 4 f(a) + f(a+h)] / 3 \quad (\text{IV-1})$$

An error bound (Taylor series residual, R) for this approximation is

$$R = - 0.000347 (\Delta x)^5 f^{(4)}(x') \quad (\text{IV-2})$$

where $\Delta x = 2h$ and x' is some point in $(a-h, a+h)$.

With Simpson's rule, the directional flux is modelled by a continuous piecewise-quadratic polynomial. Continuity is accomplished not by overlapping finite elements, but implicitly, through the use of the same auxiliary flux at the boundary of adjacent discrete elements. If the actual flux is discontinuous, or nearly so, then the model will be poor only in the element(s) in which the discontinuity(s) occur. Discontinuities at the boundaries between (directional) octants are included in this model, since the auxiliary fluxes along octant boundaries are independently computed for each octant as part of the spatial mesh walk. Consequently, vacuum boundaries parallel to principal planes can be modelled exactly by the discrete elements method, regardless of the choice of quadrature rule.

Advantages of Simpson's rule include:

- Mean streaming direction can vary over full range of the element. This could be valuable in problems with streaming ducts through shields since particles could be modelled as streaming directly down the duct, regardless of its orientation.

- Some auxiliary directions are on boundary between elements. These can be used twice, if sufficient storage is available, reducing computational cost of auxiliary fluxes.

B. Three-Point Gauss-Legendre Rule

The Gauss-Legendre (three-point) rule is of higher order than Simpson's rule, but has the same computational cost (assuming auxiliary fluxes are not reused due to storage constraints). It is the only method used here which models the flux as discontinuous piecewise polynomial. A

convenient form for use here is

$$\int_{a-h}^{a+h} f(x) dx = h [5 f(a-bh) + 8 f(a) + 5 f(a+bh)] / 9 \quad (\text{IV-3})$$

where the auxiliary flux offset factor is $b = (3/5)^{1/2}$

An error bound (Taylor series residual, R) for this approximation is

$$R = - 4.96 \times 10^{-7} (\Delta x)^7 f^{(6)}(x') \quad (\text{IV-4})$$

where $\Delta x = 2h$ and x' is some point in $(a-h, a+h)$.

Advantages of the three-point Gauss-Legendre quadrature are:

- Higher order on individual discrete elements with only slightly higher cost (no more cost than Simpson's rule if boundary auxiliary fluxes aren't reused due to memory constraints)

- Broad range of variation of mean angle, compared to two-point Gauss-Legendre, but mean angle cannot reach the edge of the element. This could interact well with spatial quadrature schemes since they are inaccurate for very small μ or η .

- The underlying model is equivalent to a piecewise-discontinuous, piecewise-quartic (fourth-order) polynomial fit to the directional flux. In this model, if any discontinuities occur at (or very near) to the boundary between elements, they may be modelled accurately, which is a potential advantage. This provides a simple way to optimize the method for problems where such discontinuities are anticipated to occur along a limited number of known directions. (Examples: hexagonally shaped or diagonally oriented absorbers, sources, or material interfaces in an otherwise rectangular system.)

C. Newton-Cotes Closed (Five-Point) Rule

The Newton-Cotes (five-point) rule is of the same order as the Gauss-Legendre (three-point) rule, and the coefficients of the error bounds are approximately equal. Newton-Cotes rule provides equivalent accuracy, but at greater computational cost due to the increased number of auxiliary fluxes needed. It is tested for use in the discrete elements method because it provides continuity at the boundaries between elements, unlike the Gauss-Legendre rule. A convenient form for use here is

$$\int_{a-h}^{a+h} f(x) dx = h [7 f(a-h) + 32 f(a-h/2) + 12 f(a) + 32 f(a+h/2) + 7 f(a+h)] / 45 \quad (\text{IV-5})$$

An error bound (Taylor series residual, R) for this approximation is

$$R = - 5.17 \times 10^{-7} (\Delta x)^7 f^{(6)}(x') \quad (\text{IV-6})$$

where $\Delta x = 2h$ and x' is some point in $(a-h, a+h)$.

The advantages are:

- Computational cost of using five auxiliary directions is offset by the fact that two of them are on the element boundaries and can be reused, as with the Simpson's rule.

- Mean streaming direction can vary over the full range of the discrete element, as with Simpson's rule, which could be beneficial in duct streaming problems, for example

- The underlying model is a continuous piecewise-quartic fit to the directional flux. The comments about the Simpson's rule model apply here, as well.

Simpson's Rule:

$$\langle s \rangle = s_0 + h \frac{f(s_0+h) - f(s_0-h)}{f(s_0+h) + 4 f(s_0) + f(s_0-h)} \quad (\text{IV-7})$$

where $h = \Delta s/2$

Gauss-Legendre Three-Point Rule:

$$\langle s \rangle = s_0 + g \frac{f(s_0+g) - f(s_0-g)}{f(s_0+g) + 1.6 f(s_0) + f(s_0-g)} \quad (\text{IV-8})$$

where $h = \Delta s/2$

$$g = (3/5)^{1/2} h$$

Newton-Cotes Five-Point Rule:

$$\langle s \rangle = s_0 + h \frac{f(s_0+h) - f(s_0-h) + c_1 [f(s_0+h/2) - f(s_0-h/2)]}{f(s_0+h) + f(s_0-h) + c_2 [f(s_0+h/2) + f(s_0-h/2)] + c_3 f(s_0)} \quad (\text{IV-9})$$

where $h = \Delta s/2$

$$c_1 = 16/7$$

$$c_2 = 32/7$$

$$c_3 = 12/7$$

Table IV-1: Flux-Weighted Mean Angle Formulas

D. Summary

The discrete element quadrature rule is used in computing the flux-weighted mean streaming direction for the element. Its only effect on the method is through this steering of particle streaming. Three quadrature rules were selected for evaluation. Simpson's rule is low order but computationally inexpensive and allows the streaming direction to be steered anywhere within the element of angle. With the same expense (three auxiliary flux calculations per element), Gauss-Legendre provides higher order and the possible advantages of a piecewise discontinuous, piecewise polynomial flux representation. Gauss-Legendre restricts the steering of the streaming angle to the center 77% of the element range (in one angular dimension), which may limit its ability to model a streaming duct, for example, but also avoids space quadrature in directions nearly parallel to the sides of the space cell, for which most space quadrature schemes have very poor accuracy. The Newton-Cotes rule uses five auxiliary fluxes per element and so is more expensive to compute. It uses a continuous, piecewise polynomial flux representation and allows the streaming direction to be steered anywhere in the element.

The above discussions of error bounds and accuracy all implicitly assume that the auxiliary fluxes ($f(s_0)$, etc.) are exact. However, they are calculated by numerical means, discrete ordinates spatial quadrature. The errors in the data for the quadrature rules, as it were, may well dominate their performance. The results of numerical experimentation are reported in later chapters. The spatial quadrature methods employed here are discussed in the next chapter.

V. Spatial Quadrature Methods

The research reported in this dissertation is primarily concerned with two-dimensional Cartesian (xy) geometry, although the special case of one-dimensional Cartesian (slab) geometry is also considered. The discrete element method uses the same spatial integration methods as the discrete ordinates method; therefore, these spatial methods are reviewed in this chapter.

A. One-Dimensional (Slab) Spatial Quadrature

Four methods of one-dimensional spatial quadrature were evaluated in this study: step, diamond difference (with negative flux fixup), step characteristic, and linear characteristic. Several recent papers have concerned these methods. Alcouffe, et al. [Ref. 3], proposed the linear characteristic (L.C.) method and reported excellent performance, in comparison with other methods, based on numerical testing. Larsen and Miller [Ref. 6] evaluated the convergence (vs. space cell size) of these methods, as did Lee and Vaidyanathan [Ref. 11]. The concepts behind the methods, their formulas, and some of their advantages and disadvantages are summarized below.

1. Coordinates and Symbols

In the one-dimensional coordinate system, x is the space coordinate; the angular coordinates are rotated (compared to xy geometry) such that θ is the angle with respect to x , and μ is the x

direction cosine ($\mu = \cos(\theta)$). For convenience in computer implementation, let F_{in} be the directional flux entering the space unit cell of width Δx and F_{out} be that leaving. This convention allows the use of the absolute value of μ and requires that the program explicitly keep track of whether F_{in} represents F_{left} and F_{out} represents F_{right} (for positive μ , i.e., for right-bound particles) or vice versa (for negative μ , i.e., for left-bound particles). Using this scheme, the spatial quadrature method need only consider positive directions. Negative directions are handled as the reflection of positive ones. With this notation, the transport equation to be solved is:

$$\mu \, dF/dx + \sigma F = \sigma Q \quad (V-1)$$

where:

$$\sigma = \sigma_{total} \quad (V-2)$$

$$c = \sigma_{scatter} / \sigma_{total} \quad (V-3)$$

$$Q = c \Phi + S/\sigma \quad (V-4)$$

The effective source parameter, Q , has dimensions of a directional flux, and is physically significant as the value the flux asymptotically approaches as $\mu \rightarrow 0$. Defining Q in this way is computationally convenient and efficient, as well as physically meaningful, and is consistent with the usage in chapter II.

2. Balance Equation

The balance equation is a conservation relation among the cell-edge and cell-average fluxes obtained by integrating equation (V-1) across a space cell:

$$\mu(F_{\text{out}} - F_{\text{in}}) / \Delta x + \sigma F_c = \sigma Q_c \quad (\text{V-5})$$

where F_c is the cell average flux and σQ_c is the cell average effective source. (The subscript on Q will be omitted, except where necessary to avoid ambiguity.) The cell optical thickness, ϵ , is the parameter defined as

$$\epsilon = \sigma \Delta x / \mu \quad (\text{V-6})$$

Using this parameter, the balance equation becomes

$$(F_{\text{out}} - F_{\text{in}}) / \epsilon + F_c = Q \quad (\text{V-7})$$

3. Conservation Considerations

Conservation of particles is assured if two conditions are met. First, the spatial quadrature scheme must be based upon the (exact) balance equation, regardless of any approximate auxiliary relations it assumes. This condition ensures conservation of particles inside each spatial mesh cell. All the spatial quadratures used here meet this condition. Secondly, particles must be conserved in crossing the interfaces between cells. In the discrete ordinates method, this is achieved by using the flux out of one cell as the flux into the next cell. More precisely, it is the component of current in the direction normal to the face of the cell which must be carried unchanged across the cell boundaries. In one dimension, this current is $J_x = \mu_m F_m$. In the discrete ordinates method, the directions, μ_m , are fixed so that continuity of flux across the cell interfaces is sufficient.

In the discrete elements method, this same logic applies to the auxiliary fluxes, whose directions are fixed. However, the main fluxes in the discrete element method use steered streaming directions which are not fixed (which is the major objective of discrete elements). Conservation is accomplished in the same two steps. Within each space cell, the streaming angle for each element is assumed to be constant. It may have a different value after each iteration, but while the spatial quadrature is performed, the flux-weighted streaming directions are treated as fixed. This assures conservation within each space cell, since the explicitly conservative spatial quadrature methods are used, as in S_N . Conservation across cell interfaces is achieved by explicitly using the normal current out of one cell as the normal current into the next cell. Since the streaming directions are discontinuous across cell interfaces, so are the fluxes, but in just such fashion as to maintain continuity of the current. Consequently, there are two physically meaningful results computed by the method, the cell-average fluxes and the cell-boundary currents.

4. Step Method

The step method assumes that the flux is constant across each space cell, with discontinuities at the inbound edges. This is equivalent to assuming the auxiliary relation:

$$F_c = F_{out} \quad (V-8)$$

This leads to a solution of the balance equation:

$$F_c = F_{out} = Q \epsilon / (1 + \epsilon) + F_{in} / (1 + \epsilon) \quad (V-9)$$

This solution has several computational advantages. The coefficients of Q and F_{in} are in the range (0,1) for all possible optical thicknesses. Therefore, the numerical method which uses these coefficients is stable and absolutely convergent. The method is positive, in that, for any positive inputs (Q and F_{in}), the computed fluxes are positive; hence, no negative flux "fixup" is required. Positive methods also have the benefit of producing solutions which vary smoothly from cell to cell across the space mesh. Finally, there are no special cases, so that no if-tests are required. This combines with the computational simplicity of equation (V-9) to make the method extremely fast.

The disadvantage of this method is its poor accuracy, which requires a prohibitively fine space mesh to provide usable results for most purposes. Since the method is smooth and positive, it may be adequate for computing the auxiliary fluxes used in steering the streaming directions. For that application, only relative levels are important, as is seen from the form of equations (II-20) and (II-21).

5. Diamond Difference

The diamond difference method assumes that the flux varies linearly across the space cell. Thus, the cell-average flux is approximated by the average of the cell-edge fluxes. This is equivalent to the familiar "diamond difference" approximation for numerical differentiation and gives the auxiliary relation:

$$F_c = (F_{out} + F_{in}) / 2 \quad (V-10)$$

This combines with the balance equation to give a solution:

$$F_{out} = Q \frac{2\epsilon}{(2 + \epsilon)} + F_{in} \frac{(2 - \epsilon)}{(2 + \epsilon)} \quad (V-11)$$

F_c is then computed directly from the auxiliary equation.

This method has several advantages. It is numerically stable and absolutely convergent; the coefficients of F_{in} and Q in the explicit solution for F_c lie in the range $(-1, +1)$, since the optical thickness is positive. As in the step method, the calculations are simple and no if-tests are required. This method is substantially more accurate than the step method, and is easily generalized to curvilinear geometries, as with cylindrical or spherical coordinates.

The diamond difference method, however, is not a positive method. It may predict negative fluxes, which are not physically reasonable. Relatively fine space meshes are needed to avoid negative fluxes. The calculation of space-integral quantities, such as total absorption rates, is insensitive to the presence of a few negative fluxes; but the pointwise values, such as scalar flux as a function of position, tend to be oscillatory and inaccurate. These inaccuracies impair its usefulness for computing the auxiliary fluxes, but it may be adequate for the main fluxes of the discrete elements method.

6. Negative Flux Fixup for the Diamond Difference Method

In order to avoid the (conceptually disconcerting) negative fluxes, a fixup scheme is often employed. This is done by computing F_{out} using the normal diamond difference equations, as shown above. If the result is negative, however, it is (arbitrarily) set to zero. This new auxiliary relation ($F_{out} = 0$) is substituted into the balance equation,

which is then solved for F_c :

$$F_c = Q + F_{in} / \epsilon \quad (V-12)$$

The advantage of this scheme is that the pointwise fluxes are more reasonable, while the space-integral values are nearly as accurate as before, assuming the fixup is invoked only infrequently.

The disadvantage of the fixup is that the numerical method becomes nonlinear and convergence is no longer assured. An oscillatory instability can result wherein the fixup is required on one iteration, but the fixed-up flux avoids the need for the fixup on the next iteration, yet that un-fixed-up flux requires the fixup on the subsequent iteration, etc. This can happen if the fixup is required too frequently, which is sometimes the case for realistic problems.

7. Considerations Regarding the Use of Fixups

There are two schools of thought regarding the use of negative flux fixups. One viewpoint is that the fixup degrades integral values and should not be used. Negative fluxes are seen as being merely inaccurate numerical representations of the (correct) positive values. Further, the presence of too many negative fluxes is considered an indication of a need to refine the space mesh. The other viewpoint is that negative flux fixups should be used since pointwise values are improved, so long as integral values are not significantly altered by the fixup. Changes in integral values are seen as an indication of the need to refine the space mesh. Since amelioration of ray effects is an objective of this research, pointwise values are of importance, and the latter point of view is taken here.

8. Step Characteristic Method

The step characteristic method is derived by assuming streaming along the "characteristic lines" of the transport differential equation, i.e., in direction . The transport equation (V-1) is integrated analytically, with the assumption that $Q(x)$ is a constant, Q_c , across the space cell. This provides an auxiliary equation for F_{out} :

$$F_{out} = e^{-\epsilon} F_{in} + (1 - e^{-\epsilon}) Q \quad (V-13)$$

The resulting value is then used in the balance equation to obtain

$$F_c = Q + (F_{in} - F_{out}) / \epsilon \quad (V-14)$$

An advantage of this method is its positivity, which avoids the need for negative flux fixups. The method also avoids the point-to-point oscillations of the diamond difference method. With both smoothness and accuracy, the method should be applicable to both the auxiliary and main fluxes of the discrete elements method.

The disadvantage of the method is the computational cost of evaluating the exponential function. This cost can be minimized if the coefficients are computed only once and stored in arrays, assuming sufficient storage is available for this use, or are computed only upon changing material regions, being passed to the step characteristic subroutine as a parameter.

It is interesting that (in this one-dimensional case, only) the diamond difference method is equivalent to the step characteristic method with the exponential approximated by $(2-\epsilon)/(2+\epsilon)$. The leading error term in this approximation is $\epsilon^3/12$.

9. Linear Characteristic Method

The linear characteristic method is derived as was the step characteristic method but with the improved approximation that the effective source, $Q(x)$, is assumed to vary linearly across the space cell. In order to estimate this variation, it is necessary to accumulate, in the outer iteration, not only the cell average effective source, Q_c , but also the edge values for each cell, Q_{in} and Q_{out} . (Note that Q_{out} of one cell and Q_{in} of the next cell are different if the cross-sections are different.) Then $Q(x)$ can be approximated by

$$Q(x) = Q_c + P (x - x_c) / \Delta x \quad (V-15)$$

where

$$P = Q_{out} - Q_{in} \quad (V-16)$$

However, if $|P| > 2 Q_c$, then $Q(x)$ will be negative at one end of the cell. Therefore, a negative source fixup is used, which reduces the slope of $Q(x)$ so that it just reaches zero at the edge of the cell. This is done by recomputing P (if $|P| > 2 Q_c$) as

$$P = 2 Q \text{ SIGN}(Q_{out} - Q_{in}) \quad (V-17)$$

The transport equation is integrated analytically to obtain F_{out} in terms of F_{in} , Q , P , and the optical thickness, ϵ :

$$F_{out} = F_{in} e^{-\epsilon} + Q (1 - e^{-\epsilon}) + P [1 - (1/2 + 1/\epsilon) (1 - e^{-\epsilon})] \quad (V-18)$$

This result is used in the balance equation to obtain F_c :

$$F_c = Q + (F_{in} - F_{out}) / \epsilon \quad (V-19)$$

Alcouffe, et al., have reported that the advantage to this method is that it is very much more accurate than the other methods considered. Although it requires more storage and computation per cell, it provides equivalent accuracy with a much coarser mesh, so that storage and execution costs are both reduced for a given accuracy of results [Ref. 3]. The disadvantage of somewhat more complicated programming is a minor one. This method is appropriate to both the auxiliary and main fluxes of the discrete element method.

B. Two-Dimensional (xy) Spatial Quadrature

Three methods of xy spatial quadrature are considered: step, diamond difference (with negative flux fixup), and step characteristic. Fine mesh spacing is used with these methods to obtain adequate accuracy, rather than the higher order methods which have been presented very recently. Conservation is achieved by the same means as in one dimension, as described above.

1. Coordinates and Symbols

The two-dimensional space and angular coordinate systems used to define the angular quadratures are used here for the spatial quadratures. The unit space cell is shown in figure V-1. As in the one-dimensional case, the direction cosines are all assumed positive and the other three octants are obtained by reflections. Due to the z-symmetry, only the upper hemisphere of directions ($\tau > 0$) need be considered. The fluxes entering the cell are $F_{in,x}$ and $F_{in,y}$ and are the fluxes on the left ($x=x_{i-1/2}$) and bottom ($y=y_{i-1/2}$) faces, respectively. Similarly, $F_{out,x}$ and $F_{out,y}$ are the fluxes on the right and top faces of the cell. These fluxes are directional fluxes in a fixed quadrature direction, $\hat{\Omega}$.

2. Balance Equation

Using the above notation, the transport equation becomes

$$\mu dF/dx + \eta dF/dy + \sigma F = \sigma Q \quad (V-20)$$

where Q is defined by equation (V-4), as before. Integrating over the area of the space cell yields the balance equation:

$$(F_{out,x} - F_{in,x}) / \alpha + (F_{out,y} - F_{in,y}) / \beta + F_c = Q_c \quad (V-21)$$

where the optical thicknesses are

$$\alpha = \sigma \Delta x / \mu \quad (V-22)$$

$$\beta = \sigma \Delta y / \eta \quad (V-23)$$

and the cell-edge fluxes are averages over their respective cell faces, F_c is the cell-average flux, and Q_c is the cell-average source term. The subscript on Q will be dropped except where required to avoid ambiguity.

3. Step Method

As in slab geometry, the step method in xy geometry assumes auxiliary relations

$$F_{out,x} = F_{out,y} = F_c \quad (V-24)$$

This assumption reduces the balance equation to a single unknown. The

balance equation is solved to obtain

$$F_c = \frac{Q + (1/\alpha) F_{in,x} + (1/\beta) F_{in,y}}{1 + (1/\alpha) + (1/\beta)} \quad (V-25)$$

The step method has the same advantages and disadvantages in two dimensions as were described above for the one-dimensional case. Another advantage is that it can be readily extended to curvilinear coordinates.

4. Diamond Difference

The diamond difference method assumes that the flux is linear in both x and y over a space cell, so that the cell-average flux is equal to the arithmetic average of the cell-edge fluxes on opposite sides of the cell. As before, the cell-edge fluxes represent averages over their respective faces of the cell. This assumption leads to an auxiliary relation for each dimension:

$$F_c = (F_{in,x} + F_{out,x}) / 2 \quad (V-26)$$

$$F_c = (F_{in,y} + F_{out,y}) / 2 \quad (V-27)$$

These relations, together with the balance equation form an algebraic system which is solved for $F_{out,x}$.

$$F_{out,x} = \frac{Q + F_{in,x} (a - b - 1/2) + F_{in,y} 2b}{a + b + 1/2} \quad (V-28)$$

where, for computational efficiency, $a = 1/\alpha$ and $b = 1/\beta$.

The remaining fluxes, F_c and $F_{out,y}$, are then evaluated using the auxiliary relations.

The diamond difference method provides good accuracy for global, i.e. space-integrated, quantities, such as total absorption; but the method is not positive and predicts negative fluxes if the space mesh is too coarse. Lathrop has researched the issue of positivity versus accuracy. He states that:

"A version of the variable weight scheme in which weights depend not only on the space-angle mesh but also on particle sources and fluxes is suggested as a means of obtaining the highest accuracy consistent with a positive difference scheme, but it is noted that such schemes are computationally more expensive than available corrective recipes used in conjunction with nonpositive schemes." [Ref. 7:475]

The only variable weight scheme used here is the step characteristic method. It will be discussed after the corrective recipes, which are considered next.

5. Negative Flux Fixup for the Diamond Difference Method

The design and application of negative flux fixup in two dimensions is similar to that used in one dimension, with the added complications that one or the other or both of the cell-exiting fluxes can be negative, so several special cases must be handled. The algorithm, optimized for minimum if-tests and computer operations, proceeds as follows:

- 1 - Compute $F_{out,x}$ from equation (V-28)
- 2 - If $F_{out,x}$ is not negative, compute $F_{out,y}$ from the diamond difference relations:

$$F_{out,y} = F_{in,x} + F_{out,x} - F_{in,y} \quad (V-29)$$

a - If $F_{out,y}$ is not negative, compute F_c from either diamond difference equation, which completes the calculations.

b - If $F_{out,y}$ is negative (but $F_{out,x}$ was not), then replace the y diamond relation, equation (V-27), with the fixup $F_{out,y} = 0$ and solve the resulting system of equations for $F_{out,x}$:

$$F_{out,x} = \frac{Q + F_{in,x} (a - 1/2) + F_{in,y} b}{a + 1/2} \quad (V-30)$$

If the revised $F_{out,x}$ is not negative, compute F_c from the x diamond relation, equation (V-26), which completes the calculations. If the revised $F_{out,x}$ is negative, then both outgoing fluxes require fixups. This case is handled in step 4, below.

3 - If the (originally) calculated value of $F_{out,x}$ is negative, then the x diamond relation is replaced by the fixup $F_{out,x} = 0$ and the resulting system is solved for $F_{out,y}$:

$$F_{out,y} = \frac{Q + F_{in,x} a + F_{in,y} (b - 1/2)}{b + 1/2} \quad (V-31)$$

If $F_{out,y}$ is not negative, then compute F_c from the y diamond relation, equation (V-27), which completes the calculations. Otherwise, both outgoing fluxes require fixups. This case is handled in step 4, next.

4 - Since both outgoing fluxes have been negative, despite application of a fixup of one of them, the final alternative is to replace both diamond relations by fixup constraints: $F_{out,x} = 0$ and $F_{out,y} = 0$ and compute F_c directly from the balance equation:

$$F_c = Q + F_{in,x} a + F_{in,y} b \quad (V-32)$$

6. Step Characteristic

The step characteristic method for xy-geometry was developed by Lathrop and compared to several other positive schemes [Ref. 7]. Figure V-1 illustrates a single space mesh unit cell, of dimensions Δx by Δy , not necessarily square. The streaming direction is assumed to lie in the principal octant, so that particles enter the cell from the left and bottom and exit on the right and top.

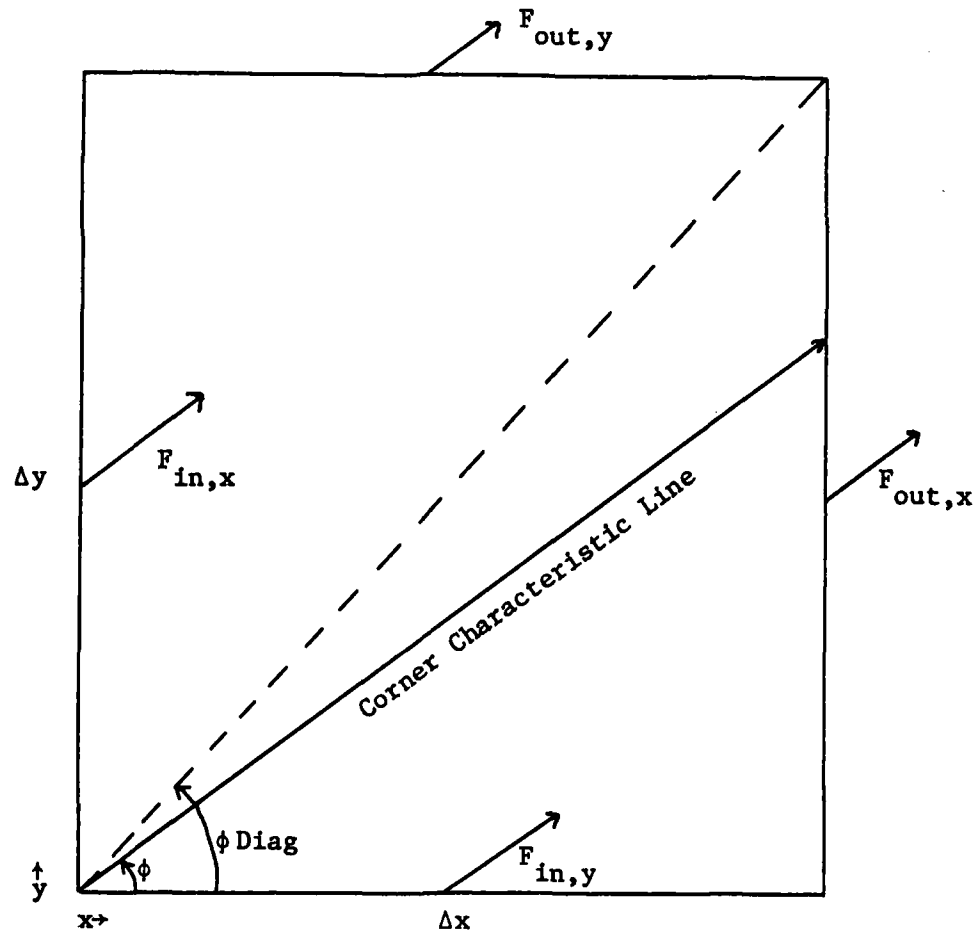


Fig. V-1: Step Characteristic Unit Cell

Rather than assume the auxiliary relations directly, as in the previous methods, the step characteristic method uses analytic integration, in the fixed single direction \hat{n} , to find the flux throughout the cell. The assumptions are:

- 1 - the source term, Q , is constant throughout the cell
- 2 - the flux entering on the left, $F_{in,x}$, is a constant (with respect to y) along the left face of the cell
- 3 - the flux entering on the bottom, $F_{in,y}$, is a constant (with respect to x) along the bottom face of the cell.

The solution for the flux is analytic throughout the cell, except that it is discontinuous across the corner characteristic line, which extends from the lower left corner in direction ϕ across the cell (unless $F_{in,x} = F_{in,y}$). The required outputs of the method are the cell average flux, F_c , and the exiting fluxes, $F_{out,x}$ and $F_{out,y}$. The exiting fluxes are obtained by analytically averaging the solution for the flux along the right and top faces. This provides a formula for the outbound fluxes in terms of the inbound fluxes, the source (Q), and the optical thicknesses of the cell (α and g). The cell average flux, F_c , could be found by analytically averaging the solution over the cell, but it is computationally more efficient to find it directly from the balance equation. The two approaches are algebraically equivalent, but not necessarily numerically equivalent, due to rounding error. Using the balance equation ensures that the method is numerically, as well as conceptually, conservative. The step characteristic method is a variable weight method, in that there are different sets of formulas used depending upon whether the corner characteristic line intersects the right face, the top face, or the top right corner of the cell.

If the corner characteristic line intersects the right face of the cell, as shown in figure V-1, then $\phi < \phi_{diag} = \arctan(\Delta y / \Delta x)$. An equivalent condition is that $\alpha < \beta$. In this case, the right cell-edge flux depends on both inbound fluxes, but the top flux does not depend on the bottom flux. The formulas are

$$F_{out,x} = Q + (1 - \alpha b) e^{-\alpha} (F_{in,x} - Q) + (1 - e^{-\alpha}) b (F_{in,y} - Q) \quad (V-33)$$

$$F_{out,y} = Q + (1 - e^{-\alpha}) a (F_{in,x} - Q) \quad (V-34)$$

where $a = 1/\alpha$ and $b = 1/\beta$. If the corner characteristic line intersects the top right corner, i.e. if $\alpha = \beta$, then the top flux depends only on the left, and the right depends only on the bottom. The formulas are

$$F_{out,x} = Q + (1 - e^{-\beta}) b (F_{in,y} - Q) \quad (V-35)$$

$$F_{out,y} = Q + (1 - e^{-\alpha}) a (F_{in,x} - Q) \quad (V-36)$$

The remaining case is that $\alpha > \beta$, so that the formulas are

$$F_{out,x} = Q + (1 - e^{-\beta}) b (F_{in,y} - Q) \quad (V-37)$$

$$F_{out,y} = Q + (1 - e^{-\beta}) a (F_{in,x} - Q) + (1 - \beta a) e^{-\beta} (F_{in,y} - Q) \quad (V-38)$$

In each case, the cell average flux is given by

$$F_c = Q + (F_{in,x} - F_{out,x}) a + (F_{in,y} - F_{out,y}) b \quad (V-39)$$

The step characteristic spatial quadrature is advantageous for use in the discrete elements method for both the auxiliary and main fluxes. It is unconditionally stable and convergent, as well as being a positive method. These features provide the smooth results needed for the auxiliary fluxes, but with much better accuracy than the step quadrature. The step characteristic quadrature also has the accuracy needed for the main fluxes. However, the accuracy of the method depends upon the relation between the streaming azimuth and the cell shape. If the streaming direction is at or near the cell diagonal, the method has excellent accuracy, but it provides comparatively poor accuracy for directions which are far from the diagonal. The nature of these inaccuracies is considered in detail in the next chapter.

C. Summary

This chapter has reviewed the spatial quadrature methods used in one- and two-dimensional discrete ordinates and for evaluation of the discrete elements method. The step method is computationally inexpensive, and is inaccurate but positive and smooth. The diamond difference method is computationally moderately expensive and is accurate in computing global quantities, such as total absorption rate, but is less accurate for pointwise quantities, such as the scalar flux as a function of position. This inaccuracy is because diamond difference is not a positive method, and hence predicts negative fluxes (if the space mesh is too coarse) or spatially oscillating fluxes, in any case. The diamond difference method may be used with negative flux fixups, which introduce nonlinearity into the method, and reduce accuracy of global quantities, but which prevent negative fluxes and so improve the

calculation of pointwise quantities. The step characteristic method is computationally relatively expensive because of the exponential function it uses, but provides both smoothness and accuracy. In one dimension, the linear characteristic method is also selected for testing. It is higher order than the step characteristic and has improved accuracy, especially with relatively coarse spatial meshes.

Later chapters report the results of testing the discrete element method with various combinations of methods of spatial quadrature used for the auxiliary and main fluxes. In order to interpret these results, it is necessary to consider the characteristics of the spatial quadratures as well as those of the angular quadratures. This is the reason for the detailed review presented here. The interaction of the spatial and angular quadratures is similarly important, and is considered in the next chapter.

VI. Interaction of Angular and Spatial Quadrature:

Ray Effects and Quasi-Ray Effects

The objective of this research is to develop and evaluate a method of numerical neutron transport which handles difficult problems better than discrete ordinates and which reduces ray effect. The discrete elements method attempts this by coupling the angular and spatial quadrature and by using a composite angular quadrature. In order to accurately interpret the results of numerical testing, it is first necessary to consider what sorts of errors are attributable to the angular quadrature in S_N and what sorts are due to the spatial quadrature, and how the two interact. The purpose of this chapter is to investigate these deficiencies and interactions. The approach is to solve a simple problem, a square source in a square non-scattering absorber, using combinations of analytic and discrete angular and spatial quadrature.

A. The Square-in-a-Square Problem: Without Scatter

Figure VI-1 shows the test problem and a benchmark solution. The problem is a 4 cm by 4 cm square absorber with an absorption cross-section of 0.75 cm^{-1} and scatter cross-section of zero, located in a vacuum. A source of strength $1 \text{ n/cm}^2/\text{sec}$ is distributed throughout the central 1 cm by 1 cm subregion. Only the upper right quadrant of the problem is actually solved. The rest of the problem is represented by

reflecting boundaries. Also shown is a benchmark solution for the y component of scalar current, J_y , along the top edge of the square. This solution used Monte Carlo spatial and azimuthal integration and 2-point Gauss-Christoffel polar integration of a Green's function kernel. The curve is obtained from 16 data points, each representing the average current in an interval 1/8 cm in width.

This benchmark solution shows several qualitatively expected features. The current is nowhere zero. The current is monotone decreasing, as a function of x (along $y = 2$ cm). The current should have zero slope with respect to x at $x=0$ (by symmetry), and the solution approximates this feature. The slight lack of smoothness is due to the variance of this Monte Carlo solution, which used 200,000 particles.

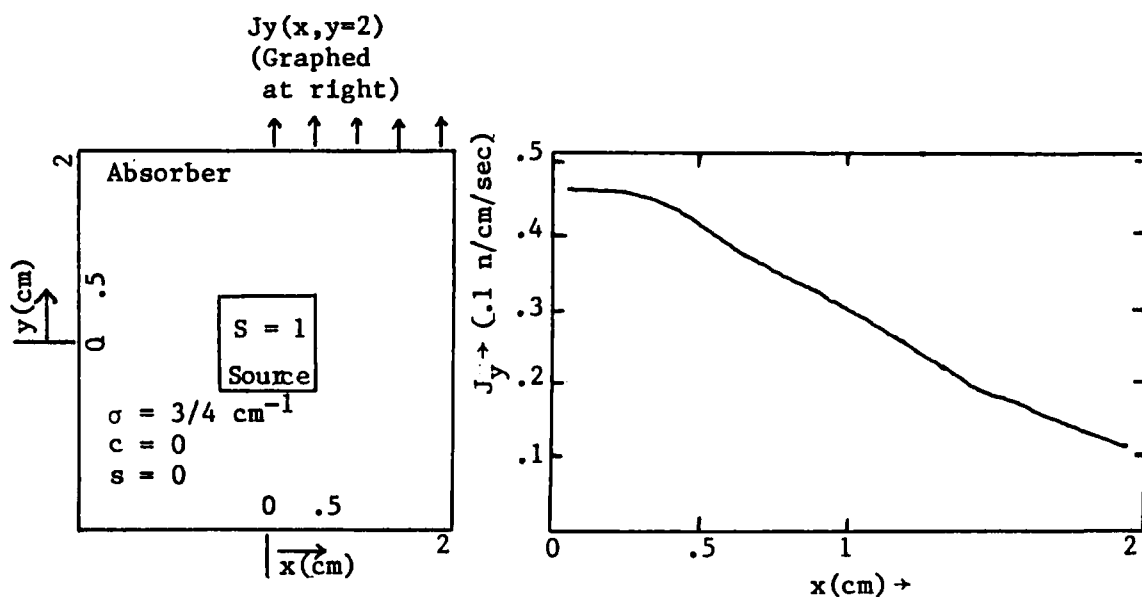


Fig. VI-1: Square-in-a-Square, Non-scattering Absorber Problem

B. Angular Truncation Error and Ray Effect

Any finite numerical representation of the angular dependence of the flux will suffer truncation error. This results in inaccuracy of the computed scalar fluxes, which feeds back through the scattering source in the transport equation to cause inaccuracy in the spatial variation as well. One of the objectives of the discrete element representation is to reduce this error and thus improve the accuracy of computed quantities.

Ray effect, however, is a particular sort of systematic error which causes computed results to be qualitatively wrong, as well as quantitatively inaccurate. The term "ray effect" is often used loosely to describe any such qualitative deficiencies. For the purposes of this discussion, a more precise definition is needed.

Ray Effect: The presence of qualitatively unreasonable numerical results caused by the use of a discrete angular representation of the directional flux, which would be present even if the spatial quadrature were performed analytically, or with a vanishingly fine mesh.

As an example of ray effect, figure VI-2 shows results for the test case of figure VI-1. These are Green's function solutions with discrete ordinates angular quadrature, evaluated at the midpoints of 16 intervals of width $1/8$ cm along the top edge of the problem. The $S_{2G,1R}$ and $S_{2G,2R}$ solutions show the results of projecting a single ray from the source region to the edge of the absorber. These solutions are neither non-zero everywhere nor monotone decreasing. However, comparison with the benchmark solution shows $S_{2G,64R}$ to be essentially converged in azimuthal quadrature.

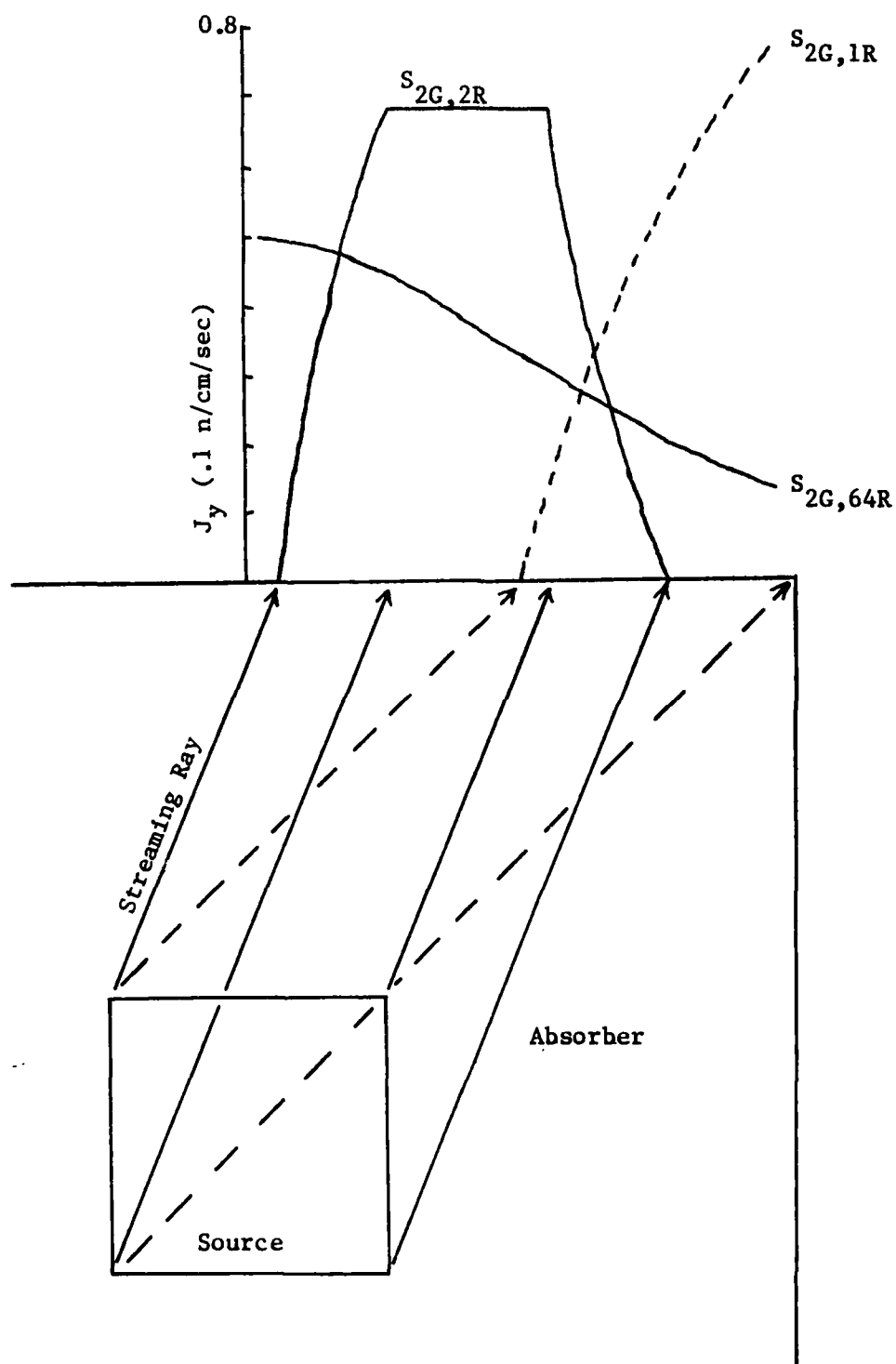


Fig. VI-2: Discrete Ordinates Solution with Analytic Spatial Quadrature

C. Quasi-Ray Effect and Spatial Truncation Error

As with the angular representation, the finite numerical representation of the spatial variation of the fluxes results in truncation error causing quantitative inaccuracy of computed results. Although less generally recognized, systematic errors can also occur, resulting in qualitative inaccuracy. These inaccuracies are, in practice, quite difficult to distinguish from those caused by the angular discretization, but the conceptual distinction is important. In view of this, the term quasi-ray effect is defined for use here.

Quasi-Ray Effect: The presence of qualitatively unreasonable numerical results caused by the use of a discrete spatial representation of the directional flux, which would be present even if the angular quadrature were performed analytically, or with a vanishingly fine mesh.

As an example of quasi-ray effect, the test case of figure VI-1 is solved by $S_{2G,64R}$ using discrete spatial quadratures. Since the angular quadrature is essentially converged, any appearance of ray effect should be attributable to the spatial quadrature. The spatial mesh used is 16 by 16 cells of size 1/8 cm by 1/8 cm. The resulting curves of J_y are thus comparable to those presented above. Figure VI-3A shows the results for two spatial quadrature methods, diamond difference with negative flux fixup (DDF) and step characteristic (SC). With a total cross-section of 0.75 cm^{-1} , the cells are slightly less than 1/10 mean free path in height and width, and this is a fine enough mesh that the DDF curve nearly matches the corresponding analytic curve in figure VI-2. The spatial oscillations of DDF, like noise, have averaged out.

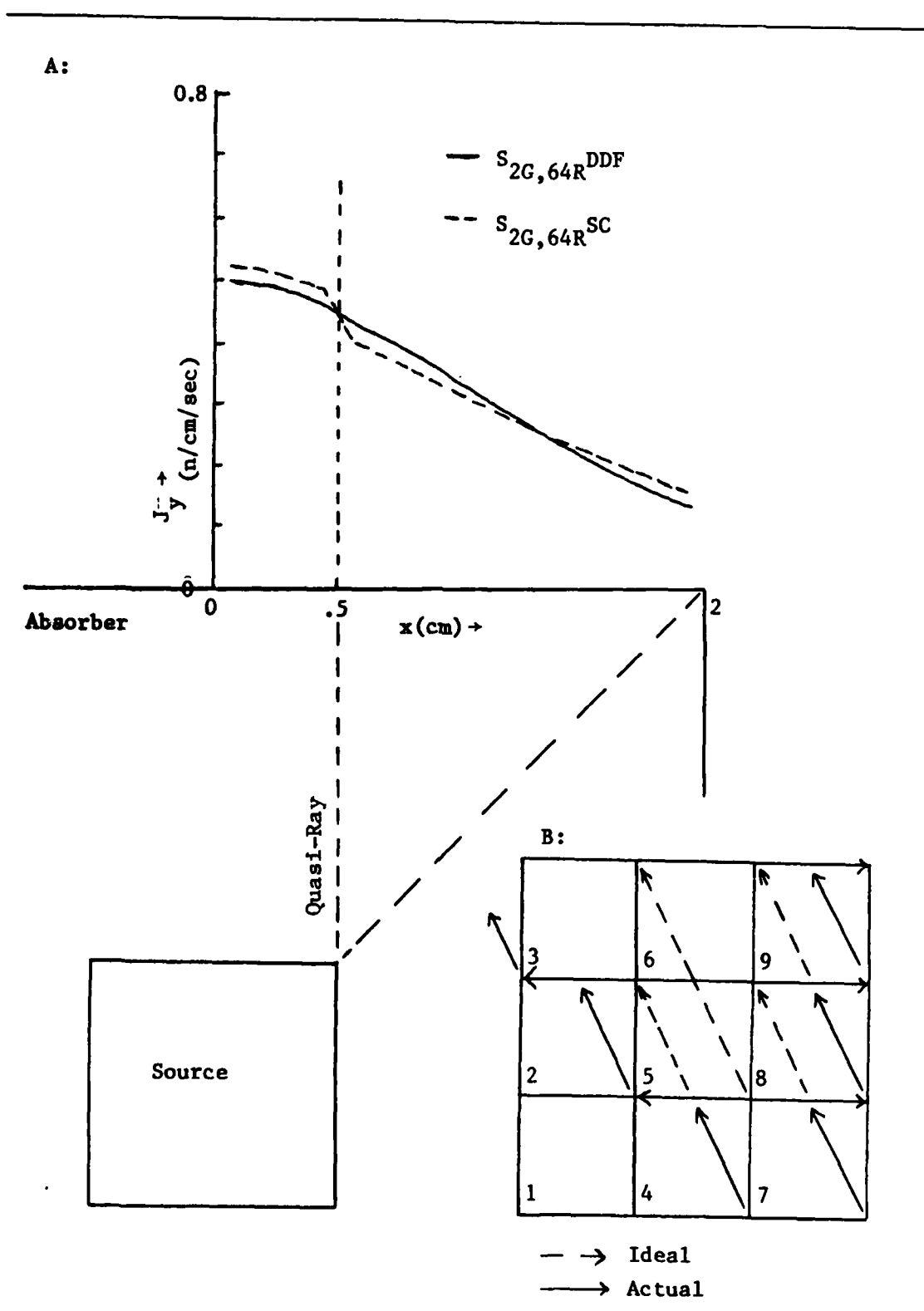


Fig. VI-3: Quasi-Ray Effect in Step Characteristic Method

The SC solution in figure VI-3A shows a distinct quasi-ray effect. The flux directly above the source region is too high and that just adjacent is too low. This comes about in the following way. Consider one of the azimuthal quadrature directions in the $S_{2G,64R}$ set which represents streaming of particles upward and to the left, as shown in figure VI-3B. If the SC method were to accurately represent a collimated beam of particles streaming in this direction, starting with a source only in cell 7, then the flux would step through the space mesh obliquely, as does a knight on a chess board, moving from cell 7 through cell 6 of that figure, so that none of the flux would reach cells 3 and 9. However, because the SC method assumes a constant flux distribution along each cell interface, part of the flux is "averaged" to the right along the 7-8 interface, and again along the 8-9 interface, arriving, incorrectly, in cell 9. Similarly, some of the flux crosses through cell 4 into cell 5, and is "averaged" to the left along the 4-5 interface, thence crossing through cell 2 into cell 3. Thus, some of the flux goes off to the left like a bishop, while most of the flux goes up the grid like a rook. Rather than a collimated beam, the streaming is modelled as a broad swath which more-or-less averages out to motion in the intended direction. The closer that direction is to diagonal, the better collimated the beam; but for directions far from the diagonal, the flux moves straight up the grid with a small smear out to one side. Since the $S_{2G,64R}$ quadrature includes many such oblique angles, this error accumulates systematically, overestimating the flux directly above the source. The flux is decreased just outside this band, i.e. at x just greater than $1/2$ cm, since the particles that should have arrived there have increased the flux above the source, instead. Similarly, transport

along the cell diagonals (like a bishop) accumulates so that the flux diagonally opposite the source (near $x = 2$ cm) is also overestimated.

The overall result is qualitative error which is similar to what one would expect for ray effect if a quadrature set which included only the verticle and diagonal directions were used. This is the quasi-ray effect defined above.

D. Combined Angular and Spatial Truncation Errors

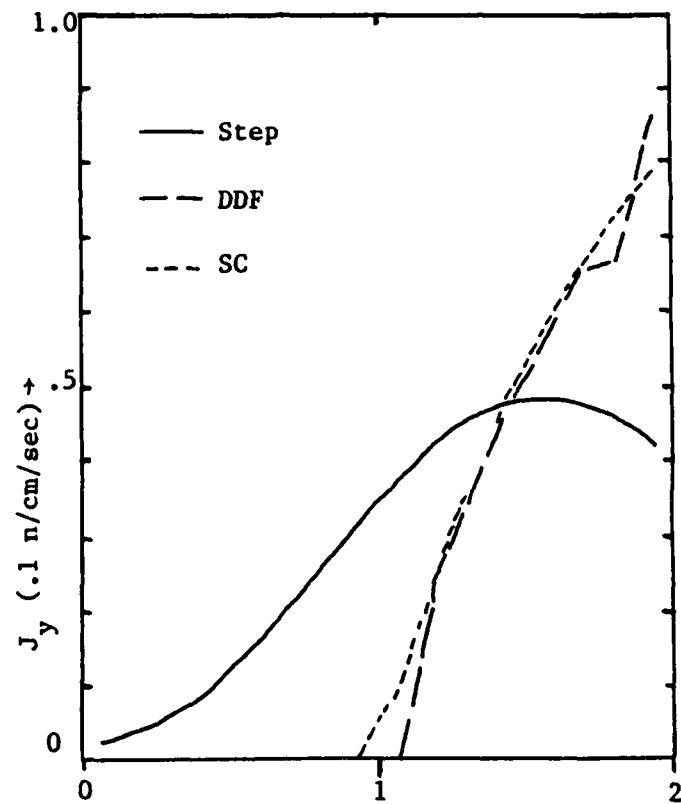
In practice, both the spatial and angular quadratures are discrete so that it is difficult to distinguish ray effect and quasi-ray effect. The use of analytic spatial or angular quadrature is normally infeasible. Only the simple example chosen here, without scatter, has made it possible to demonstrate the independent nature of each.

Figure VI-4A shows the $S_{2G,1R}$ solutions for step, DDF, and SC spatial quadratures for comparison with the analytic spatial quadrature of figure VI-2. The step method results are very smooth and show the presence of flux throughout the absorber region, for reasons similar to those discussed above with reference to the SC method. The DDF results resemble the analytic solution well in that regard (no current for $x < 1$ cm), but show the lack of smoothness typical of the method. The SC results show excellent accuracy (of spatial quadrature) for this case of diagonal streaming.

Figure VI-4B shows the $S_{2G,2R}$ solutions for DDF and SC spatial quadratures. Compared with figure VI-2, the DDF results are generally correct, but lack smoothness. The SC results are smooth, but show the beam spreading described above for this non-diagonal streaming direction.

A:

$S_{2G,1R}$



B:

$S_{2G,2R}$

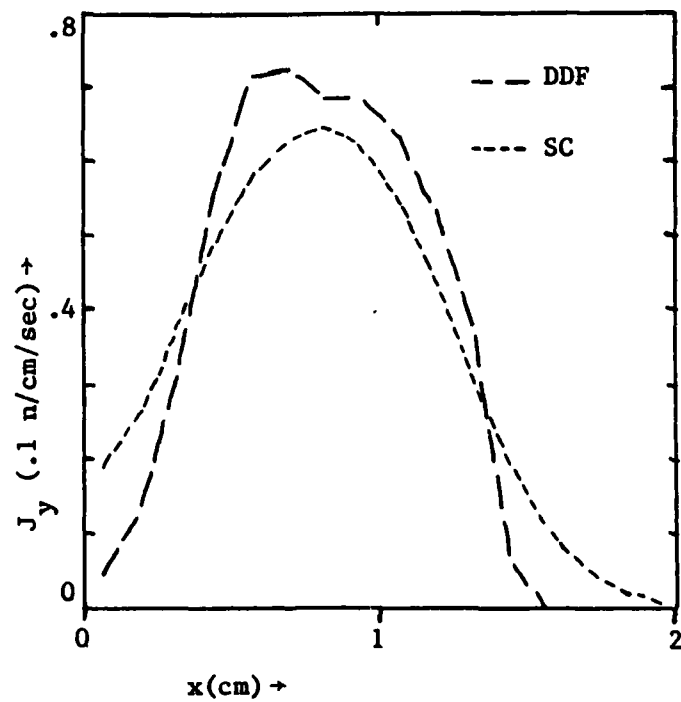


Fig. VI-4: Discrete Angular and Spatial Quadrature Results

Carlson and Lathrop have remarked upon the interaction of spatial and angular quadrature.

"Experience has shown that errors involved in spatial and angular quadrature are interdependent. Qualitatively, the error surface is like a valley between two ridges. If error is plotted against order of angular quadrature along one axis and order of spatial quadrature along an orthogonal axis, the ridges of the surface lie above these axes. Hence, if a calculation gives a result in the error valley, both quadratures must be refined to remain in this error valley. On the other hand, for a given spatial mesh, refining the angular quadrature may actually increase the error, and conversely." [Ref. 4:35]

The examples presented in this chapter tend to explain these observations. A low order angular quadrature should suffer from strong ray effect, due to the use of a few narrow beams of streaming particles; but the spatial quadrature, for a similarly coarse mesh, broadens out these narrow beams, reducing the apparent ray effect. Arbitrarily refining only the spatial mesh would narrow down the beams, letting the ray effect be seen. Conversely, a coarse spatial mesh should suffer from strong quasi-ray effect, but a correspondingly coarse angular mesh prevents this. With only a few angles, the spatial errors seem random, and are considered as mere truncation error. But arbitrarily refining only the angular mesh causes accumulation of this systematic error, letting the quasi-ray effect be seen.

E. Summary

This chapter has demonstrated some characteristics of the discrete ordinates method.

- 1 - Spatial quadrature schemes smear out the angular rays
- 2 - Use of a limited number of angular directions often ameliorates the quasi-rays of the spatial scheme

Success of S_N may be due, in part, to the combination of these two effects. On the other hand, the general truncation error implicit in the method has precluded application to some types of problem, such as vacuum ducts.

The discrete elements method avoids ray effects not by smearing out fixed rays, but rather by steering the rays. This means of coupling the spatial and angular representations then requires a spatial quadrature scheme which will accurately propagate the element flux as a collimated beam in the steered direction. Recent progress has been made in developing higher order spatial quadrature schemes, such as the linear characteristic and linear nodal methods, which should be of value in this regard. The discrete elements method may also be viewed as a higher order angular quadrature scheme, which should complement these new spatial quadratures. Success of the discrete elements method should be judged both on its ability to produce the results of a high order discrete ordinates calculation with the use of fewer rays, and on its ability to handle difficult problems more accurately than S_N . The following chapters present the results of numerical testing of this ability.

VII. Versions of the Discrete Elements Method

The previous chapters have shown that there are several degrees of freedom in designing a discrete elements scheme: quadrature rule for the individual elements, angular mesh type and size, spatial quadrature for the auxiliary and main flux calculations (not necessarily the same), and the coupling between the auxiliary and main fluxes.

A. Specification of a Discrete Elements Numerical Scheme

Notation to identify the particular combination of choices constituting a specific discrete element method is defined as follows:

Prefix - the general notation, L_N , is preceded by an abbreviation indicating the quadrature rule used within each discrete element:

SR - Simpson's rule

G3 - Gauss-Legendre three-point quadrature

NC - Newton-Cotes (five-point) rule

Subscripts - the general subscript, N , is replaced by a subscript indicating the type of angular mesh and number of mesh intervals. These subscript conventions were introduced in chapter III.

Superscripts - the superscripts indicate the spatial quadrature method(s) used for the auxiliary and main fluxes. The abbreviations for the superscripts are:

Step - step method

DD - diamond difference

DDF - diamond difference with negative flux fixup

SC - step characteristic

LC - linear characteristic

Thus, a notation of $G3-L_{2G,3}^{SC/DDF}$ would indicate a discrete elements scheme with three-point Gauss-Legendre quadrature in azimuth within each element of a three cell equal weight azimuthal mesh and with two-point Gauss-Christoffel polar quadrature, where the auxiliary fluxes are calculated by the step characteristic method and the main fluxes by diamond difference with negative flux fixup. Portions of the notation which are determined by the context of a discussion are usually omitted, for simplicity.

B. Coupling of Auxiliary and Main Fluxes

In computing the auxiliary fluxes by the discrete ordinates method, it is possible to either use the scalar flux from the main calculation or to compute a separate scalar flux directly from the auxiliary fluxes. In the former case, the auxiliary fluxes are coupled to the main fluxes by feedback through the source term. In the latter case, the auxiliary fluxes are uncoupled from the main fluxes. (Note that the main fluxes are always coupled to the auxiliary fluxes through the estimation of the streaming directions of the main fluxes, which is the object of the exercise.) Coupling would seem to offer more accurate auxiliary fluxes, and hence more accurate steering of the main fluxes, assuming stability is satisfactory. On the other hand, uncoupling preserves the linearity of the auxiliary flux calculation, ensuring convergence. Uncoupling also means that the streaming directions of the main fluxes are fixed, in the sense of being determined independently, so that the convergence of the main calculations is also assured.

The relative merits of coupling vs. uncoupling were evaluated in one-dimensional L_N and coupling was consistently the more accurate technique. Uncoupling speeded convergence only slightly, for the problems considered. Uncoupling could allow the streaming directions to be computed in advance and stored for use in the main calculations (although this would require rather vast storage resources for practical problems), but the decrease in computational effort of this scheme proved negligible. It was concluded that coupling is the scheme to use. If poor convergence is encountered, convergence can be improved by refining the spatial mesh or using a smoother spatial method, rather than by uncoupling. The results and conclusions presented in this dissertation refer implicitly to the coupled form of discrete elements.

C. Optimization

For computer implementation, a numerical method may be optimized in two important ways: with respect to execution time and/or with respect to storage. The dollar cost of a calculation may be dominated by either of these factors, depending on the computer facility. One of the objectives of this research is to identify the "best" discrete element method, based on accuracy vs. execution time with near minimum storage. The next chapter presents execution time and storage requirements for two-dimensional versions of the discrete elements method.

VIII. Computer Implementation

This chapter compares the computer execution time and memory requirements of the discrete elements and discrete ordinates methods. This information facilitates cost-effectiveness comparisons of the two methods and establishes the feasibility of the discrete elements method.

A. Problem and Quadrature Dimensions

The following memory requirements apply to a problem mesh consisting of I cells in the x direction by J cells in the y direction, and K polar directions or elements by L azimuthal directions or elements. The IJ space cells are partitioned into R regions of constant material and source parameters, not necessarily contiguously located.

B. Discrete Ordinates Memory Requirements

The discrete ordinates method requires the following arrays:

Spatial Arrays - Three arrays of size IJ are required for the all-angle flux for the previous iteration, F_{old} , the scalar flux for the iteration in progress, F_{new} , and the indexing array which records to which region each cell belongs. Three arrays of size R are required for the material constants, c , σ , and $Q_0 (= S/\sigma)$. One cell spacing array of size I is required for Δx , and one of size J for Δy , assuming non-uniform cell sizes.

Angular Arrays - For minimum storage, two arrays of size K are required: one for $\sin(\theta)$ and one for the polar weights, W_k . Two arrays of size L are required for the azimuthal angles and weights. Execution

speed is slightly enhanced if arrays of size KL are used for μ , η , and $W_{k,l}$.

Cell Boundary Flux Arrays - If two vacuum boundaries are available, then the boundary values of the directional fluxes need not be stored between iterations. Within an iteration, two arrays of size I and two of size J are required for the intercell boundary fluxes. If there are no vacuum boundaries, then KL sets of these arrays are required to save the needed boundary values of the directional fluxes between iterations.

Optical Thickness Arrays - Although not required, execution speed is improved if the optical thicknesses of cells in each region and in each quadrature direction are stored. Assuming a uniform space mesh within each region, this requires two arrays of size RKL , otherwise it would require two arrays of size $IJKL$. This is probably impractical except in the former case and with relatively small R , and it is assumed that these arrays are not used.

Minimum Memory Requirement:

With Vacuum Boundaries: $3IJ + 3R + 3(I+J) + 2(K+L)$

Without Vacuum Boundaries: $3IJ + 3R + (2KL+1)(I+J) + 2(K+L)$

C. Discrete Elements Memory Requirements

The discrete elements method requires the storage described above for the discrete ordinates method, with the element main fluxes taking the place of the ordinate fluxes, and has additional storage requirements for the auxiliary fluxes. Assuming the element quadrature rule has A auxiliary fluxes per element, the following minimum of arrays are required:

With two adjacent vacuum boundaries, $2A$ arrays of size I and of size J are needed for the intercell auxiliary fluxes and $2A$ arrays of

size K and of size L are needed for the auxiliary direction quadrature parameters. Without vacuum boundaries, KL sets of 2A arrays of size I and of size J are needed for the auxiliary flux boundary values, in addition to the auxiliary quadrature parameter arrays.

Minimum Memory Requirement:

With Vacuum Boundaries:

$$3IJ + 3R + (2A+3)(I+J) + (2A+2)(K+L)$$

Without Vacuum Boundaries:

$$3IJ + 3R + [2KL(A+1)+1](I+J) + 2(A+1)(K+L)$$

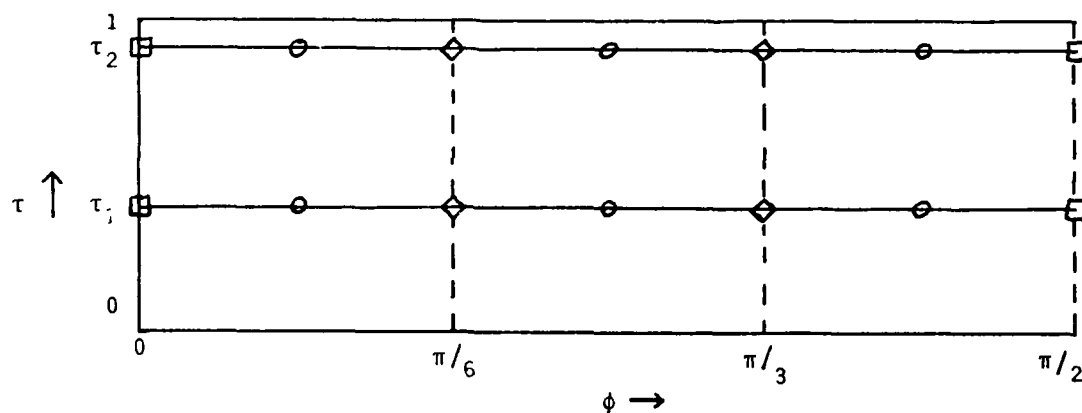


Fig. VIII-1: Quadrature Set for $SR-L_{2G,3}$

Additional memory may be used to speed execution with Simpson's rule or Newton-Cotes rule, as mentioned in chapter III. As an example, figure VIII-1 shows the quadrature set for the $SR-L_{2G,3}$ scheme for the principal octant. The circles mark the element center auxiliary directions; the squares mark the element edge auxiliary directions at the edges of the octant; the diamonds mark the element edge auxiliary directions internal to the octant. Each of these last four directions is

common to two elements, and could be computed (throughout the space mesh) only once, with the first element walk, and reused for the second element walk. This results in a 10%-15% savings in execution time for this quadrature. The cost in storage is an additional array of size IJ , if no vacuum boundaries are used, and two such arrays if vacuum boundaries are used (since octants are done in pairs: a single elements is walked in from vacuum boundary to non-vacuum boundary, reflected, and walked back out to the vacuum boundary). To take full advantage of this quadrature set overlap in $SR-L_{K,L}$ requires $(K+1)$ sets of these arrays. K sets are required for the directions marked with triangles in figure VIII-2, an example showing $SR-L_{2,3}$, and one set is needed for the diamonds. This provides about a 15% savings for this example, and up to about 25% for a fine angular mesh.

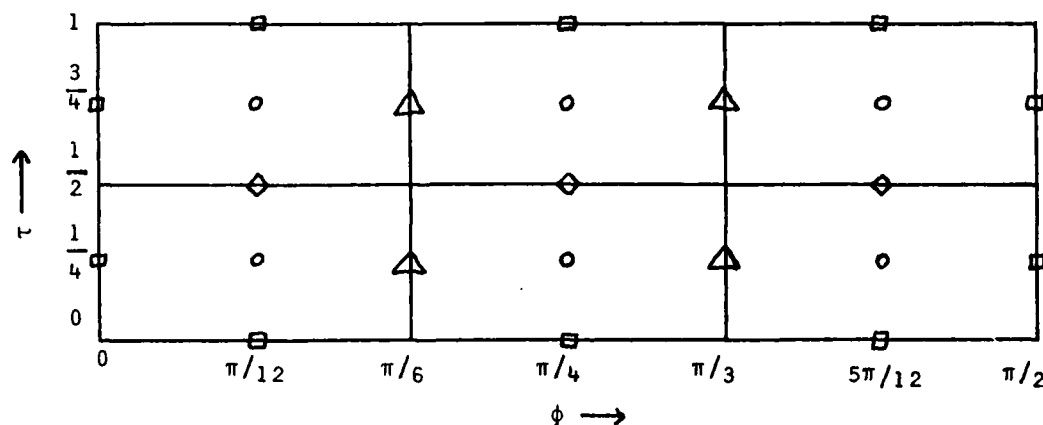


Fig. VIII-2: Quadrature Set for $SR-L_{2,3}$

This memory requirement, $(K+1)IJ$, may be prohibitive, but it can be quite reasonable when compared to the GIJ storage (for F_{old}) required for G energy groups, since G is often large and $K=4$ is probably maximum.

D. Example Comparison of Storage Requirements

Table VIII-1 shows the memory requirements for an example case of a 100 cell by 100 cell space mesh with 25 regions. The minimum memory requirements, measured in array elements, are given for two situations, with and without vacuum boundaries. The formulas for conventional S_N are slightly different than those above, and the result is shown for S_{16} .

Method	With 2 Vacuum Boundaries	No Vacuum Boundaries
S_{16}	30,783	44,783
$S_{2G,3R}$	30,685	32,685
$L_{2G,3}$	31,915	39,915
$L_{2,3}$	32,735	44,735

Table VIII-1: Example Case Memory Requirements

With two adjacent vacuum boundaries, the extra memory required for the discrete elements method is negligible. Without vacuum boundaries, it is larger, but not problematical. For very large spatial mesh problems, where memory may be a limiting factor, the three arrays of size IJ dominate all the schemes, so that the discrete element method is essentially equivalent to discrete ordinates in storage requirements.

E. Execution Times for S_N Spatial Quadratures

The execution speed of the discrete ordinates method is determined almost entirely by the spatial quadrature subroutine. Table VIII-2 gives the approximate execution costs of elementary mathematical floating point operations and function evaluations in units of Cray-1 clock cycles. A short accuracy square root routine of approximately six

decimal place accuracy is estimated to be achievable using 65 clock cycles. A short accuracy (four to six decimal places) routine for evaluating both the sine and cosine costs 46 cycles using the following formulas [Ref. 1:76]:

$$v = u * u \quad (\text{VIII-1})$$

$$\cos(u) = (.03705 * v - .49670) * v + 1.0 \quad (\text{VIII-2})$$

$$\sin(u) = ((.00761 * v - .16605) * v + 1.0) * u \quad (\text{VIII-3})$$

Operation:	+	-	*	/	if	exp	sqrt	sin & cos (both)
Clock Cycles:	4	4	5	20	8	128	65	46

Table VIII-2: Cray-1 Floating Point Execution Times

Estimates of the execution costs of the two dimensional spatial quadrature schemes of chapter V, based on the above clock times, are presented in table VIII-3. Larsen and Alcouffe [Ref. 5] have recently developed a linear characteristic method for xy geometry with a cost of about 600 clock cycles. The diamond difference method requires more than the indicated 102 clock cycles for cells where fixups are required; the step characteristic method requires slightly less than 267 cycles if the quadrature direction lies exactly on the space cell diagonal. The numbers given are generally representative, however.

XY Spatial Quadrature:	Step	DDF	SC	LC
Clock Cycles per Call:	56	102	267	600

Table VIII-3: Discrete Ordinates Spatial Quadrature Subroutine Costs

F. Execution Times for L_N Streaming Direction Averaging

The cost of execution of a discrete elements scheme is determined by the sum of three sets of subroutine calls:

- 1 - Auxiliary flux spatial quadrature (per table VIII-3)
- 2 - Streaming direction flux-weighted averaging (per table VIII-4)
- 3 - Main flux spatial quadrature (per table VIII-3)

The spatial quadratures are computed by the same subroutine(s) as in discrete ordinates, although different schemes can be used for the main vs. auxiliary fluxes. The extra cost of the discrete elements method (besides the auxiliary flux calculations) is for the computation of the flux-weighted streaming directions. These costs are presented in table VIII-4, below, and assume the use of short accuracy square root, sine and cosine algorithms. Values are given for those xy geometry methods which were tested. An alternative scheme of directly averaging the x- and y-direction cosines was tested and abandoned. It avoided the sine and cosine needed to convert the averaged (τ, ϕ) to (μ, η) , but cost 167 clock cycles and gave unsatisfactory numerical results. The short accuracy sine and cosine fits proved to have no degrading effect on the overall accuracy of the discrete elements method.

Method:	Clock Cycles:
Simpson's Rule or Gauss-Legendre (3-point):	
Azimuthal averaging only ($L_{KG,L}$)	160
Azimuthal and polar averaging ($L_{K,L}$)	288
Newton-Cotes (5-point) Rule:	
Azimuthal averaging only ($L_{KG,L}$)	186

Table VIII-4: Execution Times for L_N Streaming Direction Averaging

G. Example Execution Cost Comparison

As an example of the use of the above information, consider a comparison of S_{16}^{SC} and $G3-L_{2G,3}^{SC,SC}$. The discrete ordinates scheme, S_{16} , uses 144 total quadrature directions, for a cost of 38,448 cycles per space cell. The G3-L discrete elements method uses three auxiliary fluxes, one direction averaging, and one main flux for a cost of 1228 cycles per element per space cell. With 24 elements total, the cost is 29,472 cycles per space cell. Assuming both converge equally rapidly, these figures give the relative cost of the two methods: $G3-L_{2G,3}^{SC,SC}$ costs about 77% as much as S_{16}^{SC} .

H. Computer Programs for Testing the Discrete Elements Method

The computer programs used to test the discrete elements method were written in Fortran-IV (with extensions similar to WATFIV) and run on an Intel-8088 based microcomputer. The programs were specialized to handle the test cases efficiently and so are not of general applicability. For this reason, and because the programs were straightforward implementations of the equations and algorithms described in this report, listings of the program code are not included here, but are on file at the Physics Department of the Air Force Institute of Technology, Wright-Patterson AFB, Ohio, 45433.

The discrete ordinates codes were validated by comparison with sample cases run for that purpose by E. W. Larsen of the Los Alamos National Laboratory. The discrete elements codes were validated by use of the midpoint rule for the element quadrature and comparison with the equivalent product quadrature discrete ordinates calculations.

I. Conclusions

As with most higher order methods in numerical analysis, computer implementation of the discrete elements method entails three costs: increased program complexity, increased storage requirements, and increased execution times. The remainder of this report will deal with the question of whether the method also provides increased accuracy, and, if so, increased efficiency on the basis of cost vs. accuracy.

Chapter II presented the discrete elements algorithm, and showed that the essential simplicity of structure of the discrete ordinates method is retained.

This chapter has shown that the L_N method has only modestly increased storage requirements, if a vacuum boundary is present in both the x- and y-directions. In the absence of vacuum boundaries, the storage requirements are more substantial, but still about equivalent to S_N requirements. The storage penalty is of even less concern in multi-group problems, since the increase only applies to the one energy group being iterated at a time.

Execution times are similarly increased, but are comparable to discrete ordinates quadratures currently in use, such as S_{16} . Two approaches to minimizing execution costs are possible. One is to use the least expensive of spatial quadrature schemes for the auxiliary fluxes, since most of the cost of the method is for these calculations. The other approach is to use the highest order of spatial quadratures for both the main and auxiliary fluxes so that the spatial mesh may be coarse. The next chapter evaluates these approaches for the case of one-dimensional (slab) geometry, since high-order spatial quadratures are readily employed in this geometry.

IX. Test Cases in One-Dimensional Geometry and Results

This chapter compares the performance of L_N and S_N schemes for two problems in one-dimensional Cartesian geometry. Evaluations in xy-geometry are presented in the next chapter.

A. Scatter-Free Shield Penetration

This test problem consists of a uniform , isotropic flux incident upon the left of a shield, with vacuum on the right of the shield. The shield is 20 mean-free-paths (mfp) thick and is purely absorptive. The exact solutions for the directional flux and current within the shield are the analytic functions:

$$F(\mu, x) = F_0 e^{-\sigma x / \mu} \quad (\text{IX-1})$$

$$J_x(\mu, x) = \mu F_0 e^{-\sigma x / \mu} \quad (\text{IX-2})$$

Integrating equation (IX-2) over μ at $\sigma x = 20$ gives the current penetrating the shield:

$$J_x = 0.5 E_3(20) = 4.50456 \text{ E-11} \quad (\text{IX-3})$$

where $F_0 = 1$ and E_3 is an exponential integral.

The problem was solved using S_N with equal weight quadrature and with Gaussian quadrature, and using L_N with equal weight elements and Gaussian weight elements for various angular meshes and space schemes. In each case, 40 space cells of 1/2 mfp thickness were used. For this problem, since $Q = 0$ in every cell, the step characteristic (SC) and linear characteristic (LC) methods are identical.

Table IX-1 presents the error ratio of the current penetrating the shield for the various schemes. Error ratio is a computationally convenient measure of error, here defined as

$$\text{Error Ratio } (x, x_{\text{exact}}) = |x - x_{\text{exact}}| / |x + x_{\text{exact}}| \quad (\text{IX-4})$$

where x_{exact} is the reference or benchmark value. This has the advantage over percentage that if x is too large by a factor of 2, the relative error is 100% but if x is too small by a factor of 2, it is -50%, whereas the error ratio is 1/3 in each case. For small errors, the error ratio is approximately half the conventional relative error. An error ratio of .05 corresponds to approximately 10%, for example.

<u>Method</u>	<u>N:</u>	<u>2</u>	<u>4</u>	<u>6</u>	<u>8</u>	12	24
Three-Point-Gaussian Discrete Elements:							
$L_{\text{EW}}^{\text{Step/SC}}$.556	.303	.210	.149		
$L_{\text{GW}}^{\text{Step/SC}}$.556	.220	.0846	.0407	.0191	.00504
$L_{\text{EW}}^{\text{SC/SC}}$.395	.0488	.00880			
$L_{\text{GW}}^{\text{SC/SC}}$.395	.0106	.00122	.000506		
Simpson's Rule Discrete Elements:							
$L_{\text{EW}}^{\text{SC/SC}}$.578	.310	.146	.0670	.0169	
$L_{\text{GW}}^{\text{SC/SC}}$.578	.161	.0223	.00930	.00208	.00012
Discrete Ordinates:							
$S_{\text{EW}}^{\text{SC}}$		1.000	.978	.791	.553	.273	.0696
$S_{\text{GQ}}^{\text{SC}}$		1.000	.572	.0759	.00138	.000007	0
	<u>N:</u>	<u>8</u>	<u>16</u>	<u>24</u>	<u>32</u>	48	
$S_{\text{EW}}^{\text{SC}}$.553	.156	.0696	.0392	.0174	
$S_{\text{GQ}}^{\text{SC}}$.00138	.000007	.0000004	0	0	

Table IX-1: Error Ratio of Shield Penetration Current

1. Step vs. SC for Auxiliary Fluxes

A comparison of the $L^{\text{Step/SC}}$ results with the $L^{\text{SC/SC}}$ results indicates the superiority of using the higher order method for the auxiliary calculations. Even if allowance is made for the lower cost of the step method, SC is more effective. For example, assuming the step method costs 1/4 as much as the SC method, then with three auxiliary fluxes per element, $L_{8\text{EW}}^{\text{Step/SC}}$ costs about the same as $L_{4\text{EW}}^{\text{SC/SC}}$, but has three times as much error. For larger N, the disparity in performance is even greater.

2. Simpson's Rule vs. Gauss-Legendre (3-point) Quadrature

A comparison of the $G3-L^{\text{SC/SC}}$ and $SR-L^{\text{SC/SC}}$ results shows consistently better results for the G3 method. Even if the SR scheme reuses the overlapping auxiliary fluxes, and so costs only 3/4 as much as the G3 scheme, it still cannot compete. For example, the $G3-L_{6\text{EW}}$ and the $SR-L_{8\text{EW}}$ cost about the same, but the SR scheme has over 7 times larger error.

3. Equal Weight vs. Gaussian Weight Discrete Elements

The Gaussian weight discrete elements outperforms the equal weight quadrature mesh for this problem. The reason is that the flux penetrating completely through a 20 mfp thickness of non-scattering absorber is strongly forward-biased, so that the element(s) closest to $\mu = 1$ carry all the information. With Gaussian weights, the discrete elements are crowded toward the poles and sample this information more effectively.

4. Discrete Elements vs. Discrete Ordinates

When compared on the basis of number of elements/ordinates, the $G3-L^{\text{SC/SC}}$ schemes have smaller error than the S^{SC} schemes, but also

have slower convergence as N is increased. For large enough N , it is expected that S_N will be the more accurate. These discrete element methods, however, have roughly four times the cost per element of the discrete ordinates schemes. Comparing S_8 to L_2 , etc., the Gauss-Legendre quadrature discrete ordinates method is quite clearly the most cost effective scheme tested, for this problem. The bottom rows of table IX-1 facilitate this comparison. This is not necessarily a representative comparison, however, because the problem is ideally suited for the S_N quadrature in two ways. First, the angular flux distribution which S_N seeks to represent with a high-order polynomial is in fact an analytic function well suited to such a representation, namely, the function in equation (IX-1). Secondly, the SC spatial quadrature is exact (except for rounding error accumulation) for this source-free, scatter-free medium, so that the data points used to obtain the high-order fit have essentially no error.

B. Two-Region Problem

This problem consists of a strongly scattering source region with weakly scattering shielding and vacuum outer boundaries. Only half of the system is solved, using a symmetry boundary on the left and vacuum on the right. The problem parameters are summarized in table IX-2.

<u>Region</u>	<u>Source</u> (#/cm ² /sec)	<u>c</u>	<u>Region Width</u> (cm)	<u># of Cells</u>	<u>Cell Width</u>
Source	1	0.5	5	40	0.125
Shield	0	0.1	15	120	0.125

Table IX-2: Parameters for Two Region Test Problem

1. Error "Norms"

Two error norms are used in each region. (The term "norm" is used loosely here; no attempt is made to demonstrate that these are true norms in the function-analytic sense.) One is an integral norm: the error ratio of the integral of the scalar flux over the region. This is a measure of the ability of the method to compute reaction rates or related eigenvalues. The other is a pointwise norm: the error ratio of the scalar flux as computed for each spatial cell, averaged over the cells of the region. Tables (IX-3) through (IX-6) present these results.

<u>Method</u>	<u>Quadrature:</u>	<u>2</u>	<u>4</u>	<u>6</u>	<u>8</u>	<u>48</u>
Three-Point-Gaussian Discrete Elements:						
L _{EW} Step/DDF		.000112	.000058	.000044	.000038	
L _{EW} Step/LC		.000097	.000040	.000025	.000019	
L _{GW} Step/LC		.000097	.000054	.000035	.000026	
L _{EW} LC/LC		.000021	.000012	.000011	.000010	
L _{GW} LC/LC		.000021	.000014	.000012	.000011	
Simpson's Rule Discrete Elements:						
L _{EW} LC/LC		.000103	.000004	.000006	.000009	
Gaussian Quadrature Discrete Ordinates:						
S ^{Step}		.00619	.00200		.000983	.000639
S ^{DDF}		.00534	.00125		.000286	.000025
S ^{SC}		.00537	.00128		.000329	.000022
S ^{LC}		.00535	.00126	.000553	.000307	Benchmark
	<u>Quadrature:</u>	<u>8</u>	<u>16</u>	<u>24</u>		
S ^{LC}		.000307	.000071	.000027		

Table IX-3: Error Ratio of Scalar Flux Integrated over Source Region

2. Step/LC vs. Step/DDF

The least expensive discrete element scheme, per cell per element, which might produce reasonable accuracy, is the $L^{\text{Step/DDF}}$ scheme. The step auxiliary calculations are smooth and the DDF main calculations are relatively accurate. Comparison of the results with those of the $L^{\text{Step/LC}}$ scheme shows the latter to be more accurate on an equal N basis and to have faster convergence in N, but (allowing for twice the cost per element) the two are about equally cost-effective.

Method	Quadrature:	<u>2</u>	<u>4</u>	<u>6</u>	<u>8</u>	<u>48</u>
Three-Point-Gaussian Discrete Elements:						
$L^{\text{Step/DDF}}$ _{EW}		.00122	.000630	.000476	.000414	
$L^{\text{Step/LC}}$ _{EW}		.00105	.000432	.000268	.000201	
$L^{\text{Step/LC}}$ _{GW}		.00105	.000586	.000382	.000283	
$L^{\text{LC/LC}}$ _{EW}		.000228	.000129	.000115	.000109	
$L^{\text{LC/LC}}$ _{GW}		.000228	.000148	.000125	.000116	
Simpson's Rule Discrete Elements:						
$L^{\text{LC/LC}}$ _{EW}		.00112	.000041	.000070	.000093	
Gaussian Quadrature Discrete Ordinates:						
S^{Step}		.0630	.0214		.0106	.00693
S^{DDF}		.0548	.0134		.00312	.00109
S^{SC}		.0552	.0138		.00357	.000241
S^{LC}		.0550	.0136	.00600	.00334	Benchmark
Quadrature: <u>8</u> <u>16</u> <u>24</u>						
S^{LC}		.00334	.000771	.000293		

Table IX-4: Error Ratio of Scalar Flux Integrated over Shield Region

3. Equal Weight vs. Gaussian Weight Elements

For both integrated and pointwise errors and in both source and shield regions, L_{EW} is more accurate, and hence more cost-effective, than L_{GW} . The only exception in the four tables is the L_4 average error ratio in the shield region. This observation holds for both the Step/LC and the LC/LC spatial quadratures. The introduction of scatter and an interior material boundary make this problem more realistic than the non-scattering shield, and show the validity of equal weight composite quadrature for less well-behaved fluxes.

<u>Method</u>	<u>Quadrature:</u>	<u>2</u>	<u>4</u>	<u>6</u>	<u>8</u>	<u>48</u>
Three-Point-Gaussian Discrete Elements:						
$L_{EW}^{Step/DDF}$.00106	.000540	.000392	.000356	
$L_{EW}^{Step/LC}$.000816	.000276	.000142	.000087	
$L_{GW}^{Step/LC}$.000816	.000441	.000253	.000162	
$L_{EW}^{LC/LC}$.000314	.000073	.000057	.000046	
$L_{GW}^{LC/LC}$.000314	.000109	.000068	.000061	
Simpson's Rule Discrete Elements:						
$L_{EW}^{LC/LC}$.00169	.000433	.000186	.000133	
Gaussian Quadrature Discrete Ordinates:						
S^{Step}		.00761	.00258		.00211	.00259
S^{DDF}		.00855	.00241		.000780	.000303
S^{SC}		.00850	.00232		.000639	.000056
S^{LC}		.00846	.00227	.00104	.000597	Benchmark
	<u>Quadrature:</u>	<u>8</u>	<u>16</u>	<u>24</u>		
S^{LC}		.000597	.000149	.000058		

Table IX-5: Average Error Ratio of Scalar Flux in the Source Region

4. LC/LC vs. Step/LC

For both integrated and pointwise errors, and in both source and shield regions, and even allowing for a 2:1 or greater cost ratio, $L^{LC/LC}$ is more accurate and more cost-effective than $L^{Step/LC}$. Similar comparisons with $L^{SC/SC}$ (data not shown) reveal the same trend: the higher-order the spatial quadrature, the more accurate and cost-effective the discrete element method. The use of LC for both auxiliary and main fluxes can be even more efficient if its ability to use a coarser spatial mesh is used to advantage.

<u>Method</u>	<u>Quadrature:</u>	<u>2</u>	<u>4</u>	<u>6</u>	<u>8</u>	<u>48</u>
Three-Point-Gaussian Discrete Elements:						
$L_{EW}^{Step/DDF}$.0474	.0270	.0188	.0139	
$L_{EW}^{Step/LC}$.0404	.0203	.0124	.00770	
$L_{GW}^{Step/LC}$.0404	.0130	.0446	.00287	
$L_{EW}^{LC/LC}$.0340	.000914	.000094	.000027	
$L_{GW}^{LC/LC}$.0340	.000483	.000123	.000033	
Simpson's Rule Discrete Elements:						
$L_{EW}^{LC/LC}$.203	.0425	.0107	.00360	
Gaussian Quadrature Discrete Ordinates:						
s^{Step}		.601	.185		.223	.224
s^{DDF}		.707	.0785		.00700	.00593
s^{SC}		.704	.0737		.000915	.000260
s^{LC}		.704	.0738	.00324	.00113	Benchmark
	<u>Quadrature:</u>	<u>8</u>	<u>16</u>	<u>24</u>		
s^{LC}		.00113	.000231	.000088		

Table IX-6: Average Error Ratio of Scalar Flux in the Shield Region

5. G3 vs. SR Element Quadrature

For pointwise errors, in both source and shield regions, the three-point Gauss-Legendre quadrature provides clearly superior performance. Even allowing for a 2:1 cost ratio (the actual ratio is closer to 1.2:1), the $G3-L_{EW}^{LC/LC}$ scheme is more cost-effective than the $SR-L_{EW}^{LC/LC}$ scheme.

For the integrated flux errors, the evidence is not so clear-cut. In the source region, for example, both methods converge toward an error ratio of 0.000010, indicating this much residual error in the benchmark (S_{48}^{LC}) solution. But they converge from opposite directions. The $G3-L_4$ is nearly converged, at 0.000012, and is actually closer than the $SR-L_6$ which is also nearly converged, at 0.000004. However, neither of these errors is large enough for meaningful comparisons. Similar logic applies to the data for the shield region.

6. Discrete Elements vs. Discrete Ordinates

Comparison of the best discrete elements method tested, namely $G3-L_{EW}^{LC/LC}$, with the best discrete ordinates quadrature tested, S_N with Gauss-Legendre quadrature, shows that the L_N method is very much more accurate, for the same N . On a cost basis, allowing for a 4:1 cost ratio, the bottom row of each table can be compared directly with the L_N rows. In terms of the integrated flux errors, the L_N method is the better performer. Even L_2 has less error than S_{24} , and at 1/4 the computational cost. In terms of the average errors in the source region, L_N is somewhat more cost-effective. Only in terms of the average errors in the shield region is S_N the more accurate for a given cost. This occurs for reasons similar to those which applied to the non-scattering, non-source shield penetration problem.

It might be argued that a double-range Gauss-Legendre quadrature would improve the performance of the discrete ordinates method for this problem by modeling the flux discontinuity at $\mu = 0$ exactly, as with the double P_N method. With this quadrature, S_N could possibly be more cost-effective than L_N . However, Carlson and Lathrop have reported that the single-range quadrature is more accurate for problems with optically thick regions, while double-range is better for problems with many thin regions [Ref. 4:34]. The regions in this problem are optically thick (10 and 15 mfp), so that the comparison with single-range S_N should be a fair one.

C. Conclusions

This chapter has presented the results of numerical testing of various discrete element and discrete ordinate schemes in slab geometry. As a proof of concept, two test cases were used. While more extensive testing would be needed to support categorical conclusions, the data presented do indicate the following trends.

1 - Equal weight discrete elements are generally more accurate than Gauss-Legendre weight elements, for realistic problems.

2 - Three-point Gauss-Legendre element quadrature is superior to Simpson's rule.

3 - L_N method can be more cost-effective than Gaussian S_N when the linear characteristic space scheme is used for both the auxiliary and main fluxes, and the three-point Gauss-Legendre rule is used for the element quadrature.

4 - The expectation that "the harder the problem, the more advantageous the L_N method" is supported by this evidence.

5 - Convergence and accuracy of L_N are degraded by use of inaccurate or, especially, non-smooth space schemes for the auxiliary fluxes. L_N with step characteristic or linear characteristic auxiliary quadrature converged in the same number of iterations as S_N , however.

The above tests in one dimension implicitly avoided consideration of ray effects, since there are no ray effects, per se, in one dimensional (time independent) problems. The next chapter uses two test problems, one of which is similar to the ray effects problem of chapter V. An objective of those tests is to determine the applicability in two dimensions of the observations made here in one dimension.

X. Test Cases in Two-Dimensional Geometry and Results

This chapter compares the performance of L_N and S_N schemes for two problems in two-dimensional Cartesian geometry. The first problem is a variation of the square source in a square absorber problem introduced in chapter VI. A review of results from the literature provides qualitative comparisons of performance in ameliorating ray effects. The second problem models a shielded plane source with a vacuum duct in the shield, and is used for quantitative as well as qualitative comparisons of performance on a difficult problem.

A. Ray Effect Problem and Comparison of Results

A test problem which has been used in the literature for evaluation of ray effect is inset in figure X-1. The problem is similar to the one used in chapter VI, but with the source square increased in size and with scatter included. The results used for comparison are the cell-average scalar fluxes along the top row (or up the right column, by symmetry) of a 30 cell by 30 cell spatial mesh. This mesh is nearly twice as fine as that used in chapter VI, so the quasi-ray effect should be reduced.

1. Conventional Discrete Ordinates

Lathrop used this problem with several angular quadrature schemes. Figures X-1 through X-4 are taken directly from reference 8 for qualitative comparisons. Figure X-1 shows the results for S_2 , S_4 , and S_{16} , using conventional (totally-symmetric) quadrature using TWOTRAN (and presumably, diamond difference spatial quadrature). The substantial wobbles in the curves are described by Lathrop as ray effect.

2. Rotationally Symmetric Discrete Ordinates

Figure X-2 shows the results using discrete ordinates with a product quadrature set consisting of a single row of directions at a fixed latitude (polar angle), equally spaced in azimuth and equally weighted, i.e., the "rotationally invariant" quadratures. In Lathrop's notation, these are R_2 , R_4 , R_8 , and R_{16} . These show decreased, but still significant, ray effect.

3. "Consistent" Discrete Ordinates

Figure X-3 compares the S_{16} result with that of Lathrop's CS_2 method. This "consistent S_N " method [Ref. 10] used explicit coupling of the directional flux distribution to the spatial quadrature (as does discrete elements) derived by a first-order Taylor expansion of the flux about the S_N quadrature angles. This scheme shows a vast improvement over the S_2 scheme (to which it degenerates if the coupling is omitted), and might seem quite promising. Its limitation seems to be that the "consistent" treatment is an approach rather than a numerical method, in that to increase either the set of quadrature angles or the order of the coupling terms, or both, requires a complete rederivation of the equations to be solved. With the discrete elements method, however, increasing the quadrature set is a strictly mechanical procedure, and increasing the coupling order requires only the use of a different element quadrature rule.

4. Spherical-Harmonics-Like Discrete Ordinates

In any case, Lathrop abandoned the CS_2 scheme in favor of "spherical-harmonics-like" discrete ordinates. This method uses fictitious sources to cause the discrete ordinates equations to conserve the same moments as the spherical harmonics method [Ref. 8]. Results

with these schemes, $S_2 \rightarrow P_1$, $S_4 \rightarrow P_1$, $S_6 \rightarrow P_3$, $S_8 \rightarrow P_5$, are shown in figure X-4. They show no "ray effect" in that they are shaped correctly, but they have angular quadrature truncation error which systematically affects the level rather than the shape. The convergence in amplitude (vs. N) is relatively slow, as with the P_N method. The method also has substantially increased computational cost.

5. Compatible Product Quadrature Discrete Ordinates

Abu-Shumays [Ref. 2] investigated the possibilities of improved performance through use of specialized "compatible" product quadrature sets (with diamond difference spatial quadrature). He concluded that the Gauss-Christoffel polar / quadruple-range azimuthal product quadrature has more accuracy and less ray effect, for this problem, than any of the other quadratures he investigated. The results for this quadrature, $S_{3G,6Q}$ and $S_{4G,8Q}$, are shown in Figure X-5, taken directly from reference 2.

6. Discrete Elements

A variety of discrete element schemes were tested for this problem using a 16 by 16 spatial grid. For the auxiliary fluxes, the step method was found to be unacceptable in accuracy, while the diamond difference method (with or without negative fixups) was inaccurate and slow to converge ($L_{KG,L}$), or prevented convergence ($L_{K,L}$). With the step characteristic method for the auxiliary fluxes and either diamond difference or step characteristic for the main fluxes, convergence was as fast as for the S_N method. As in the one-dimensional test problems, the Gauss-Legendre three-point element quadrature was generally more accurate than the Simpson's Rule. The Newton-Cotes rule was about as accurate as the Gauss-Legendre, but at greater execution cost.

The results of two calculations with the 30 by 30 spatial grid are shown in figures X-6 and X-7. The schemes used were $G3-L_{2G,3}^{SC/DDF}$ and $G3-L_{2G,3}^{SC/SC}$. The SC/DDF solution shows a small amplitude wiggle which can be attributed to the spatial quadrature, since it is not present in the SC/SC solution, and so is quasi-ray effect. The SC/SC solution also shows a quasi-ray effect, in that there is a slight break in slope at $x = 1$ which corresponds to the edge of the source region (as was seen in chapter VI). These quasi-ray effects were reduced by refining the spatial grid from 16 by 16 to 32 by 32. The SC/SC curve falls between the $S_6 \rightarrow P_3$ and $S_8 \rightarrow P_5$ curves of figure X-4.

Comparing figure X-6 with figures X-1 through X-5, it may be concluded that, for this problem, the discrete element method, with as few as three elements in azimuth per azimuthal quadrant, ameliorates ray effect as well as the best of previous methods.

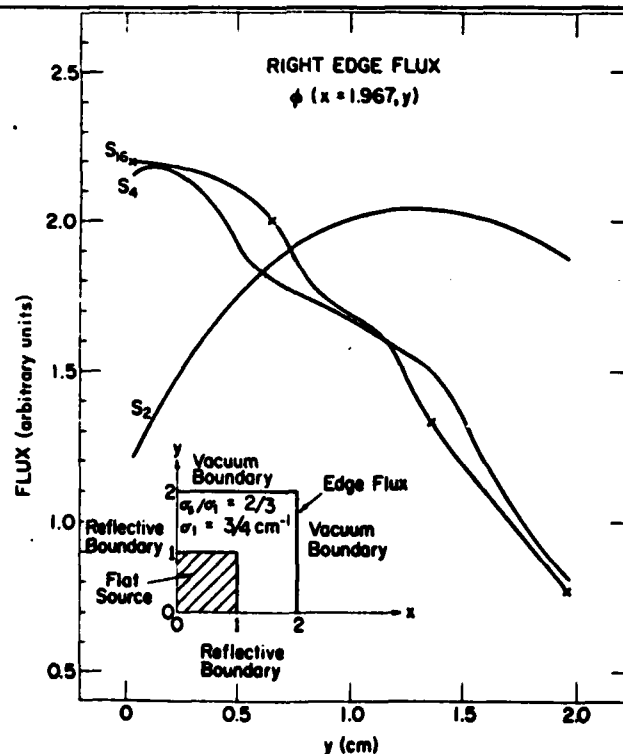


Fig. X-1: Ray Effects: Conventional S_N [Ref. 8:257]

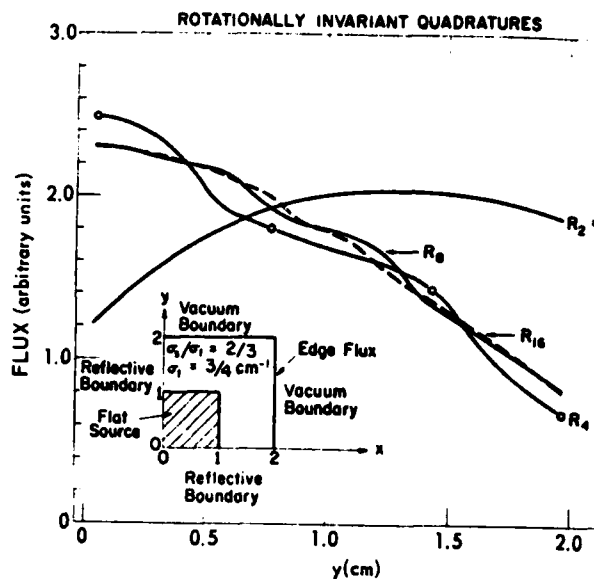


Fig. X-2: Ray Effects: Rotationally Symmetric S_N [Ref. 8:258]

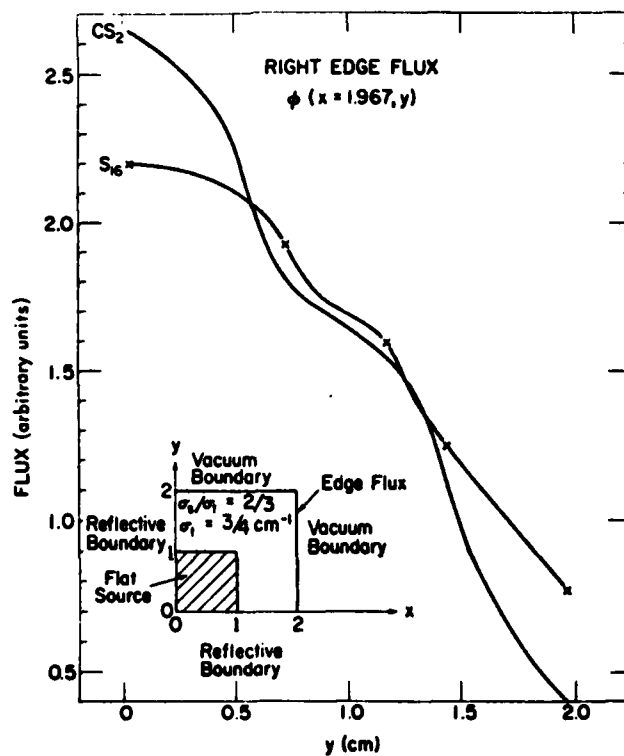


Fig. X-3: Ray Effects: "Consistent" Discrete Ordinates [Ref. 8:259]

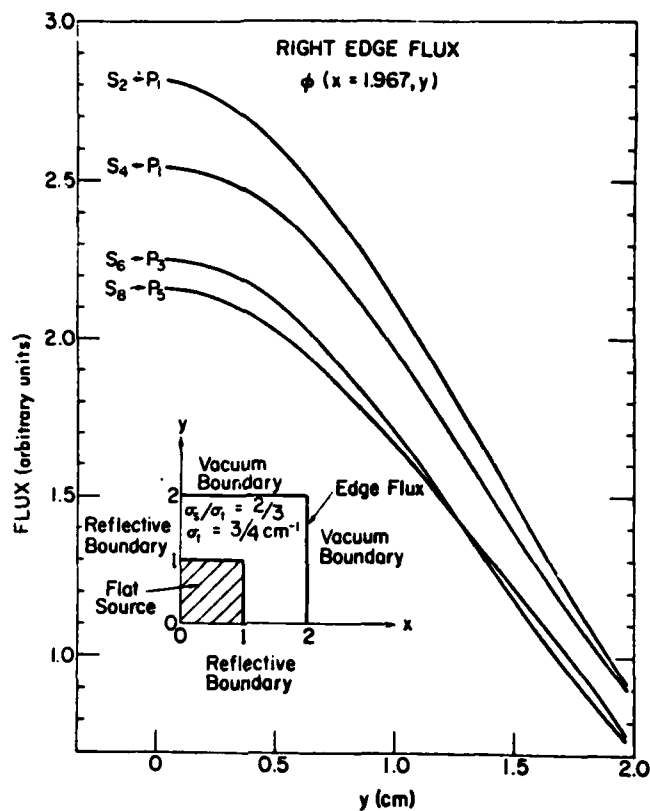


Fig. X-4: Ray Effects: Spherical-Harmonics-Like S_N [Ref. 8:263]

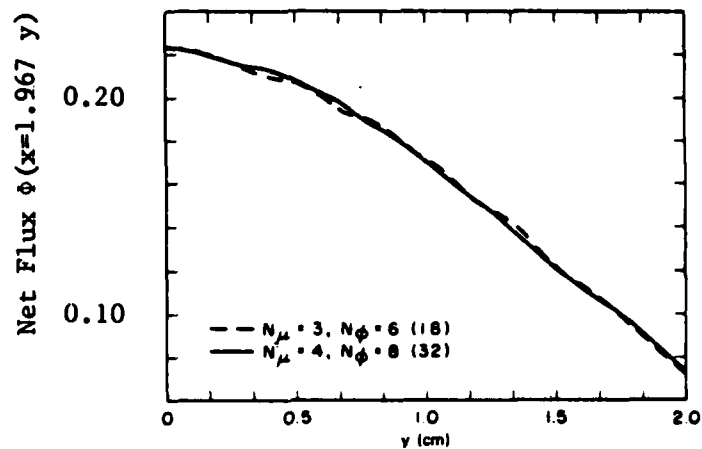


Fig. X-5: Ray Effects: Gauss-Christoffel/Quadruple-Range S_N [Ref. 2:313]

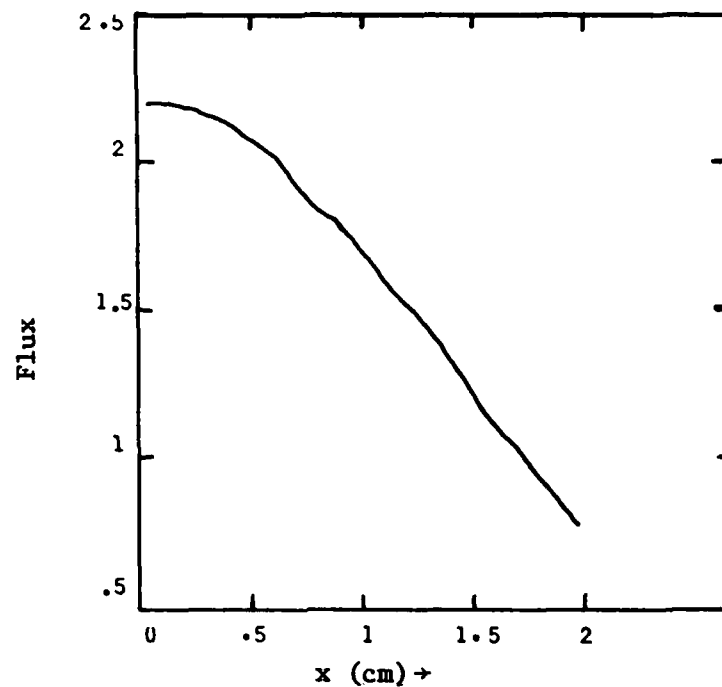


Fig. X-6: Ray Effects: Discrete Elements $G3-L_{2G,3}^{SC/DDF}$

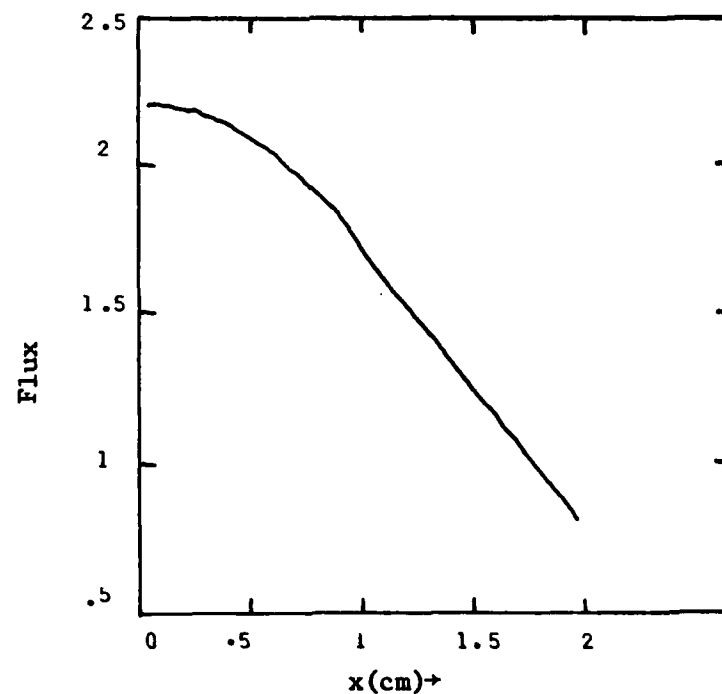


Fig. X-7: Ray Effects: Discrete Elements $G3-L_{2G,3}^{SC/SC}$

B. Vacuum Duct Problem: Qualitative Comparison of Results

The second test case is a duct problem which is difficult for discrete ordinates. A quantitative comparison of L_N and S_N is made. Streaming ducts in shields are a common design problem for which empirical thumb-rules are often used. Where better solutions are needed, Monte Carlo methods provide accurate but expensive answers. This section presents graphs of numerical results and qualitative comparison; the next section presents quantitative comparisons.

1. The Test Problem

Figure X-8 defines a test problem consisting of a thin source region along the bottom of a shield with vacuum boundaries along the top, right, and bottom. The left side of the problem is a symmetry boundary, with a deep, narrow vacuum duct, or channel, along the edge. It is expected that the major leakage through the shield will be by streaming up the duct. This particular problem was selected as an idealized representation of an access port in a fusion reactor design. Such access ports are required for plasma injection, charged particle heating beams, laser instrumentation, etc.

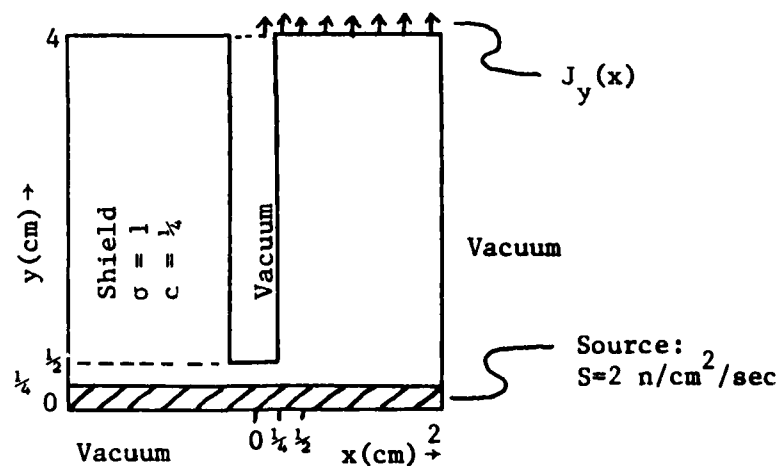


Fig. X-8: Vacuum Duct Problem Parameters

2. Monte Carlo Benchmark Solution

In order to accurately assess the performance of both the discrete elements and discrete ordinates methods, a benchmark solution known to be both accurate and free of ray effect was required. The Monte Carlo solution used for this purpose is shown in figures X-9 through X-13. The solution entailed the simulation of 10^6 particles. Data recorded included total leakage, total absorption, and leakage through each of 16 equal segments along the top edge of the problem, corresponding to the 16 cell by 16 cell spatial grid used for the discrete elements and discrete ordinates calculations. The relative variance of the results was approximately 1% at the one-sigma level of confidence for the least accurate of the 16 top face leakages. This solution was provided by W. T. Urban of Los Alamos National Laboratory in support of this research.

3. Conventional Discrete Ordinates

Conventional S_N quadrature solutions using various spatial quadrature schemes were provided by E. W. Larsen in support of this research. Diamond difference solutions are shown in figure X-9. There are two striking observations to be made about S_N^{DDF} : the results are not good, and they don't improve much as N is increased. The currents are in error by factors of two to four over most of the top face of the problem, even for S_{16} , which uses 36 quadrature directions per octant. The step characteristic solutions are smoother and more accurate in level, and are shown in figure X-10. Larsen and Alcouffe have developed a linear characteristic spatial quadrature method for xy-geometry [Ref. 5]. Results with this quadrature, shown in figure X-11, have some improvement over the step characteristic method.

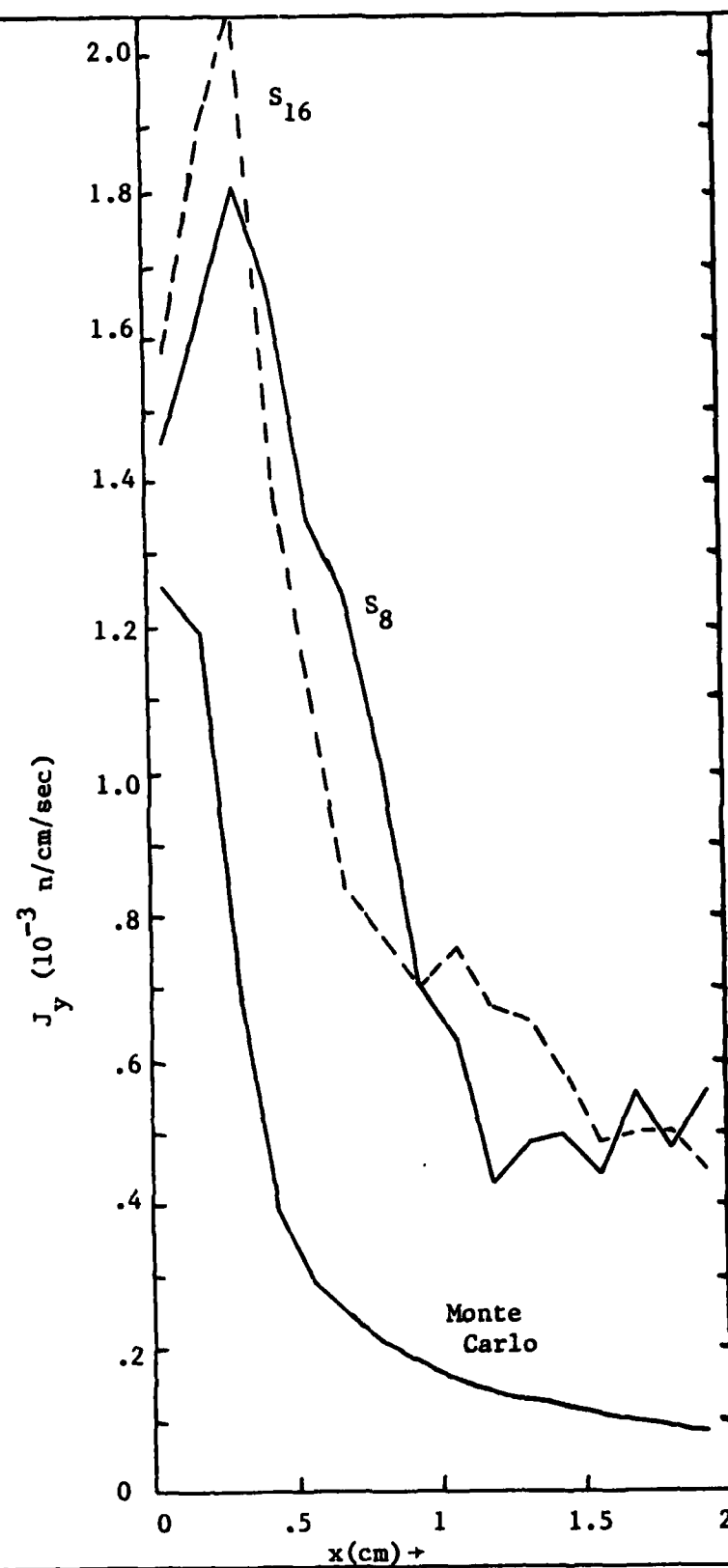


Fig. X-9: Vacuum Duct: Conventional S_N^{DDF}

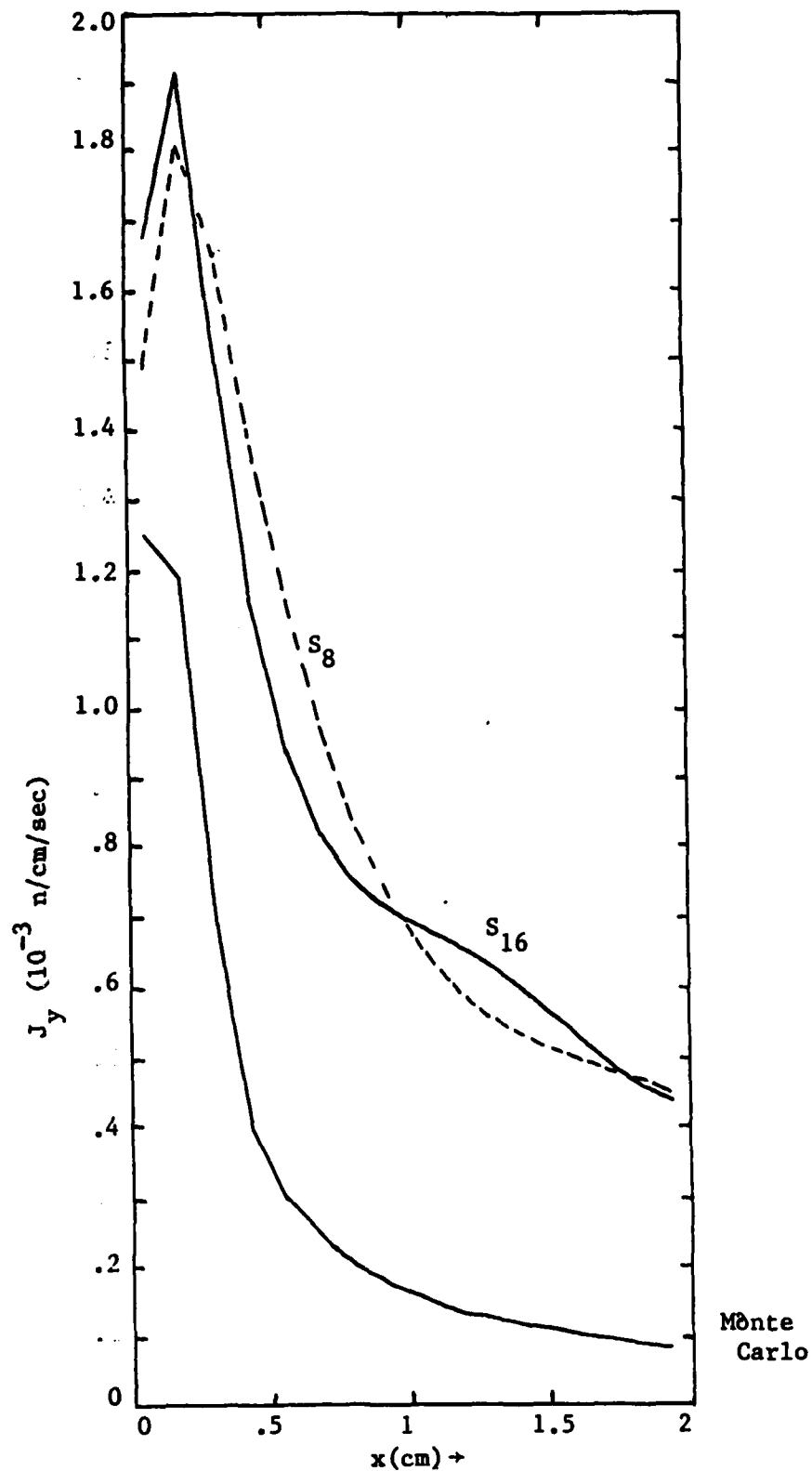


Fig. X-10: Vacuum Duct: Conventional S_N^{SC}

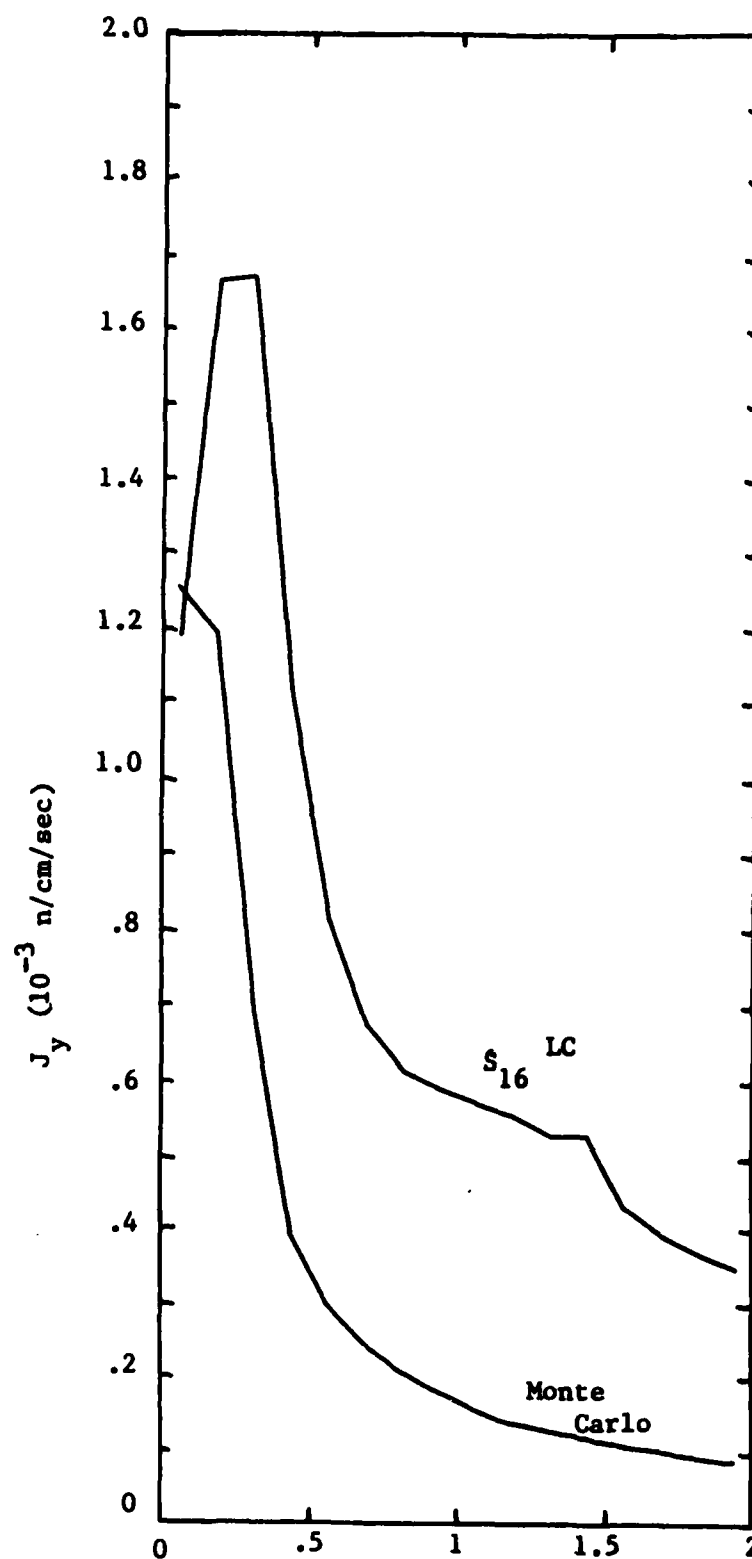


Fig. X-11: Vacuum Duct: Conventional S_N^{LC}

4. Product Quadrature Discrete Ordinates

Figure X-12 shows the results of a discrete ordinates calculation using a Gauss-Christoffel / rotationally symmetric product quadrature and step characteristic spatial quadrature: $S_{2G,3R}^{SC}$. This is the angular quadrature underlying the discrete elements results considered next. These results are greatly improved over the conventional S_N results, both in overall level and in shape. The conventional S_N gave a ratio of less than 4:1 for the leakage in the duct to that on the right half of the top of the shield, even for S_{16} . The product quadrature gives a ratio of about 6:1, while the benchmark ratio is about 12:1. In the next section, a "level norm" and a "shape norm" are introduced to properly quantify these observations.

5. Discrete Elements

Figure X-13 shows the results for the discrete elements method: $G3-L_{2G,3}^{SC/SC}$, with 16 by 16 and 32 by 32 spatial meshes. The ratio of duct current to that on the right is about 11:1, much improved over all the discrete ordinates methods. Also, the leakage is monotone decreasing from left to right, as expected from the problem symmetry. None of the discrete ordinates methods were correct in this regard. Deficiencies of this discrete element solution are:

- a - The leakage through the duct is overestimated by 20%-30%
- b - There is a slight hump to the curve at about $x = 1.5$ cm
- c - The leakage through the shield away from the duct is overestimated by about 15%

Item b is a ray effect and is eliminated in the $L_{3G,4}$ solution. The other two deficiencies are at least partially quasi-ray effect and are reduced by the refined (32 by 32) spatial mesh.

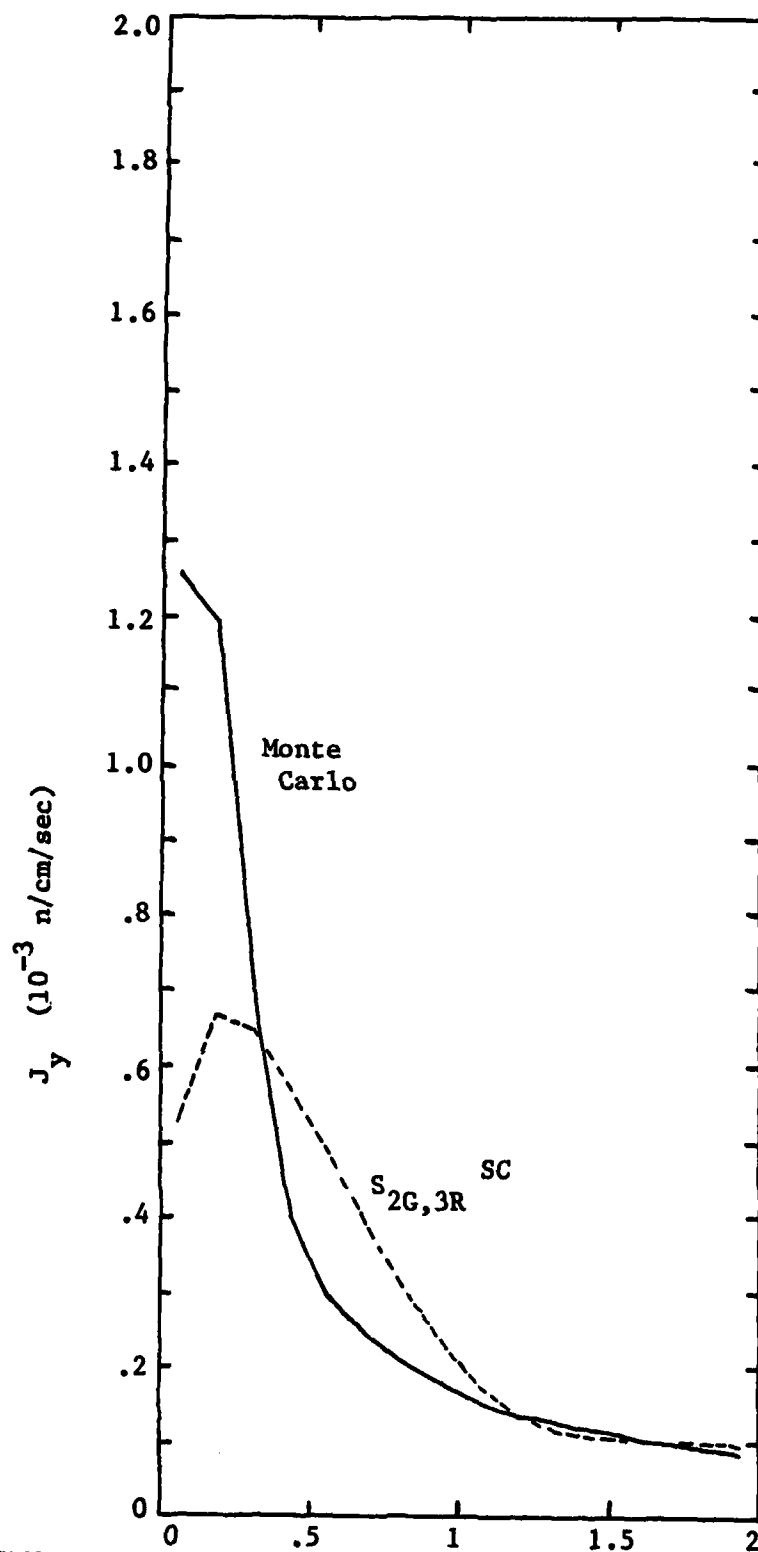


Fig. X-12: Vacuum Duct: Product Quadrature Discrete Ordinates S_{2G,3R}^{SC}

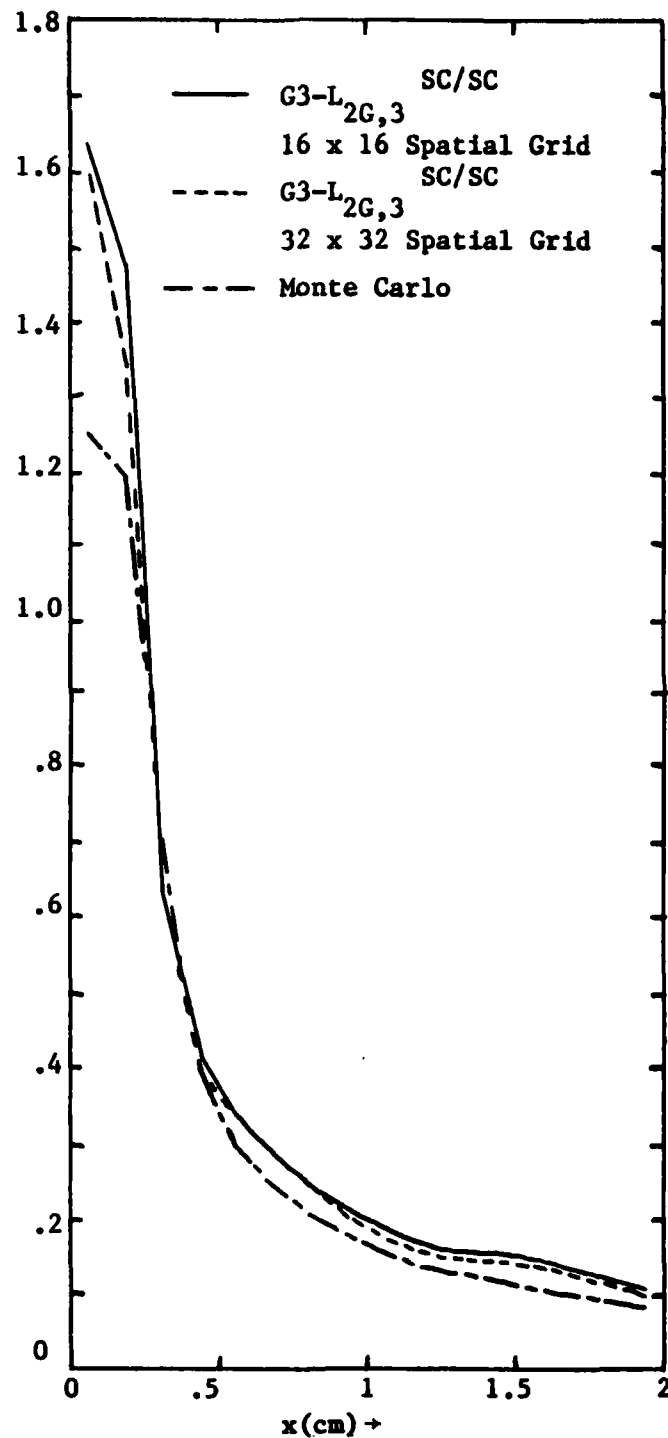


Fig. X-13: Vacuum Duct: Discrete Elements G3-L_{2G,3} SC/SC

C. Vacuum Duct Problem: Quantitative Comparison of Results

This section makes a quantitative comparison of the accuracy of discrete elements solutions with that of discrete ordinates solutions, for the problem presented in the previous section. As in chapter IX, informal "norms" are used for this purpose. Two such measures of error are used. One is sensitive to the over-all amplitude of the top face leakage. This "level norm" is the error ratio (defined by equation IX-4) of the total leakage through the top face of the problem, i.e., through the duct and through the shield, with respect to the Monte Carlo benchmark solution. The table indicates the sign of the error: positive for overestimated leakage, negative for underestimated leakage. The other measure of error is sensitive to the relative distribution of leakage through the top face. This "shape norm" is the average of the error ratios of the 16 normalized cell currents. The currents are normalized to give the same total leakage as the benchmark solution, so that the norm will be sensitive to shape but not level. The performance of various schemes tested is presented in table X-1, in terms of these norms. Data is presented for the step characteristic spatial quadrature, since the SC/DDF results show poor performance in the shape norm as a result of spatial oscillations (quasi-ray effect). S_{16}^{LC} results are also included. Observations based on this data are presented next.

1. Convergence of Conventional S_N

Refining the angular quadrature from S_8 to S_{16} provided negligible quantitative improvement in either shape or level. Refining the spatial quadrature from S_{16}^{SC} to S_{16}^{LC} , however, improved the level but not the shape. The conventional S_N angular quadrature is essentially converged, and with poor results.

<u>Method</u>	<u>Elements or Ordinates per Octant</u>	<u>Level Norm</u>	<u>Shape Norm</u>	<u>Grid</u>
G3-L _{2G,2}	4	.1018	.0594	16x16
SR-L _{2G,3}	6	.0776	.0503	16x16
G3-L _{2,3}	6	.1121	.0400	16x16
G3-L _{2G,3}	6	.0895	.0370	16x16
SR-L _{3G,4}	12	.0693	.0417	16x16
G3-L _{3G,4}	12	.0750	.0381	16x16
NC-L _{3G,4}	12	.0741	.0386	16x16
G3-L _{3G,6}	18	.0672	.0370	16x16

S _{2G,3R}	6	(-) .0608	.1525	16x16
S ₈	10	.4533	.2420	16x16
S _{3G,4R}	12	(-) .0012	.1130	16x16
S ₁₆	36	.4451	.2380	16x16
S ₁₆ ^{LC}	36	.3846	.2285	16x16
S _{2G,18R}	36	.0611	.0366	16x16
S _{3G,12R}	36	.0562	.0344	16x16
S _{2G,3Q}	6	.0336	.0641	16x16
S _{2G,3Q}	6	(-) .0006	.0954	32x32

G3-L _{2G,3}	6	.0658	.0319	32x32
G3-L _{3G,6}	18	.0471	.0257	32x32

Table X-1: Vacuum Duct: Error Norms for L_N and S_N Results

2. Convergence in Polar Quadrature

Increasing the accuracy of polar quadrature by increasing K for product quadratures should improve level but have little effect on shape. This effect is seen in a comparison of $S_{2G,18R}$ and $S_{3G,12R}$, both of which are essentially converged in azimuth. Also, the hybrid discrete element method, $G3-L_{2G,3}$ is significantly more accurate in level than the corresponding $G3-L_{2,3}$ method, but only a little better in shape, indicating its superiority in polar quadrature. The hybrid method is more accurate and less expensive.

3. Convergence in Azimuthal Quadrature

Each of the product quadratures $S_{2G,18R}$ and $S_{3G,12R}$ use 36 ordinates per octant and thus have the same computational cost as S_{16} . Because they apply most of their effort to the difficult azimuthal quadrature, and because they use a composite quadrature scheme (composite midpoint rule) to treat the ill-behaved azimuthal flux variations, they greatly outperform the conventional quadrature. The azimuthal quadrature is converged at a shape norm of about .035-.038 for the various product quadrature discrete elements and discrete ordinates schemes tested, for a 16 cell by 16 cell spatial grid. Thus, to the accuracy of this spatial quadrature, the $G3-L_{2G,3}$ scheme is essentially converged in azimuthal quadrature. The Simpson's rule method, however, is less effective, not being converged in shape at $SR-L_{2G,3}$. The Newton-Cotes rule method is as accurate as the Gauss-Legendre method, but costs more to compute.

4. Convergence of Spatial Quadrature

For the 16x16 grid, the spatial cell size is 1/8 mfp in width (Δx) and 1/4 mfp in height (Δy). The improvement in level (but not shape) resulting from the use of the new linear characteristic method with S_{16} indicates that the spatial quadrature is not converged. The spatial grid was therefore refined to 32x32 for a limited number of calculations.

The composite Gauss-Christoffel / quadruple-range quadrature, $S_{2G,3Q}$, was evaluated for both space mesh sizes. The level error decreased with the refined spatial grid, but the shape error increased. This inconsistent behavior, together with the average 19% pointwise error, indicates that the nearly exact total leakage for the method is coincidental, as for the $S_{3G,4R}$.

The improvement in the $G3-L_{2G,3}$ method resulting from the spatial grid refinement was more significant than that resulting from a refinement of the angular grid to $G3-L_{3G,6}$ (still on a 16x16 spatial grid). This improvement was both in level and in shape. The reasons for these improvements are considered below. With this refined spatial grid, further improvement was noted by then refining the angular mesh as well, to $G3-L_{3G,6}$.

Since the errors of shape and level remaining in the discrete elements solutions, such as $G3-L_{2G,3}^{SC/SC}$, are dominated by the spatial quadrature, and since it was not possible to refine the spatial mesh to convergence within the scope of this research, precise comparisons of cost-effectiveness of the various schemes could not be made. A more important consideration, perhaps, is the confidence level (in an engineering sense) of the various methods, which is considered next.

5. Confidence of Results

The foregoing discussions of accuracy and convergence have implicitly presumed that the benchmark solution is known. From the viewpoint of practical engineering, however, the objective of numerical calculations is to estimate an (unknown) answer and its confidence limits.

Taking this view, and supposing the duct problem is to be solved only by the discrete ordinates method, the results obtained above lead to a low level of confidence. Different families of quadrature sets apparently converge to different results, both in shape and level. The convergence is inconsistent with respect to the two. In terms of the error valleys that Lathrop described, the dilemma is simply stated: "how is one to know which solutions are in the valley?" As seen with the total top-face leakage and the $S_{KG,LR}$ quadratures, the hills on one side may be positive error while the hills on the other side of the valley are negative error. The properly conservative engineering answer is that the shield leakage is the median of the collection of discrete ordinates results, to within a factor of about two (for this example). This is the reason nuclear power reactor shielding is typically over-designed.

If this same engineering problem were to be solved by discrete elements, however, the consistent convergence in polar, azimuthal, and spatial quadratures, toward the same answer, using different element quadrature rules and different quadrature types ($L_{KG,L}$ vs. $L_{K,L}$) allow a much more useful conclusion to be drawn. The result can be estimated to a confidence of about plus or minus 10%. There may still be an "error valley", but all the results in table X-1 are on one side of it, and the hills are lower.

D. Interaction of Spatial and Angular Quadrature

The discrete elements solutions for the vacuum duct problem were not fully converged in spatial quadrature. As a consequence, the auxiliary fluxes were not as accurate as possible, so that the coupling of angular and spatial quadratures is not as effective as possible. The errors of the $G3-L_{2G,3}^{SC/SC}$ solution were observed to be of three types:

- 1 - The leakage through the duct is overestimated by 20%-30%
- 2 - There is a slight hump to the curve at about $x = 1.5$ cm
- 3 - The leakage through the shield away from the duct is overestimated by about 15%.

The second item is a ray effect and is eliminated by refining the angular mesh, but the other two are quasi-ray effects, and are reduced by refining the spatial mesh. The objective of this section is to evaluate the causes of these quasi-ray effects and the possibility of reducing or eliminating them through the use of a higher order spatial quadrature.

1. Leakage Through the Shield

Since it is a simpler problem, the overestimation of the leakage through the shield, away from the vacuum duct, is considered first. The step characteristic scheme assumes a flat source distribution within each spatial cell. This source term is Q and includes scatter. As the flux penetrates a shield, it should be monotone decreasing, so that the scatter-source should be decreasing across each cell (in the direction of shield penetration). But, the step characteristic scheme computes the cell-average value, redistributing Q uniformly across the cell. This is a systematic error which consistently transports scattered particles deeper into the shield, as shown in figure X-14A.

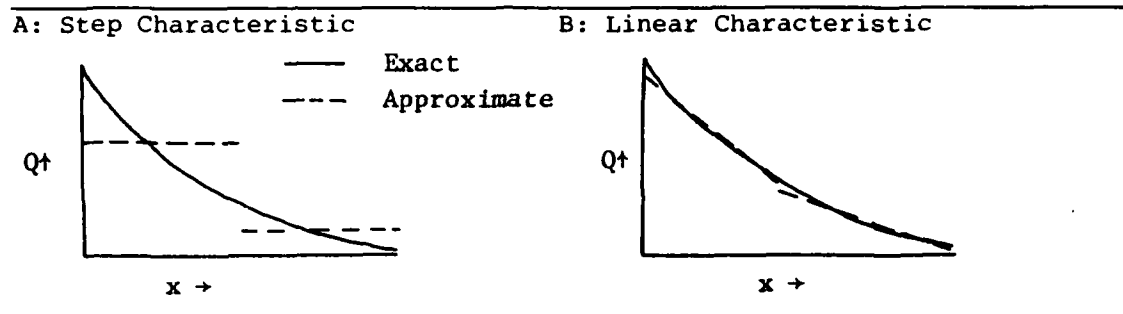


Fig. X-14: SC and LC Shield Penetration Errors

The linear characteristic method models the scatter-source term, Q , as linearly varying across each spatial cell so as to approximate both its average and its first (spatial) moment. This eliminates, to the accuracy of the approximation, the systematic artificial transport of particles into the shield, as shown in figure X-14B. It is expected, then, that use of the LC spatial quadrature with the discrete elements method would substantially reduce the overestimation of the leakage through the shield, away from the streaming duct.

2. Leakage Through the Duct

The presence of the duct enhances overall leakage through the shield in two ways. Particles that originate below the duct (or scatter below the duct) may stream freely through the shield, provided only that they start in the right direction. This is illustrated as path A of figure X-15. Discrete ordinates is inaccurate for this problem because few, if any, of the quadrature directions represent this path. Discrete elements, however, can steer the streaming into this path. The second effect of the duct is to decrease the optical thickness of the shield for paths which cross through the duct and ultimately leak out through the main body of the shield, as illustrated by path B.

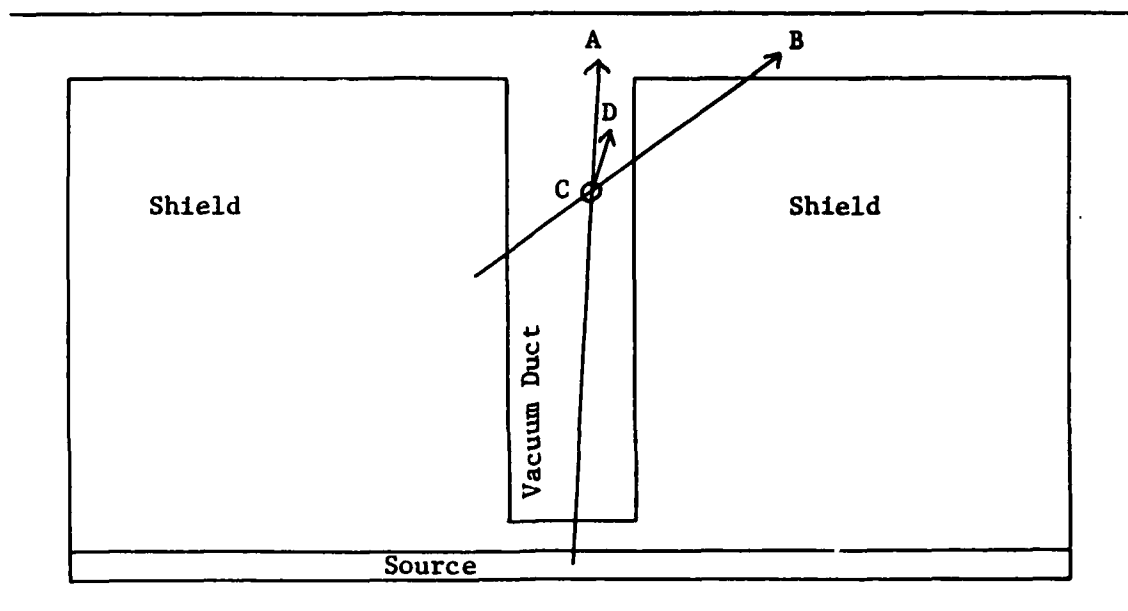


Fig. X-15: Paths Through the Vacuum Duct

The discrete elements method errs in a different way in handling path B. The flux in an angular element at point C of figure X-15 would consist of mostly path A type particles with an admixture of some path B type particles, and would be represented by a flux-weighted average streaming direction such as D. Assuming analytic spatial quadrature were somehow employed, the particles in the element would be moved precisely in direction D; the result would be to walk the B's across the duct and the A's up the duct. But, with step characteristic spatial quadrature, this is not the result. Since direction D is close to the duct axis (y), and hence far from the cell diagonal, the method is numerically inaccurate and (as shown in section VI-C) walks the flux, like a chess rook, straight up the duct. The renormalizing of the spatial distribution along the cell edge to a flat approximation moves the particles (falsely) to the left at each cell interface. The path B particles, in effect, become trapped in the duct and escape absorption.

The linear characteristic scheme would minimize this form of error by representing the flux along each cell interface with a linear fit which, at least approximately, matches the average and the first (spatial) moment along the cell boundary. This eliminates the flattening process which moved particles leftward, and would allow the B's to cross the duct and the A's to stream up the duct. The B's would not arrive at the top of the duct, so that the overestimation of the duct leakage by the step characteristic scheme should be largely eliminated. Since the B's would be exposed to further absorption upon reentering the shield material, only some would survive to leak through the shield, so that the total leakage would be reduced. This same feature would reduce or eliminate the quasi-ray effect of the SC scheme seen in the square-in-a-square problems in sections VI-C and X-A.

The linear characteristic scheme is not merely higher order than the step characteristic scheme, but it also corrects the specific deficiencies which are the source of the errors observed in the discrete elements solutions. Thus, the linear characteristic method is expected to correct both the level and shape errors of the step characteristic method, when used for both the main and auxiliary flux calculations of the discrete element method.* A demonstration of the validity of this logic by actually programming the combined linear characteristic / discrete elements method was beyond the scope of this project, but refining the spatial mesh ameliorates the deficiencies of the SC scheme, and was observed to improve both the shape and level of the results in the manner anticipated from this analysis.

* The linear nodal method, recently developed by Walters and O'Dell [Ref. 13] should also be appropriate for this application.

E. Conclusions

The conclusions derived from the one-dimensional test cases of chapter IX have been further supported by the two-dimensional test cases of this chapter. In respect to xy-geometry, specific conclusions are:

1 - The hybrid Gauss-Christoffel (fixed) polar / equal weight composite (discrete element) azimuthal angular quadrature is most efficient and accurate.

2 - The minimum number of Gauss-Christoffel latitudes should be two, since with only one latitude, the quadrature is not of high enough order to meet the diffusion limit. Numerical performance indicates the importance of this consideration.

3 - The coupling of angular and spatial quadrature by the mechanism of "steered" element fluxes is highly successful in ameliorating ray effects, provided at least three (azimuthal) elements are used.

4 - The three-point Gauss-Legendre rule was the most effective element quadrature tested.

5 - As in chapter IX, the expectation that "the harder the problem, the more advantageous the discrete elements method" is supported by the evidence of these two tests.

6 - The discrete elements schemes showed better accuracy and more consistent convergence toward the benchmark solution than the discrete ordinates schemes tested.

7 - An evaluation of the full accuracy and cost-effectiveness of the method will require the use of a spatial quadrature of higher order, compatible with the higher order of the discrete elements angular quadrature (in order to take full advantage of the angular-spatial coupling).

XI. Conclusions and Recommendations

The objective of this research has been to develop and demonstrate "proof of concept" of the discrete elements method of numerical neutral particle transport. This chapter summarizes the conclusions which were drawn in the previous chapters and presents recommendations for use of the discrete elements method and for further study.

A. Conclusions

1. Sound Theoretical Basis

The discrete elements method has a sound basis in numerical analysis and transport theory. It is not an ad hoc fixup to discrete ordinates.

2. Practical for Computer Implementation

The discrete elements algorithm retains the essential structure of the discrete ordinates method. Its requirements for computer storage and run time are comparable to S_N ; in the absence of vacuum boundaries, $L_{2G,3}$ uses 22% less storage and run time than S_{16} . The method could be incorporated within existing production codes.

3. Amelioration of Ray Effects

The method is effective in ameliorating ray effects, but is more sensitive to quasi-ray effects than discrete ordinates. In this regard, a low-order L_N method behaves like a high order S_N method. Use of high-order spatial quadrature should ameliorate the quasi-ray effect.

4. Accuracy

The method is consistently more accurate than S_N with the same quadrature set. For example, $G3-L_{2G,3}^{SC/SC}$ is more accurate than $S_{2G,3R}^{SC}$. For the vacuum duct problem, L_N was the most consistently accurate and convergent (as angular or spatial mesh is refined) method.

5. Cost Effectiveness

The discrete elements method is the most cost-effective alternative for some problems. This was demonstrated in slab geometry, but could not be fully demonstrated in xy-geometry since the spatial quadrature dominated the remaining errors in the vacuum duct solutions. The discrete elements method was more cost-effective than conventional S_N for the xy-geometry duct problem. Both theory and testing supported the conjecture that the more difficult the problem, the more advantageous the discrete elements method would be, as compared to S_N .

6. Element Quadrature Rules

Gauss-Legendre three-point quadrature was consistently the most effective element quadrature rule tested. It was more accurate and cost-effective than Simpson's rule, and as accurate as Newton-Cotes five-point rule, but less expensive.

7. Angular Quadrature for XY-Geometry

The hybrid Gauss-Christoffel (fixed) polar / equal weight (steered) azimuthal quadrature, $L_{KG,L}$, was consistently more accurate and less expensive than the equal weight (steered) polar / equal weight (steered) azimuthal quadrature, $L_{K,L}$.

8. Spatial Quadrature

One approach considered was to use the least expensive spatial quadrature available, the step method, for the auxiliary fluxes (used to

steer the streaming directions of the element "main" flux) with the consideration that any accuracy of steering would be better than none, i.e., S_N , and that the cheap auxiliary calculations could then give the best cost-effectiveness. This approach proved ineffective.

The alternative approach was to use the highest order, most accurate spatial quadrature for both the auxiliary and main fluxes so that with really precise steering, the method would produce sufficient accuracy to pay for the expense of the high order auxiliary calculations. This proved to be the case. In one-dimensional geometry, the linear characteristic method produced the most accuracy and was more cost-effective than Gauss-Legendre discrete ordinates. In two-dimensional geometry, the most effective method tested was discrete elements with step characteristic spatial quadrature.

An analysis of the quasi-ray effect errors in the $L_{2G,3}^{SC/SC}$ solution to the vacuum duct problem indicated that the use of linear characteristic spatial quadrature for both the main and auxiliary fluxes would reduce or eliminate those errors.

B. Recommended General Purpose Discrete Elements Schemes

From the experience gained in testing these methods, the following quadratures are recommended for general purpose application:

1-D (Slab): L_4 2-D (xy): $L_{2G,3}$

No three-dimensional codes were used, but based on its two-dimensional performance and on the expectation that composite quadrature with angle-space coupling is effective for ill-behaved distributions, $L_{2,3}$ or $L_{3,3}$ is recommended for use in 3-D problems. These methods should all use Gauss-Legendre three-point element quadrature and the highest order spatial quadrature available.

C. Recommended Topics for Further Research

This initial study has developed the discrete elements method and demonstrated some of its potential. Of necessity, many areas of interest were not pursued. The following topics are recommended as being of most value in developing the discrete elements method as a useful tool.

1. Evaluation with Higher Order Spatial Quadratures

A cost-effectiveness study of discrete elements in two-dimensional geometry with linear characteristic or linear nodal spatial quadrature and a range of test problems could further explore the value of the method.

2. Extension to Curvilinear Coordinates

Characteristic quadratures have not been applied in curvilinear coordinates. Step and diamond difference methods have been, but the former is insufficiently accurate and the latter is insufficiently smooth for use in discrete elements. Extension of the method to curvilinear coordinates could be possible using the linear discontinuous spatial quadrature.

3. Extension to Anisotropic Scatter

Since the zeroth and first angular moments of the flux are computed and used in the discrete ordinates method, including linearly anisotropic scatter should be straightforward. Higher order anisotropy could be included by approximating the higher moments by numerical quadrature over each element as is done for the first moment, or alternatively, the full collection of auxiliary fluxes could be used as a single quadrature set to approximate the higher angular moments. Research is needed to find the most accurate and least expensive scheme.

4. Higher Order Space-Angle Coupling

The discrete elements method developed here couples the angular distribution to the spatial quadrature only through the mean streaming direction. In a sense, this is the first order member of a family of discrete element methods, with discrete ordinates as the zeroth order member. Higher order schemes could possibly be developed by treating the flux distribution over each element of angle as a known polynomial (from the auxiliary fluxes) and integrating that distribution across the space cell analytically, as an element characteristic spatial quadrature rather than the (steered) ordinate characteristic spatial quadratures used here. Using the symbolic tensor algebra capabilities of the MACSYMA system, such methods could conceivably be extended to curvilinear coordinates. Such higher order schemes would abandon some of the algorithmic simplicity of S_N and L_N , but could allow the use of coarse spatial grids and still provide acceptable accuracy. Such a hybrid of discrete ordinates, finite elements, and space-angle synthesis might prove highly effective.

Bibliography

1. Abramowitz, Milton and Irene A. Stegun, ed. Handbook of Mathematical Functions. National Bureau of Standards, Applied Mathematics Series 55. U. S. Government Printing Office, Washington, D.C. Issued June 1964, Fifth Printing, August 1966, with corrections.
2. Abu-Shumays, I. K. "Compatible Product Angular Quadrature for Neutron Transport in x-y Geometry," Nuclear Science and Engineering, 64: 299-316 (1977)
3. Alcouffe, R. E., E. W. Larsen, W. F. Miller, Jr., and B. R. Wienke. "Computational Efficiency of Numerical Methods for the Multigroup, Discrete-Ordinates Neutron Transport Equations: The Slab Geometry Case," Nuclear Science and Engineering, 71: 111-127 (1979)
4. Carlson, Bengt G. and Kaye D. Lathrop. Transport Theory - The Method of Discrete Ordinates. Los Alamos Scientific Laboratory of the University of California, Los Alamos, New Mexico, Report LA-3251-MS, Special Distribution, distributed April 1, 1965, under contract W-7405-ENG. 36 with the U. S. Atomic Energy Commission.
5. Larsen, E. W. and R. E. Alcouffe. "The Linear Characteristic Method for Spatially Discretizing the Discrete-Ordinate Equations in x,y Geometry," Proceedings of the American Nuclear Society Topical Meeting on Advances in Mathematical Methods for the Solution of Engineering Problems, Munich, FRG, April 27-29, 1981, Vol. 1: 99-113
6. Larsen, Edward W. and Warren F. Miller, Jr. "Convergence Rates of Spatial Difference Equations for the Discrete-Ordinates Neutron Transport Equations in Slab Geometry," Nuclear Science and Engineering, 73: 76-83 (1980)
7. Lathrop, K. D. "Spatial Differencing of the Transport Equation: Positivity vs. Accuracy," Journal of Computational Physics, 4: 475-498 (1969)
8. Lathrop, K. D. "Remedies for Ray Effects," Nuclear Science and Engineering, 45: 255-268 (1971)
9. Lathrop, K. D. and B. G. Carlson. Discrete Ordinates Angular Quadrature of the Neutron Transport Equation. Los Alamos Scientific Laboratory of the University of California, Los Alamos, New Mexico, Report LA-3186, UC-32, Mathematics and Computers, TID-4500 (36th Ed.), distributed February 12, 1965, under contract W-7405-ENG. 36 with the U. S. Atomic Energy Commission.
10. Lathrop, K. D. and B. G. Carlson. "Properties of New Numerical Approximations to the Transport Equation," Journal of Quantitative Spectroscopy and Radiative Transfer, 11: 921-948 (1971)

11. Lee, Suresh M. and R. Vaidyanathan. "Comparison of the Order of Approximation in Several Spatial Difference Schemes for the Discrete-Ordinates Transport Equation in One-Dimensional Plane Geometry," Nuclear Science and Engineering, 76: 1-9 (1980)
12. Rhoades, W. A. and R. L. Childs. An Updated Version of the DOT 4 One- and Two-Dimensional Neutron/Photon Transport Code. Oak Ridge National Laboratory, Oak Ridge, Tennessee, Report ORNL-5851, Distribution Category UC-79d, published July 1982, under contract W-7405-eng-26 for the Department of Energy
13. Walters, Wallace F. and R. Douglas O'Dell. "Nodal Methods for Discrete-Ordinates Transport Problems in (X,Y) Geometry," Proceedings of the American Nuclear Society Topical Meeting on Advances in Mathematical Methods for the Solution of Engineering Problems, Munich, FRG, April 27-29, 1981, Vol. 1: 115-129

Vita

Kirk Alan Mathews was born on 12 May 1949 in Boise, Idaho. He graduated from high school in Federal Way, Washington in 1967 and attended the California Institute of Technology, Pasadena, California, from which he received the degree of Bachelor of Science with majors in Physics and English Literature, in June 1971. He attended the University of Washington, Graduate School of Nuclear Engineering until called to active duty at the Naval Officer Candidate School in January 1972. He received his regular commission as a Distinguished Naval Graduate on 12 May 1972. He graduated at the head of his class at the Naval Nuclear Power School, Mare Island, California, in November 1972, and completed Nuclear Prototype training at the D1G prototype, at West Milton, New York, in May 1973. He qualified in submarines while serving in USS George Washington, SSBN 598, until November 1975. He then taught nuclear reactor dynamics and core characteristics to officer students at the Nuclear Power Schools at Mare Island, Calif., and Orlando, Florida, qualifying as a nuclear propulsion plant Engineer Officer during this period. He reported aboard USS Birmingham, SSN 695, at her launching in November 1977, as Navigator and Operations Officer. He was a shift senior supervisor for the nuclear propulsion plant construction and testing of USS Birmingham, which was commissioned 16 December 1978. He entered the School of Engineering, Air Force Institute of Technology, in June 1981, from which he recieved the degree of Master of Science (Nuclear Engineering) in December 1982. He is a member of Tau Beta Pi.

REPORT DOCUMENTATION PAGE		READ INSTRUCTIONS BEFORE COMPLETING FORM
1. REPORT NUMBER AFIT/DS/PH/83-5	2. GOVT ACCESSION NO. 147-A138080	3. RECIPIENT'S CATALOG NUMBER
4. TITLE (and Subtitle) DISCRETE ELEMENTS METHOD OF NEUTRAL PARTICLE TRANSPORT		5. TYPE OF REPORT & PERIOD COVERED Ph.D. Dissertation
		6. PERFORMING ORG. REPORT NUMBER
7. AUTHOR(s) LCDR Kirk A. Mathews, USN		8. CONTRACT OR GRANT NUMBER(s)
9. PERFORMING ORGANIZATION NAME AND ADDRESS		10. PROGRAM ELEMENT, PROJECT, TASK AREA & WORK UNIT NUMBERS
11. CONTROLLING OFFICE NAME AND ADDRESS Air Force Institute of Technology Wright-Patterson AFB, Ohio 45433		12. REPORT DATE October, 1983
		13. NUMBER OF PAGES 129
14. MONITORING AGENCY NAME & ADDRESS (if different from Controlling Office)		15. SECURITY CLASS. (of this report) UNCLAS
		15a. DECLASSIFICATION/DOWNGRADING SCHEDULE
16. DISTRIBUTION STATEMENT (of this Report) Approved for Public Release; distribution unlimited		
17. DISTRIBUTION STATEMENT (of the abstract entered in Block 20, if different from Report)		
18. SUPPLEMENTARY NOTES Approved for public release; LAW AFR 190-17 <i>Lynn E. Wolaver</i> 7 Feb 84 LYNN E. WOLAVER Dean for Research and Professional Development Air Force Institute of Technology (AIC) Wright-Patterson AFB OH 45433		
19. KEY WORDS (Continue on reverse side if necessary and identify by block number) Neutron Transport, Boltzmann Equation, Numerical Methods		
20. ABSTRACT (Continue on reverse side if necessary and identify by block number)		

Abstract

A new "discrete elements" (L_N) transport method is derived and compared to the discrete ordinates S_N method, theoretically and by numerical experimentation. The discrete elements method is more accurate than discrete ordinates and strongly ameliorates ray effects for the practical problems studied. The discrete elements method is shown to be more cost effective, in terms of execution time with comparable storage to attain the same accuracy, for a one-dimensional test case using linear characteristic spatial quadrature. In a two-dimensional test case, a vacuum duct in a shield, L_N is more consistently convergent toward a Monte Carlo benchmark solution than S_N , using step characteristic spatial quadrature. An analysis of the interaction of angular and spatial quadrature in xy-geometry indicates the desirability of using linear characteristic spatial quadrature with the L_N method.

The discrete elements method is based on discretizing the Boltzmann equation over a set of elements of angle. The zeroth and first angular moments of the directional flux, over each element, are estimated by numerical quadrature and yield a flux-weighted average streaming direction for the element. (Data for this estimation are fluxes in fixed directions calculated as in S_N). The spatial quadrature then propagates the element flux in this "steered" direction. Since the quadrature directions are not fixed, but are coupled to the fluxes, the method strongly ameliorates ray effect. This is verified using the square-in-a-square test case originated by Lathrop. A variety of spatial, angular, and element quadrature schemes are evaluated for both L_N and S_N . The best discrete elements method uses a hybrid of Gauss-Christoffel polar and composite 3-point Gauss-Legendre azimuthal quadrature.